Impact of Sex Differences and Small Molecules on Pro-Inflammatory Lipid Mediator Biosynthesis

Dissertation

To Fulfil the
Requirements for the Degree of
“doctor rerum naturalium“ (Dr. rer. nat.)

Submitted to the Council of the Faculty
of Biological Sciences
of the Friedrich Schiller University Jena

by Dipl.-Pharm Verena Sophia Krauth
born on October 31st, 1986 in Munich

Reviewers:

1. Prof. Dr. Oliver Werz
   Friedrich-Schiller-University Jena
   Institute of Pharmacy
   Department of Pharmaceutical and Medicinal Chemistry
   Philosophenweg 14
   07743 Jena

2. Prof. Dr. Gerhard K. E. Scriba
   Friedrich-Schiller-University Jena
   Institute of Pharmacy
   Department of Pharmaceutical and Medicinal Chemistry
   Philosophenweg 14
   07743 Jena

3. Prof. Dr. Nils Helge Schebb
   Bergische University Wuppertal
   Faculty of Mathematics and Natural Sciences
   Food Chemistry Department
   Gaussstrasse 20
   42119 Wuppertal

Date of public defense: 22. November 2018

TABLE OF CONTENTS

ABBREVIATIONS

[^{3}H]-AA	Tritium labelled arachidonic acid
15-PGDH	15-hydroxy prostaglandin dehydrogenase
AA	Arachidonic acid
ADA	Adenosine deaminase
AP-1	Activator protein 1
APC	Allophycocyanin/ antigen-presenting cells
ASA	Acetylsalicylic acid
ATP	Adenosine triphosphate
C5a	Complement component 5a
cAMP	Cyclic adenosine monophosphate
CD	Cluster of differentiation cell surface marker
CLP	Coactosin-like protein
COPD	Chronic obstructive pulmonary disease
COX	Cyclooxygenase
cPGES	Cytosolic prostaglandin E synthase
CREB	CAMP response element-binding protein
cys-LT	Cysteinyl leukotrienes
D'PBS	Dulbecco's phosphate buffered saline
DAPI	4',6-diamidino-2-phenylindole
DCFH-DA	2'-7'-dichlorofluorescin diacetate
DHA	Docosapentaenoic acid
DHT	Dihydrotestosterone
DP	PGD_2 receptor
DPI	Diphenyleneiodonium
DPPH	2,2-diphenyl-1-piperylhydrazyl
DTT	Dithiotreitol
EDTA	Ethylenediaminetetraacetic acid
EGF	Epidermal growth factor
ELISA	Enzyme-linked immunosorbent assay
EP	PGE_2 receptor
EPA	Eicosapentaenoic acid
ERK	Extracellular signal-regulated kinase
ES	Estradiol
FACS	Fluorescence activated cell sorting
FCS	Fetal calf serum
FITC	Fluorescein isothiocyanate
FLAP	5-lipoxygenase activating protein
fMLP	*N*-formyl-methionyl-leucyl-phenylalanine
FP	$PGF_{2\alpha}$ receptor
GPCR	G protein-coupled receptor
GSH	Glutathione
H(p)ETE	Hydroxy(peroxy)eicosatetraenoic acid
HEK	Human embryonic kidney cell line

RP-HPLC	Reversed phase high-performance liquid chromatography
CSS	Charcoal-stripped human serum
IFN	Interferon
IKK	Inhibitor of nuclear factor kappa B kinase
IL	Interleukin
IL-1R	Interleukin 1 receptor
IP	PGI_2 receptor
IRAK	Interleukin 1 receptor-associated kinase
IRF-3	Interferon response factor 3
JNK	C-Jun N-terminal kinase
LDL	Low-density lipoprotein
LO	Lipoxygenase
LPB	LPS-binding protein
LPS	Lipopolysaccharide
LRR	Leucine-rich-repeat motif
LT	Leukotriene
LTA_4H	Leukotriene A_4 hydrolase
LTC_4S	Leukotriene C_4 synthase
MAPEG	Membrane-associated proteins in eicosanoid and glutathione metabolism
MAPK	Mitogen-activated protein kinase
MCP-1	Monocyte chemotactic protein 1
MD-2	Myeloid differentiation factor 2
MEKK	MAPK kinase kinase
mPGES	Microsomal prostaglandin E synthase
MTT	3-(4,5-dimethylthiazol-2-yl)-2,5-diphenyltetrazolium bromide
MyD88	Myeloid differentiation primary response gene 88
NADPH	Nicotinamide adenine dinucleotide phosphate-oxidase
NF-κB	Nuclear factor “kappa-light-chain-enhancer” of activated B-cells
NO	Nitric oxide
NOD	nucleotide binding oligomerisation domain
NSAID	Nonsteroidal anti-inflammatory drugs
PAF	Platelet activating factor
PAMPs	Pathogen-associated molecular patterns
PBMC	Peripheral blood mononuclear cells
PC	Phosphatidylcholine
PCR	Polymerase chain reaction
PG	Prostaglandin
PKA	Protein kinase A
PLA_2	Phospholipase A_2
PMA	Phorbol-12 myristate 13-acetate
PMNL	Polymorphonuclear leukocyte
PMSF	Phenylmethane sulfonyl fluoride
PPAR	Peroxisome proliferator-activated receptor
PRP	Platelet rich plasma

PRR	Pattern-recognition receptor
Ras	Rat sarcoma protein
RIP1	Receptor interacting protein 1
RNS	Reactive nitrogen species
ROOH	Hydroperoxide
ROS	Reactive oxygen species
RT-qPCR	Quantitative reverse transcription PCR
SDS	Sodium dodecyl sulfate
SDS-PAGE	SDS-polyacrylamide gel electrophoresis
SLE	Systemic lupus erythematosus
SPE	Solid phase extraction
SPM	Specialized pro-resolving mediators
SRS-A	Slow reacting substance involved in anaphylaxis
STI	Soybean trypsin inhibitor
TAK1	TGF-β-activated kinase 1
TAM	Tumor-associated macrophages
TANK	TRAF family member-associated NF-κB activator
TBK1	TANK binding kinase 1
TGF-β	Transforming growth factor β
Th	T helper cells
TIR	Toll/Interleukin 1 receptor homology domain
TIRAP	TIR-associated protein
TLR	Toll-like receptor
TNF(R)	Tumor necrosis factor (receptor)
TP	TxA_2 receptor
TRAF	Tumor necrosis factor receptor-associated factor
TRAM	TIR domain-containing adaptor
TRIF	TIR domain-containing adaptor inducing INFβ
Tx	Thromboxane
UPLC-MS/MS	Ultra performance liquid chromatography tandem mass spectrometry

SUMMARY

The focus of this thesis was set on the modulation of the arachidonic acid (AA) cascade. In the first part, the influence of sex on the prostanoid formation in human whole blood and isolated cells was of interest, whereas the second part was dedicated to the search for suitable 5-lipoxygenase (5-LO) inhibitors. The prostanoids are generated by the cyclooxygenase (COX)-1/2 enzymes, which convert AA in a two-step reaction to prostaglandin (PG)H_2. PGH_2 is then further metabolized to distinct prostanoids by terminal synthases [1]. The role of COX and prostanoids in inflammation is well characterized and so is the existence of a sexual dimorphism in immunity and inflammatory diseases [2, 3]. However, little is known about the role prostanoids are playing in the observed sex differences. Recent findings suggest a differential regulation of the prostanoid expression in animal models of inflammation and also of the leukotriene (LT) biosynthesis by 5-LO in human male and female leukocytes, another class of lipid mediators [4, 5]. Hence, the regulation of the prostanoid expression in human whole blood and freshly isolated cells was evaluated in the first part of this thesis. Analysis of human blood cells showed generally higher cell numbers of lymphocytes and neutrophils in female blood, whereas monocyte numbers were higher in male blood. Long term incubations (24 h) of whole blood with various stimuli like lipopolysaccharide (LPS), the Ca^{2+} ionophore A23187 or *N*-formyl-methionyl-leucyl-phenylalanine (fMLP) resulted in significant enhanced levels of PGs, mainly PGE_2, in males compared to females. The observed elevated prostanoid formation in males was not influenced by pre-incubation of the blood with sex hormones prior to LPS stimulation. It was also independent of COX-2 protein as well as COX-2 mRNA expression analyzed in freshly isolated monocytes and peripheral blood mononuclear cells (PBMC). Furthermore, a contributing role of COX-1 and of the ionophore A23187-induced release of AA in polymorphonuclear leukocytes (PMNL) could be excluded. It is noteworthy that the observed sex difference in prostanoid formation was not detectable in human whole blood or in isolated PMNL in short term incubations (up to 30 min). The influence of the time-dependent prostanoid degradation was evaluated using SW033291, a specific inhibitor of the metabolizing enzyme 15-hydroxy prostaglandin dehydrogenase (15-PGDH). The results obtained in early time points (6h) suggested an involvement of 15-PGDH in the regulation of prostanoid levels. In female blood treated with the inhibitor the amount of PGE_2 was increased to the same levels detected in male blood without previous inhibitor treatment. Additionally, PMNL and PBMC were isolated from human whole blood and stimulated separately or together after co-incubation to analyze the effect of cell-cell interactions on prostanoid formation. In co-incubations, a more pronounced biosynthesis in males compared to females was observed. In conclusion, the underlying mechanisms leading to the sex difference of prostanoid formation in human whole blood upon stimulation with LPS, A23187 or fMLP for 24 h could not be elucidated completely. Nevertheless, the results suggest differences in the time-dependent prostanoid degradation and in cell-cell interactions within the whole blood as contributing mechanisms.

Besides COX and the prostanoids, the 5-LO enzyme and leukotrienes play an important role in inflammation. 5-LO converts AA to 5(*S*)-hydroperoxy-6-*trans*-8,11,14-*cis*-eicosatetraenoic acid (5-HpETE), which is further metabolized by 5-LO to LTA_4 [6]. Upon cell stimulation, 5-LO and the cytosolic phospholipase (cPL)A_2 translocate to the nuclear envelope, where together

with the 5-LO activating protein (FLAP) they are responsible for LT formation [7]. Recent investigations revealed the plant-derived compound embelin as potent 5-LO inhibitor [8]. Using embelin as lead structure, its 1,4-benzoquinone core was systematically modified resulting in three distinct series of potential 5-LO inhibitors: series (I) comprised sixteen 1,4- and 1,2-benzoquinones substituted in 3-position with *n*-alkyl chains of 8 to 15 carbon atoms, series (II) containing five 1,2-benzohydroquinones with *n*-alkyl chains of 11 to 13 carbon atoms in 3-position, and series (III) comprised fifteen 1,2-benzohydroquinones with rather bulky aromatic residues in 4-position. The first series was categorized according to their methylation pattern of the hydroxy groups on the benzoquinone core into the series A, B, C, and D. Evaluations of the inhibitory capacity in cell-based and cell-free settings revealed EA-110C of series C as most potent with IC_{50} values in the nanomolar range (IC_{50} = 50 - 120 nM). In series (II), the most promising 1,2-benzoquinones of series (I) were reduced to 1,2-benzyo-hydroquinones and their inhibitory potential on 5-LO was analyzed in cell-free and cell-based settings. The reduced form of EA-110C (EA-110C RED) showed IC_{50} values in the nanomolar range as well (IC_{50} cell-free = 30 – 60 nM) confirming a 1,2-quinone/ hydroquinone core combined with a C13-*n*-alkyl residue as optimal structure to interfere with 5-LO product formation. Animal models of acute inflammation confirmed efficacy *in vivo* and additional analysis revealed a non-competitive inhibitory mechanism, supported by docking simulations proposing a binding site for EA-110C opposite of the substrate channel. In series (III) the two most potent hydroquinones F-XII and F-XVI were analyzed in detail. Both compounds showed highly potent inhibition of 5-LO with IC_{50} values in the nanomolar range in cell-based (IC_{50} F-XII = 70 nM; F-XVI = 60 nM) as well as in cell-free preparations (IC_{50}: F-XII und F-XVI = 20 nM). 5-LO inhibition was reversible, independent of exogenously added AA and not primarily mediated due to radical scavenging and antioxidant properties. Docking simulations proposed binding of the 1,2-benzohydroquinone moiety to the amino acid Asp-166, which is involved in the salt bridge connecting the C-terminal catalytic domain with the N-terminal C2-like domain. Furthermore, inhibition of 5-LO was independent of interference with cellular activation signals required for the 5-LO activation. The obtained results in the second part of the thesis revealed the benzohydroquinones F-XII and F-XVI as highly potent, direct, rather non-redox-type or novel type inhibitors of 5-LO with high selectivity in nanomolar concentrations, confirmed by investigations in human whole blood and in zymosan-induced peritonitis in mice as possible new drug candidates.

ZUSAMMENFASSUNG

In der vorgelegten Arbeit lag der Fokus auf der Modulation der Arachidonsäure (AA)-Kaskade. Im ersten Teil wurde der Einfluss von Sexualhormonen auf die Prostanoidbiosynthese in humanem Vollblut und daraus isolierten Zellen untersucht, wohingegen der zweite Teil der Suche nach geeigneten Inhibitoren der 5-Lipoxygenase (5-LO) gewidmet wurde. Die Prostanoide werden durch die Cyclooxygenasen(COX)-1/2 gebildet, welche die AA in zwei Schritten zu Prostaglandin (PG)H_2 umwandeln. PGH_2 wird danach durch terminale Synthasen weiter zu den einzelnen Prostanoiden umgesetzt [1]. Die Rolle der COX Enzyme und der Prostanoide in Entzündungen ist weitreichend untersucht und das Vorliegen eines Geschlechtsdimorphismus des Immunsystems und in entzündlichen Erkrankungen ist ebenfalls bekannt [2, 3]. Wenig untersucht ist dagegen die Rolle, welche die Prostanoide innerhalb der beobachteten geschlechtsspezifischen Unterschiede spielen. Neue Veröffentlichungen zeigen eine unterschiedliche Regulation der Prostanoidbiosynthese in Tiermodellen von Entzündungsreaktionen und ebenfalls in der Leukotrienbiosynthese in menschlichen weiblichen und männlichen Leukozyten, einer weiteren Klasse von Lipidmediatoren [4, 5]. Aufgrund dieser Ergebnisse wurde im ersten Teil der Arbeit die Bildung der Prostanoide sowohl in menschlichem Vollblut als auch in frisch daraus isolierten Zellen untersucht. Die Analyse der Bestandteile des Vollblutes ergab zunächst eine grundsätzlich erhöhte Zellzahl an Lymphozyten und neutrophilen Granulozyten in weiblichem Blut, wohingegen Monozyten in höherer Anzahl in männlichem Vollblut zu finden waren. Langzeitinkubationen (24 Stunden) mit verschiedenen stimulierenden Agenzien wie Lipopolysaccharid (LPS), dem Ca^{2+} Ionophor A23187 oder *N*-Formyl-Methionyl-Leucyl-Phenylalanin (fMLP) resultierten in signifikant erhöhten Prostanoidspiegeln, vorwiegend PGE_2, in männlichen Proben im Vergleich zu weiblichen. Die beobachtete Erhöhung der Prostanoide in den männlichen Blutproben wurde nicht durch die Vorinkubation mit Sexualhormonen vor der eigentlichen Stimulation mit LPS beeinflusst und war unabhängig von der COX-2 Protein- und mRNA-Expression, die in isolierten Monozyten und mononukleären Zellen des peripheren Blutes (PBMC) untersucht wurde. Des Weiteren konnte eine Beteiligung von COX-1 und von der Ionophor A23187-induzierten AA Freisetzung in polymorphkernigen Leukozyten (PMNL) ausgeschlossen werden. In Kurzzeitinkubationen (bis 30 min) von humanem Vollblut und PMNL wurde ebenfalls kein geschlechtsabhängiger Unterschied der Prostanoidbiosynthese beobachtet. Mit SW033291, einem spezifischen Inhibitor der 15-Prostaglandindehydrogenase (15-PGDH) wurde der Einfluss auf den Prostanoidabbau untersucht. Die Ergebnisse aus Kurzzeit-untersuchungen (6 Stunden) stützen die Vermutung einer Beteiligung von 15-PGDH an der Regulation der Prostanoidspiegel. Nach Vorbehandlung weiblichen Blutes mit dem Inhibitor wurde die PGE_2-Menge auf das gleiche Niveau angehoben, das in männlichem Blut ohne Inhibitorvorbehandlung festzustellen war. Zusätzlich wurden PBMC und PMNL aus humanem Vollblut isoliert und entweder getrennt oder nach Koinkubation stimuliert, um Einflüsse von Zell-Zell-Interaktionen auf die Prostanoidbiosynthese zu untersuchen. In Koinkubationen von männlichen Zellen konnte im Vergleich zu weiblichen eine verstärkte Bildung der Prostanoide beobachtet werden. Zusammenfassend kann gesagt werden, dass die zugrundeliegenden Mechanismen, die nach 24 stündiger Stimulation mit LPS, A23187 oder fMLP zu dem geschlechtsspezifischen Unterschied der Prostanoidbiosynthese in humanem Vollblut führen, nicht vollständig aufgeklärt werden konnten. Dennoch zeigen die

Ergebnisse eine Beteiligung des zeitabhängigen Prostanoidabbaus und einer unterschiedlich ausgeprägten Biosynthese durch Zell-Zell Interaktionen nach Stimulation als mögliche Ursachen.

Neben COX und den Prostanoiden, spielen die 5-LO und die LTs eine wichtige Rolle im Entzündungsgeschehen. Die 5-LO wandelt AA zu dem Produkt 5(*S*)-hydroperoxy-6-*tans*-8,11,14-*cis*-eicosatetraensäure (5-HpETE) um, welches von der 5-LO weiter zu LTA_4 metabolisiert wird [6]. Nach Zellaktivierung translozieren 5-LO und die zytosolische Phospholipase (PL)A_2 zur Kernmembran, wo sie zusammen mit dem 5-LO aktivierenden Protein (FLAP) für die Biosynthese der LTs verantwortlich sind [7]. Kürzlich veröffentlichte Ergebnisse identifizierten den pflanzlichen Inhaltsstoff Embelin als potenten 5-LO Inhibitor [8]. Embelin wurde in dieser Studie als Leitsubstanz verwendet und dessen 1,4-Benzochinonstruktur systematisch modifiziert, so dass drei unterschiedliche Substanzserien synthetisiert werden konnten: Serie (I) enthielt 16 1,4- und 1,2-Benzochinone, die in 3-Position mit einer *n*-Alkylkette mit 8 bis 15 Kohlenstoffatomen substituiert wurden, Serie (II) enthielt fünf 1,2-Benzohydrochinone mit *n*-Alkylketten von 11 bis 13 Kohlenstoffen in 3-Position und Serie (III), bestehend aus 15 1,2-Benzohydrochinonen mit eher sperrigen aromatischen Resten in 4-Position. Serie (I) wurde je nach Hydroxylierungsmuster des Benzochinonkerns nochmals in A, B, C und D unterteilt. Die Untersuchung des Potentials der Substanzen die 5-LO in zellulären und zellfreien Experimenten zu hemmen, identifizierte EA-110C aus der C-Serie als potenteste Substanz mit IC_{50}-Werten im nanomolaren Bereich (IC_{50}= 50 - 120 nM). In Serie (II) wurde bei den vielversprechendsten Substanzen aus Serie (I) das 1,4-Benzochinongerüst zu einem 1,2-Benzohydrochinongerüst reduziert und deren Fähigkeit die 5-LO zu hemmen in zellfreien und zellbasierten Experimenten analysiert. Die reduzierte Form der Substanz EA-110C (EA-110C RED) zeigte erneut IC_{50}-Werte im nanomolaren Bereich (IC_{50} = 30 - 60 nM) was ein 1,2-Benzochinon/-Benzohydrochinongrundgerüst kombiniert mit einer *n*-Alkylkette mit 13 Kohlenstoffatomen in 3-Position also optimale Struktur auszeichnete um mit der 5-LO Produktbildung zu interagieren. Die Untersuchung in Entzündungsmodellen am Tier bestätigte die Effektivität *in vivo*. Weitere Untersuchungen deckten eine nicht-kompetitive Hemmung auf, die zusätzlich durch Docking Simulationen gestützt wurde. Diese zeigten eine sehr wahrscheinliche Bindung von EA-110C RED auf der gegenüberliegenden Seite des AA-Substratkanals. In Serie (III) wurden die zwei potentesten Substanzen F-XII und F-XVI im Detail untersucht. Beide Substanzen wiesen eine überaus potente Hemmung von 5-LO mit IC_{50}-Werten im nanomolaren Bereich in zellbasierten (IC_{50} F-XII = 70 nM; F-XVI = 60 nM) und in zellfreien Experimenten (IC_{50}: F-XII und F-XVI = 20 nM) auf. Die Hemmung der 5-LO war reversibel, unabhängig von der zugesetzten Substratmenge (AA) und nicht hauptsächlich durch Radikalfänger- oder antioxidative Eigenschaften vermittelt. Docking Simulationen deuteten auf eine Bindung des 1,2-Benzohydrochinonkerns an die Aminosäure Asp-166, die Teil einer verbindenden Salzbrücke zwischen der C-terminale katalytische Domäne und der N-terminale C2-ähnliche Domäne ist. Die Hemmung der 5-LO war darüber hinaus unabhängig von zellulären Signalen, die für die 5-LO Aktivierung notwendig sind. Die erhaltenen Ergebnisse aus dem zweiten Teil der vorgelegten Arbeit identifizierten die Benzohydrochinone F-XII und F-XVI als außerordentlich potente, direkte Inhibitoren der 5-LO vom sogenannten „non-redox-type“ oder „novel type“ mit hoher Selektivität in nanomolaren Konzentrationen, was in Experimenten mit Vollblut und in einem Zymosan-induzierten Peritonitis Tiermodell bestätigt werden konnte.

1 INTRODUCTION

1.1 Acute inflammation and resolution

Inflammation is defined as a complex biological process involving microbial invasion, trauma or irritation by toxins or non-degradable particles (e.g. asbestos) that causes tissue damage accompanied by the five typical pathological phenomena: *tumour* (swelling), *calor* (elevated temperature), *rubor* (redness), *dolor* (pain) and *functio laesa* (loss of function). Under normal conditions, acute inflammation is understood as a beneficial reaction of the host innate immune system to erase invading pathogens and restore tissue homeostasis. If dysregulated or unresolved, inflammation can become detrimental and progress to a chronic status, driving a wide range of diseases like atherosclerosis, intestinal bowl diseases, diabetes and asthma [9, 10]. Invading pathogens and their secreted products are recognized by soluble receptors (e.g. nucleotide binding oligomerisation domain(NOD)-like receptors) or cell-surface receptors (e.g. toll-like receptors (TLR)) leading to the release of mediators like histamine, eicosanoids, cytokines and chemokines by mast cells and macrophages. The secretion of histamine and leukotrienes lead to an increase of vascular permeability, whereas formation of prostaglandins and nitric oxide (NO) leads to vasodilation [11-13]. Secretion of pro-inflammatory cytokines like tumor necrosis factor (TNF) and interleukins promotes the recruitment of neutrophils from the circulating blood to the site of infection or inflammation [14]. Following chemotactic factors (e.g. LTB_4, fMLP) neutrophils eventually interact with endothelial cells, initiating their extravasation into the inflamed tissue to kill pathogens directly by engulfment or by degranulation releasing toxic granule contents like reactive oxygen species (ROS), proteinases and antibiotic proteins [12, 13]. Migration of classical monocytes to the inflamed tissue typically occurs after neutrophil recruitment with a maximum after 72 to 96 h.

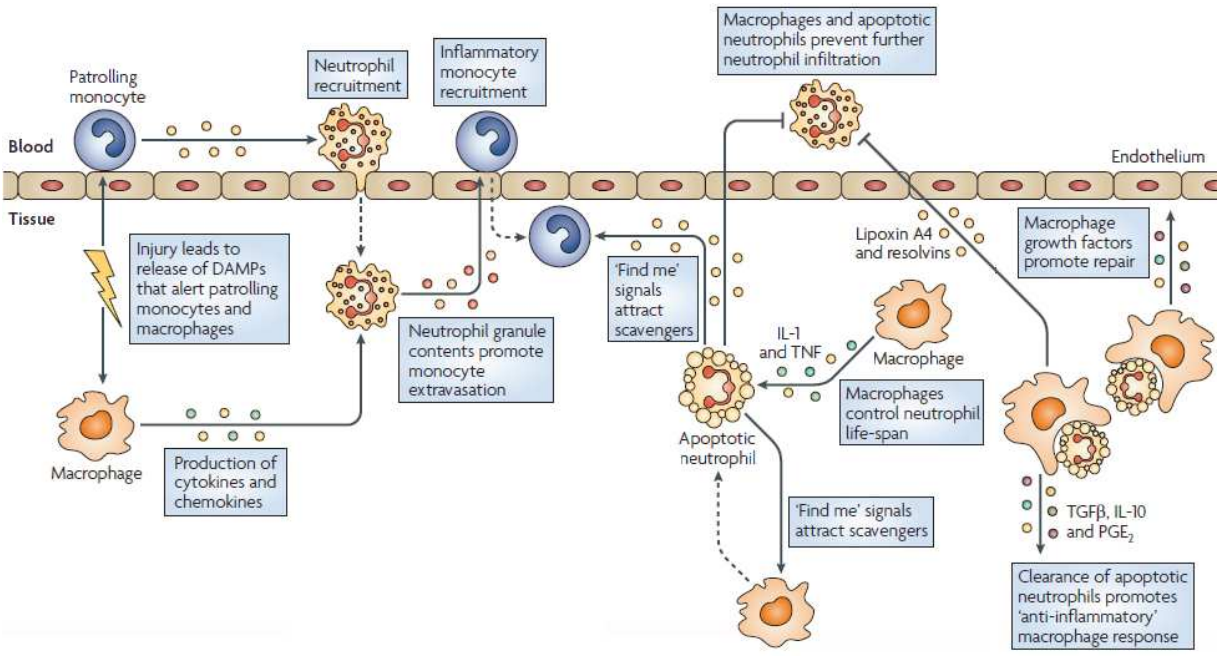

Figure 1.1: The inflammatory reaction and the resolution phase. Modified from Soenhlein et al. [14].

At sites of inflammation, monocytes can differentiate to macrophages or dendritic cells, producing mediators like TNFα and NO to enhance microbial clearance [15, 16]. After successful elimination of the pathogens, neutrophils undergo apoptosis thereby signaling their own clearance by macrophage-driven phagocytosis and additionally prompt macrophage differentiation to an anti-inflammatory phenotype promoting wound healing [17, 18]. However, these processes not only eradicate pathogens but can also cause collateral damage of host tissue [19, 20]. Therefore, resolution of inflammation is a complex and actively regulated process, which also involves soluble mediators like specialized pro-resolving mediators (SPM), namely lipoxins, resolvins, maresins and protectins derived from AA and the omega-3-fatty acids eicosapentaenoic acid (EPA) and docosapentaenoic acid (DHA) [21]. Already in the early stages of inflammation activated neutrophils start producing lipoxins together with endothelial cells or platelets by transcellular biosynthesis, switching from a pro- to an anti-inflammatory response [22, 23]. SPMs, reduce neutrophil infiltration, enhance the phagocytic capability of macrophages, cause recruitment of anti-inflammatory monocytes and have wound healing properties [21, 24-26]. Furthermore, COX-2 produces 15deoxy-PGJ_2 (15d-PGJ_2) via PGD_2 exerting similar effects as the lipoxins, e.g. promotion of neutrophil apoptosis and dampening of monocyte migration [18]. In contrast, to other classical nonsteroidal anti-inflammatory drugs (NSAID) acetylsalicylic acid (ASA) initiates the formation of so called aspirin-triggered epimeric forms of SPMs by COX-2 or the P450 pathway exhibiting pro-resolving activities. Thereby, ASA dampens the inflammatory reaction and supports the resolution as well [24]. In sum, acute inflammation and resolution are highly complex processes, where mediators and cells have to function together in a fine tuned clockwork to eliminate invading pathogens, prevent potential necrotic damage and restore tissue integrity and homeostasis.

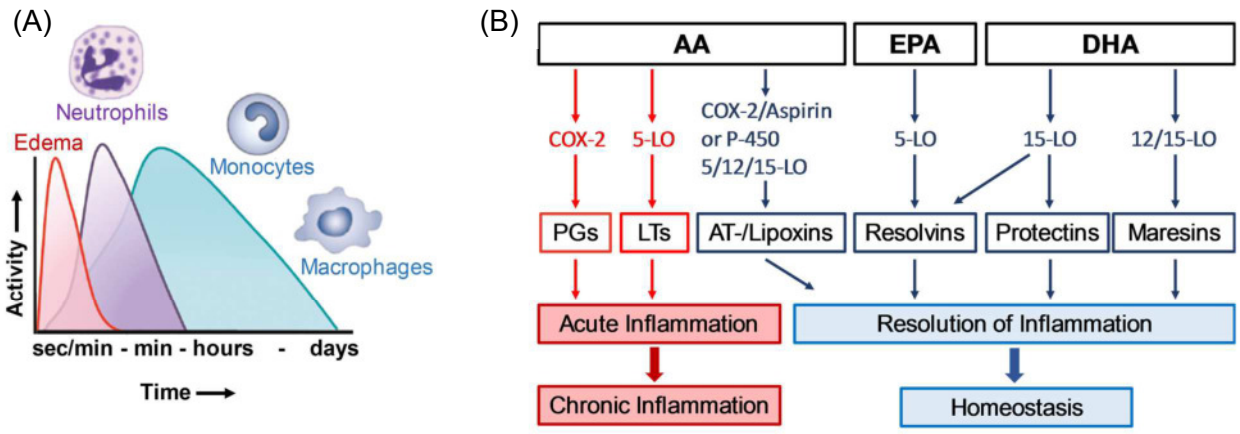

Figure 1.2: (A) Time course of inflammation and resolution, (B) Overview of selected lipid mediators and their actions regarding inflammation and resolution. Modified from Serhan et al. [21].

1.1.1 Chronic inflammation and related diseases

When resolution fails, inflammation persists and escalates to chronic conditions leading to tissue degeneration and can finally peak in chronic diseases like atherosclerosis, asthma, inflammatory bowel diseases, rheumatoid arthritis and cancer [10]. Although the involvement of inflammatory pathways in the initiation of chronic inflammatory diseases is well-established,

the specific role by which inflammation contributes to their pathogenesis is not fully understood. The persistence of inflammatory stimuli of an exogenous origin often entails non-resolving inflammation. In fact, in many chronic infections not the toxins produced by the foreign organisms are responsible for the inflammatory tissue damage but the host response itself [10, 27]. Impaired recruitment of neutrophils or the disability to undergo apoptosis can accelerate inflammatory conditions. Moreover, not fully cleared apoptotic neutrophils undergo secondary necrosis generating pro-inflammatory signals due to the release of intracellular products. These defects in resolution and the deficiency to clear phagocytic macrophages into lymphatic drainages are linked to systemic lupus erythematosus [10, 17, 18]. Additionally, resolution fails when the production and release of soluble mediators like SPMs is deficient or inhibited [21]. Another important player in inflammatory conditions is the transcription factor NF-κB, regulating the formation of pro- vs. anti-inflammatory interleukins. An enhanced NF-κB activation can lead to chronic and serious inflammatory diseases, since an overactivation of NF-κB is linked to atherosclerosis, asthma and ulcerative colitis [28, 29]. Especially in rheumatoid arthritis an excessive secretion of interleukins (mainly IL-17) is obvious that causes degradation of the synovial joint tissue by the release of oxidants and proteases [30]. Furthermore, prostaglandins which exert important roles in the onset of acute and chronic inflammation, and partially also in the resolution phase, can additionally prolong inflammation by acting as “cytokine amplifier”. PGE_2 can enhance the expression of pro-inflammatory cytokines in macrophages and stimulate the production of leukocyte attracting chemokines [31]. Additionally, failure in tissue regeneration and in reconstitution of the vasculature can result in atrophy and fibrosis leading to loss of function of the affected organ [32].

1.1.2 Chronic inflammation and the development of cancer

Epidemiological data indicate that over 25% of all cancer are related to chronic infections or other types of unresolved inflammation [33]. Both, persistent infection and sterile chronic inflammation are triggers for the development of cancer, seen in infections with *Helicobacter pylori* linked to gastric cancer or inflammatory bowel diseases linked to colon cancer [34, 35]. Even though in many cases tumor cells use inflammatory responses to promote their own growth and survival, not all chronic inflammatory diseases lead to the susceptibility to develop cancer (e.g. rheumatoid arthritis or psoriasis) [34, 36]. Inflammation plays an important role in the initiation of tumor growth due to the release of ROS and therefore the promotion of DNA alterations [37, 38]. The tumor develops due to an enhanced expression of cytokines and chemokines in cancer cells, attracting inflammatory leukocytes to the site of malignancy where they release cytokines themselves, fostering the establishment of an inflammatory microenvironment [36, 37, 39]. During the progression stage, COX-2 is found among other enzymes highly expressed producing PGE_2, which represents an angiogenetic factor and sustains proliferation [31]. Moreover, a high number of tumor associated macrophages (TAM) together with regulatory T (Treg) cells suppress the antitumor response of the adaptive immune system promoting cell survival, angiogenesis, tumor growth and metastasis [36, 37, 39, 40].

1.1.3 Toll-like receptor mediated signaling

Upon pathogen invasion toll-like receptors (TLR) recognize distinct microbial components (pathogen-associated molecular patterns; PAMPs) and activate an intracellular signaling cascade leading to the formation of pro-inflammatory cytokines and chemokines. TLRs are pattern-recognition receptors (PRR) that are expressed constitutively, mainly on immune cells, including macrophages, monocytes and dendritic cells. To date, 13 TLRs have been identified in mammals, 10 in humans and 13 in mice whereas TLR4 is the most intensely studied [41]. The TLRs can be divided in two subfamilies, depending on their localization and the PAMPs they recognize. TLR1, TLR2, TLR4, TLR5, TLR6 and TLR11 are expressed on the cell surface and recognize bacterial membrane components such as lipids and lipoproteins, whereas TLR3, TLR7, TLR8 and TLR9 are localized in intracellular components (e.g. endosomes, endoplasmic reticulum) recognizing microbial nucleic acids. TLR4 is able to recognize a variety of different ligands including lipopolysaccharide (LPS) from the outer membrane of gram-negative bacteria [42]. TLRs are type I integral membrane glycoproteins, characterized by an extracellular domain containing leucine-rich-repeat (LRR) motifs and an intracellular Toll/Interleukin 1 receptor (TIR) domain. Following PAMP binding, the TLRs form active homo- or heterodimers (TLR2/TLR1, TLR2/TLR6) to induce signal transduction. TLR4 activation requires further association with the soluble protein myeloid differentiation factor 2 (MD-2) with the extracellular LRR domain. For LPS activation, LPS has to bind to the plasma protein LPS binding protein (LPB) and is then provided via the cluster of differentiation 14 protein (CD14) to the MD-2/TLR4 complex [43, 44]. Formation of cytokines and chemokines follows two distinct signaling pathways: The myeloid differentiation primary response gene 88 (MyD88)-dependent pathway used by all TLRs except TLR3 which is considered to mediate signaling in the early phase or the MyD88-independent/ TIR domain-containing adaptor inducing IFN-β (TRIF)-dependent pathway used by TLR3 and TLR4 observed with delayed kinetics. Both signaling cascades result in the activation of NF-κB and the formation of pro-inflammatory cytokines (TNFα, IL-6, IL-8, IL-1β) and the expression of COX-2 or in the activation of TBK1 directly activating the interferon response factor 3 (IRF-3) and thereby inducing the transcription of type I interferons (INF-α/β) (Figure 1.3) [42, 44]. Upon LPS stimulation, the delay in NF-κB and IRF-3 activation in the MyD88-independen/ TRIF-dependent pathway is considered to be due to the internalization of the LPS/CD-14/MD-2/TLR4 assembly. Endocytosis creates an early endosome, where the association with the TIRAP/MyD88 complex is disrupted and paves the way for interactions with TRAM/TRIF complex [45, 46].

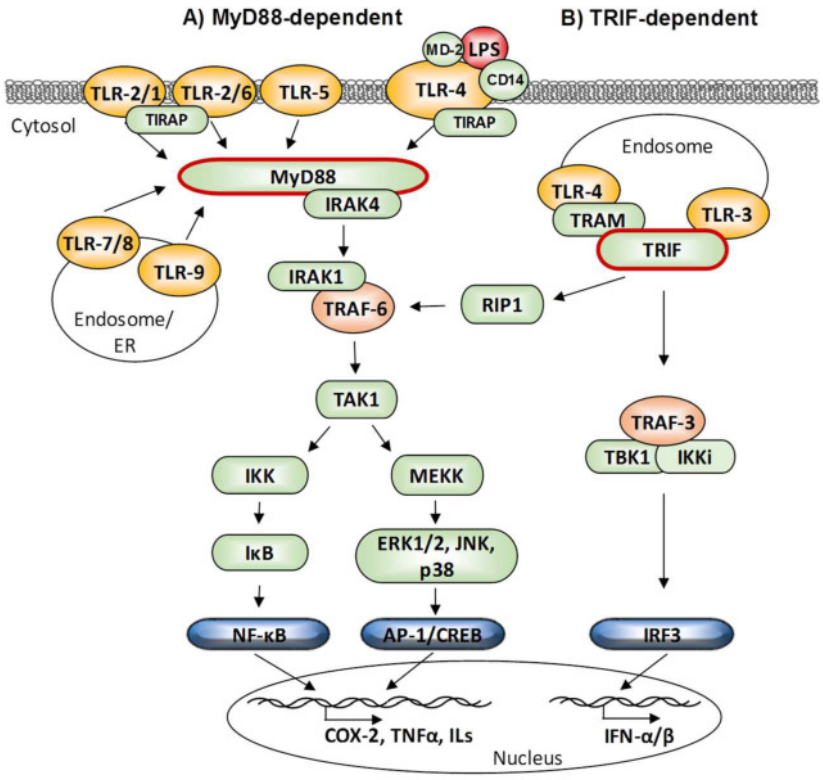

Figure 1.3: TLR-signaling. A) MyD88-dependent, B) TRIF-dependent signaling. TIRAP, TIR-associated protein; IRAK, Interleukin 1 receptor (IL-1R)-associated kinase; TRAF, tumor necrosis factor receptor-associated factor; TAK1, TGF-β-activated kinase; MEKK, mitogen-activated protein kinase (MAPK) kinase kinase; ERK1/2, extracellular signal-regulated kinase; JNK, c-Jun N-terminal kinase; AP-1, activator protein 1; CREB, cAMP response element-binding protein; IKK, inhibitor of κB (IκB) kinases; TRIF, TIR domain-containing adaptor inducing IFN-β; TRAM, TRIF-related adaptor molecule; RIP1, receptor-interacting protein 1; TBK1, TRAF family member-associated NF-κB activator (TANK)-binding kinase 1; IRF3, interferon response factor 3.

1.2 The arachidonic acid cascade

Eicosanoids and docosanoids are formed by conversion of ω3 and ω6 20- and 22-carbon fatty acids, whereas arachidonic acid (AA) and docosahexaenoic acid (DHA) play crucial roles. AA is stored esterified in phospholipids in cellular membranes and is released by phospholipases (PLAs) allowing the conversion to the diverse eicosanoids. Eicosanoids represent a family of hormonally active mediators, which exert autocrine and paracrine functions. They can be divided into prostanoids produced by cyclooxygenases, leukotrienes and lipoxins produced by lipoxygenases and epoxy and dihydroxy fatty acids formed by the cytochrome P450 system [47].

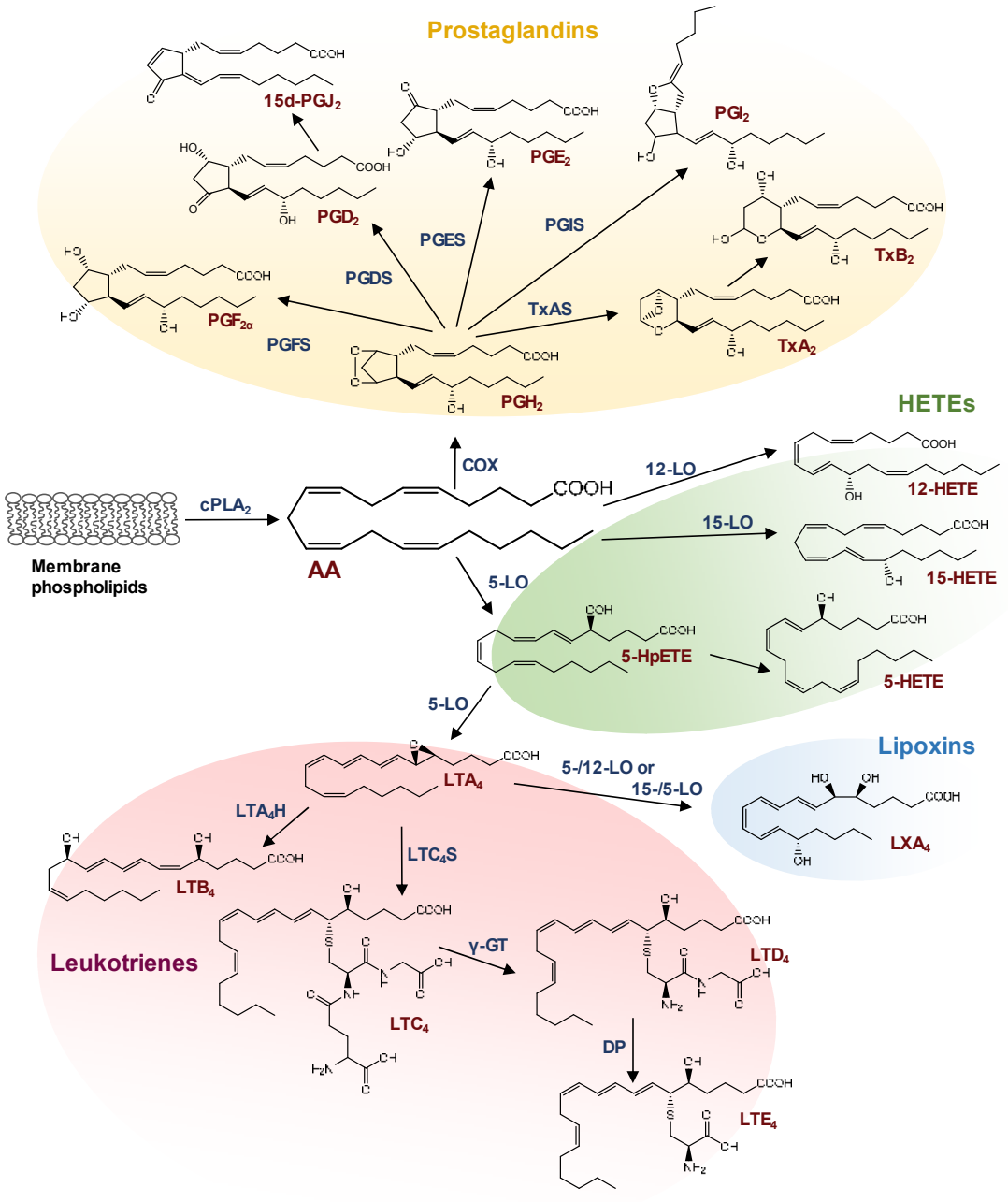

Figure 1.4: The arachidonic acid cascade. The biosynthetic pathway of eicosanoids, modified after Nakamura, M. et al. [141]. PGES, PGE_2 synthase; PGDS, PGD_2 synthase; PGFS, $PGF_{2\alpha}$ synthase; PGIS, PGI_2 synthase; TxAS, TxA_2 synthase; LTA_4H, LTA_4 hydrolase; LTC_4S, LTC_4 synthase; γ-GT, γ-glutamyl-transpeptidase; DP, dipeptidase.

1.2.1 Cyclooxygense-1/2 expression and protein function

In the 1970s and 1980s, cyclooxygenase (COX) enzymes were purified and cyclooxygenase and hydroperoxidase activities were identified. COXs are present in nearly every cell type of the human organism and are the key enzymes in the formation of prostaglandins, prostacyclins (PIs) and thromboxanes (Txs), together referred to as prostanoids. Formation of prostanoids occurs after the release of AA from cell membrane phospholipids via PLAs in two steps: AA is first converted to prostaglandin G_2 (PGG_2) and in a second step to the intermediary

prostaglandin endoperoxide H_2 (PGH_2) followed by formation of the single prostanoids via terminal synthases. Prostanoids are involved in a wide range of physiological and pathological processes including regulation of inflammation, fever and pain, platelet aggregation, ovulation and maintenance of renal function [48]. Two distinct COX isoforms have been described, the constitutively and ubiquitously expressed COX-1 exerting housekeeping functions like platelet aggregation, renal water balance and gastric cytoprotection and COX-2, induced as a response to pro-inflammatory stimuli like cytokines, endotoxins and mitogens involved in inflammatory diseases and cancer [49, 50]. However, constitutive COX-2 expression could be shown as well, for example in the brain, the kidney and the female reproductive systems and COX-2 could also be found contributing to gastric mucosal defense [51, 52]. The two isoforms arise from different genes but share 60% sequence homology. The gene for COX-1 is located on chromosome 9, is approximately 22 kb in length and contains 11 exons, whereas the gene for COX-2 is located on chromosome 1, is about 8.6 kb in length and contains 10 exons. In contrast to COX-1 mRNA, COX-2 mRNA is relatively unstable [48]. The translated enzymes contain three domains, including the epidermal growth factor-like (EGF-like), membrane binding, and catalytic domain [53], also see figure 1.5 after Smith et al [54].

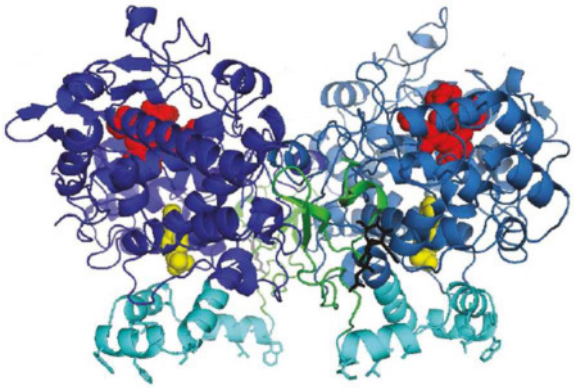

Figure 1.5: Ribbon diagram of ovine COX-1 with flurbiprofene bound to the active site. Epidermal growth factor-like (EGF) domain is shown in green, membrane binding (MBD) domain in cyan, heme group at the peroxidase active site in red, catalytic domains in dark and light blue, flurbiprofene in yellow. Saccharide unit of glycosylation is shown in the ball-and-stick form in black. Modified after Smith et al. [54].

Both are located in the endoplasmic reticulum (ER) and the nuclear envelope, whereas COX-2 is reported to be localized to a greater extend at the nuclear envelope than in the ER [55, 56]. The constitutive expression of COX-1 in most tissues makes transcriptional studies difficult, but investigations revealed a preferential expression in specific cells like vascular endothelial cells, monocytes or platelets and cells undergoing development or mimicking developmental processes [47]. Nevertheless, the expression of COX-1 can be induced as well, for example via shear stress or growth factors in vascular endothelial cells or via phorbol esters (PMA) in monocytes [48, 57]. In contrast to COX-1, several potential transcriptional regulatory elements have been identified in the promotor region of COX-2, e.g. two NF-κB sites. After LPS stimulation COX-2 expression is regulated in monocytes and macrophages via TLR4 involving ERK1/2, JNK, and p38 MAPK together with NF-κB. Upon stimulation with inflammatory cytokines (e.g. IL-1β) JNK and p38 mediate the expression of COX-2, whereas the active proto-oncogene Ras requires ERK1/2 activation to mediate COX-2 expression [48].

1.2.1.1 Prostanoid formation

Formation of the precursor PGH_2

AA, bound at the sn2 position of glycerophospholipds in cellular membranes, is released via activated phospholipases, mainly the cytosolic (c) or secretory (s) PLA_2, converted by COX to PGH_2 and further processed to distinct prostanoids by specific synthases. The COX enzymes are active as homodimers and are bifunctional catalysing both a cyclisation and a subsequent reduction. The peroxidase reaction occurs at a heme-containing active site, whereas the cyclooxygenase reaction occurs in a hydrophobic channel [54]. First, released AA is bisoxygenized with two molecules O_2 to PGG_2. Second, the 15-hydroperoxyl group of PGG_2 is subsequently reduced to PGH_2 in a peroxidase reaction, where other peroxidases like glutathione peroxidase may contribute. The COX enzymes require oxidation from the resting state to the catalytically active form. This oxidation is achieved by alkyl hydroperoxides or peroxynitrite formed by inflammatory cells [58]. During activation, an electron is transferred from the peroxidase heme iron to Tyr-385 generating a tyrosyl radical, which is able to remove the 13-pro-*S* hydrogen from AA bound in the oxygenase active site. Thereby, a free radical is created, which allows the regioselective addition of oxygen at the C11 atom. The caused hydroperoxid radical forms a cyclic peroxide with C9 leaving an adjacent carbon radical leading to a cyclopentane ring, in which a bond is formed between C8 and C12. After addition of the second O_2 molecule in C15, another peroxyl radical is created, which is reduced by a hydrogen atom provided by Tyr-385 to from PGG_2. Subsequently, the peroxidase activity reduces the 15-hydroperoxyl by two electrons to PGH_2 containing a hydroxyl group [54, 59]. In contrast to COX-2, COX-1 requires a higher concentration of peroxides to become activated and to sustain the formation of PGG_2 and furthermore, needs higher concentrations of AA (> 10 µM AA) than COX-2 to initiate the formation of PGH_2 [50]. Originating from PGH_2 the prostanoids are formed by specific synthases: PGD_2 by the hematopoietic and the lipocaline-type PGD synthase (H-/L-PGDS), PGE_2 by microsomal (m) PGE synthase-1/2 (mPGES-1/2) and the cytosolic (c) PGES, $PGF_{2\alpha}$ by the PGF synthase (PGFS), PGI_2 by PGI synthase (PGIS) and TxA_2 by the TxA synthase (TxAS) [54].

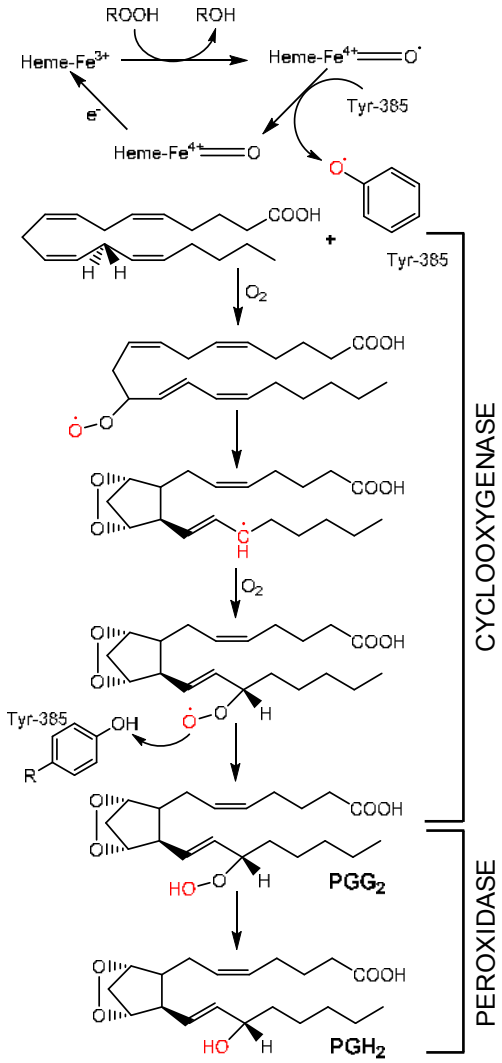

Figure 1.6: Proposed reaction mechanism of PGH_2 formation, modified after Smith, W. L. [54], Kim, S. F. [58] and Seo, M. J. et al. [60].

PGD_2

PGD_2 is formed via the isomerization of the endoperoxide of PGH_2 to a 9-hydroxy and 11-keto group by H- or L-PGDS. H-PGDS is predominantly found in mast cells, dendritic cells, and Th2 cells, whereas L-PGDS is mostly found in tissue of the heart, testis or kidney, and monocytes after LPS treatment [54, 60]. PGD_2 is an important mediator in allergic rhinitis and asthma, which exerts its biological activity via two GPCRs, DP1 and DP2 [61]. Eventually, dehydration of PGD_2 leads to the formation of 15d-PGJ_2 in various inflammatory tissues, which modulates the synthesis of pro-inflammatory cytokines [62].

PGE_2

The conversation of PGH_2 to PGE_2 is mediated by three different synthases, mPGES-1/-2 and cPGES. mPGES-2 and cPGES are constitutively expressed with unclear importance, whereas mPGES-1 is an inducible key enzyme simultaneously expressed with COX-2 upon inflammatory stimuli [63-65]. mPGES-1 is a member of the membrane-associated proteins in eicosanoid and glutathione metabolism (MAPEG) family, requires GSH as cofactor and is active as a homotrimer [66, 67]. Isomerization of the 9,11-endoperoxide of PGH_2 to a 11-hydroxy and 9-keto group via GSH forms PGE_2. PGE_2 is the most abundant product of COX challenged with AA and plays a pivotal role in inflammatory reactions, inflammatory diseases, cancer and in resolution of inflammation via its four distinct receptor subtypes EP1-4 [61, 68].

$PGF_{2\alpha}$

Formation of $PGF_{2\alpha}$ can be achieved by two electron reduction of the PGH_2 peroxide or additionally, by the reduction of the 9-keto group of PGE_2 or the 11-keto group of PGD_2. PGFS enzymes are classified as aldo-keto reductases, containing a NADPH-dependent oxido-reductase activity [54]. $PGF_{2\alpha}$ is a widely distributed prostaglandin in various organs and mediates contraction of smooth muscle in the vasculature, the bronchial tubes and most important in the human uterus via the $PGF_{2\alpha}$ receptor (FP).

PGI_2

The PGIS is a member of the cytochrome P450 family (CYP8A1) where heme is bound via the thiolate anion of Cys-441 to the iron. The initial step of the PGI_2 synthesis seems to be a radical reaction involving the heme iron with subsequent cyclisation and double bond formation [54, 60]. PGIS is preferentially co-localized with COX-2 in the nuclear envelope and plays a protective role in cancer development [69, 70]. PGI_2 is primarily produced by endothelial cells and mediates vasodilatory, anti-thrombotic and atheroprotective effects via the PGI_2 receptor (IP), maintaining cardiovascular homeostasis.

TxA_2

Like the PGIS, the TXAS is a member of the P450 family with a heme bound iron. TxA_2 is synthesized by creation of a radical and subsequent formation of the characteristic oxirane ring. Besides synthesis of TxA_2, TXAS catalyzes the formation of 12-hydroxy-heptadeca-trienoic acid (12-HHT) from PGH_2 possessing wound healing properties [60, 61, 71]. Platelets release TxA_2 formed by COX-1 and TXAS, whereas in macrophages and monocytes COX-2 can be involved. The pro-thrombotic vasoconstrictor TxA_2 plays a crucial role in regulation of cardiovascular homeostasis and platelet aggregation via the TP receptor expressed in thymus, spleen, kidney, platelets, endothelium and smooth muscle of vasculature [72].

1.2.1.2 COX in inflammatory diseases and cancer

Since prostanoids play a pivotal role in inflammatory reactions, persistent activation of COX-2 is linked to the development of numerous inflammatory diseases, e.g. rheumatoid arthritis, colitis, asthma and allergic conditions [31, 54]. As mentioned above, COX-2 and mPGES-1 overexpression is also found in many types of cancer, including colorectal, gastric and breast cancer [48]. Overexpression of both enzymes mediates elevated levels of PGE_2, which can exert immunosuppressive and angiogenetic effects. An increase in PGE_2 levels entails a decrease in PGD_2 simultaneously decreasing the formation of anti-inflammatory 15d-PGJ_2 [62]. The treatment with NSAIDs has been shown to reduce cancer risk and cancer related death via inducing apoptosis or cell cycle rest, thereby decreasing cellular proliferation [73, 74]. Although, cyclooxygenases are not only involved in the onset of inflammation but also in resolution and wound healing, treatment with anti-inflammatory drugs like NSAIDs can prolong the inflammation and delay the resolution.

1.2.2 Sex differences in immunity and inflammation

Already in the 1960s a differential immune response between male and female children to bacterial infection has been observed [75]. Up to now it is known that female individuals are more resistant to certain bacterial infections but suffer from a higher incidence of autoimmune diseases, for example rheumatoid arthritis, asthma or systemic lupus erythematosus (SLE), whereas males are more susceptible to infections, sepsis/septic shock and atherosclerosis. This circumstance is based on different mechanisms of the innate and adaptive immunity of males and females, also called the sexual dimorphism in immunity [76, 77]. In infections, the higher immune response of females results in the accelerated clearance of the pathogens but also increases the risk of developing an autoimmune or inflammatory disease. The number and activity of immune cells differ between the sexes and so the production of cytokines. Whereas the number of T lymphocytes is lower in males compared to females, the number of monocytes is higher producing elevated levels of pro-inflammatory cytokines (IL-1β, IL-6, IL-12 and TNFα) in males. In contrast, granulocytes are found in higher numbers in females and they exert an increased phagocytic effectivity as compared to males [2, 78]. Moreover, antigen presenting cells (APCs) are more efficient in females resulting in an increased activation of naïve T cell differentiation to T helper 1 cells [79]. The sex-specific difference in immune responses involves effects of the sex hormones. Both, the estrogen receptor and the androgen receptor are found in numerous cell types, including T and B cells, dendritic cells, macrophages, and endothelial cells [79]. Besides the capability to modulate neutrophil activity and the T cell expression, estrogen decreases the formation of TNFα, IL-6 and IL-12 and is able to increase the nitric oxide (NO) synthase. Additionally, estrogen enhances the production of antibodies by B cells (IgG and IgM) and has been reported to promote the expression of mediators responsible for B cell survival. Thus, strengthening the adaptive immune response, these mechanisms eventually lead to the induction of autoantibody formation and elevate the susceptibility to autoimmune diseases [2]. Also, the involvement of estrogen in the regulation of ROS mediated damages and expression of antioxidant enzymes together with the ability to decrease low-density lipoprotein (LDL) serum levels are discussed effects of atherosclerotic protection [80, 81]. However, recent findings suggest a cardioprotective role of androgens in

men but not in woman [82, 83] and show that testosterone improves vasodilation [84]. Regarding the difference in the immune responses to pathogens of males and females, the expression of TLRs and associated proteins, as well as the COX-2 pathway was evaluated intensively in animal models and in human diseases with inconsistent results, however indicating a rather higher expression level of TLR4 and COX-2 in male individuals [85-87]. Besides, differential expression of lipid mediators between sexes could be determined. The predominant expression of leukotrienes in female monocytes and neutrophils compared to males seems to be regulated by androgens via activation of ERK1/2 and a different subcellular distribution of the 5-LO [4, 88]. Taken together, sex plays a crucial role in the immune response and the severity of certain diseases. However, little is known about the mechanisms underlying these differences. The dimorphism has to be elucidated in further studies to enlighten the understanding of the underlying mechanisms, and to be able to treat male and female individuals with optimal customized pharmacotherapy.

1.2.3 Human lipoxygenases

Besides COX enzymes the lipoxygenases (LOs) play a prominent role in inflammatory conditions, diseases and cancer. The LO superfamily consists of lipid-peroxidizing enzymes that catalyze the dioxygenation of polyunsaturated fatty acids containing a series of cis double bonds. Six human LOs are known, 5-LO, 12-LO, 12/15-LO, 15-LO type 2, 12(*R*)-LO and epidermal LO, named after the position of oxygen insertion. Except for the 12(*R*)-LO the stereochemistry of the oxygenated carbon is *S* [89].

1.2.3.1 5-lipoxygenase expression and regulation of activity

In 1976, an enzyme converting AA to 5(*S*)-hydroperoxy-6-*trans*-8,11,14-*cis*-eicosatetraenoic acid (5-HpETE) in rabbit polymorphonuclear leukocytes (PMNL) has been discovered and soon its significance in human became evident [90, 91]. The 5-lipoxygenase is one of the six human lipoxygenases mainly found in leukocytes, responsible for leukotriene and lipoxin formation [92]. Upon leukocyte activation, AA is released by $cPLA_2$ from cellular membranes and delivered to 5-LO by the 5-LO activating protein (FLAP). Subsequently, the leukotrienes are biosynthesized via 5-H(p)ETE forming the unstable epoxide LTA_4, which is further converted to LTB_4 by enzymatic hydrolysis or to the cysteinyl LTs (cys-LTs) LTC_4, LTD_4 and LTE_4 by addition of GSH [93]. LTs promote chemotaxis of leukocytes and increase vascular permeability, driving hypersensitivity reactions and allergic responses, like allergic rhinitis and asthma through distinct GPCRs [94, 95]. Furthermore, they are involved in the development of atherosclerosis and cancer [96, 97]. 5-LO expression is primarily restricted to leukocytes and the promoter region shows typical properties of a housekeeping gene, which is constitutively expressed. The expression of 5-LO can be regulated via DNA-methylation and can be up-regulated by TGF-β and 1,25-dihydroxyvitamin D_3 ($1,25(OH)_2D_3$) in differentiating Mono Mac 6 cells due to posttranscriptional events and by GM-CSF in mature neutrophils [98, 99]. 5-LO is a soluble 78 kDa protein containing 672 or 673 amino acids consisting of two domains, the regulatory N-terminal C2-like domain (residues 1-112) and the catalytic C-terminal domain (residues 126-673). The C2-like domain contains the binding site for Ca^{2+}, for membrane phosphatidylcholines (PC) and coactosin-like proteins (CLP), whereas the

catalytic domain contains the non-heme iron active site [100]. The two domains are connected via a salt bridge between Arg-101 on the C2-like domain and Asp-166 on the catalytic domain [101]. Recently, a mutated form of the 5-LO protein could be crystallized, the "stable-5-LO" with some sequence modifications [102]. The crystallized structure revealed a unique property of the small helix α2 in the catalytic domain, of which the side chains of Phe-177 and Tyr-181 appear to be able to block the entrance to the active site ("FY cork"), controlling access to the catalytic iron [89, 102]. The iron is coordinated by three conserved histidines (His-367, 372, 550), Asn-554 as well as the carboxylate of the C-terminal Ile-673. In the inactive state, the iron is present in the ferrous from (Fe^{2+}) while activation with lipid hydroxyperoxides (LOOH) like 5-HpETE or 12-HpETE transfer it to the active ferric form (Fe^{3+}) [103]. The cavity of the active site is formed by the hydrophobic chains of the amino acids Leu-368, 373, 414, 607 and Ile-406, positioning the pentadien structure of AA in the required position [102]. The mechanism how AA enters the cavity, is not exactly known, but there exist two hypotheses. AA could either enter the cavity with its ω-end or the "FY-cork" is somehow unplugged and AA enters with its carboxyl head first [6].

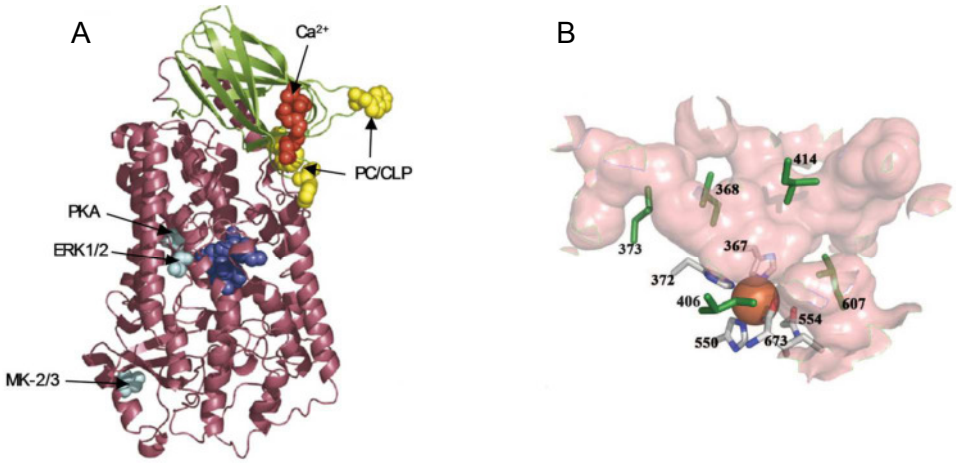

Figure: 1.7: Structure of human 5-LO. A) Model of 5-LO based on the crystal structure of rabbit reticulocyte 15-LO. C2-like domain: green; catalytic domain: purple; active site: dark blue; phosphorylated serine residues: light blue; Ca^{2+} binding site: red; PC/CLP binding site: yellow. According to Rådmark et al. [100]. B) The 5-LO active site. Amino acids coordinating the iron (orange sphere): His-367, His-372, His-550, Ile-673, Asn-554 in white sticks. Amino acids creating the elongated cavity: Leu-368, Leu-373, Leu-414, Leu-607, Ile-406 in green sticks, according to Gilbert et al. [102].

Calcium and ATP

Activation of 5-LO is induced by Ca^{2+}-mediated binding to PCs or CLP and further increased by ATP-binding. The stimulatory effect of ATP appears to increase with the number of phosphates (AMP < ADP < ATP) even though without the need to be hydrolyzed [104]. The C2-like domain has been shown to bind Ca^{2+} in a stoichiometry of about 2:1 per 5-LO protein with a Kd of about 6 μM. The half-maximal activation is obtained in presence of 1-2 μM calcium, whereas fully *in vitro* activation is reached at a concentration of 4-10 μM. Ca^{2+}-binding mediates the translocation to the nuclear envelope and increases the hydrophobicity of the enzyme by neutralizing negatively charged amino acids, allowing to associate close to the membrane [105, 106]. Mutagenesis studies revealed the amino acids Asn-43, Asp-44 and Glu-46 situated in the loop 2 of the regulatory C2-like domain important for Ca^2 binding [107].

Membranes and phosphatidylcholines

The binding of 5-LO to membranes activates the enzyme and could be mimicked using PC containing vesicles, which act as scaffold factors. Like Ca^{2+}, PCs increase the hydrophobicity and are required for basal and Ca^{2+}-activated 5-LO activity. The PC selectivity is suggested to direct 5-LO to the nuclear envelope and stabilizes the structure of the enzyme as well as of the membrane. Responsible for membrane binding are the three tryptophans in the C2-like domain, i.e. Trp-13, 75 and 102 [100].

Coactosin-like protein

The CLP is a member of actin-binding protein family able to bind F-actin. The binding sites for F-actin and 5-LO are similar and overlap, resulting in a competition for CLP binding [108]. CLP functions as a scaffold for 5-LO and can additionally support Ca^{2+}-mediated activity in the absence of PCs leading to 5-HETE formation but nearly no LTs. When CLP was present together with PCs activity was enhanced leading to a 3-fold higher LTA_4 formation [109].

Phosphorylation

Activation of 5-LO can be mediated by phosphorylation of different serine residues. Upon cell stress (e.g. phorbol esters, osmotic stress, heat shock), activated p38 MAPK phosphorylates the MAPK activated kinases-2/3 (MK-2/3), which in turn phosphorylates 5-LO at Ser-271 [110] whereas the MAPK ERK1/2 phosphorylate 5-LO at Ser-663 [111]. Both phosphorylations induce translocation and increase the 5-LO enzyme activity, in particular when both residues are phosphorylated at the same time. The activation by both kinases is promoted by fatty acids including AA [112]. In contrast, exogenous adenosine and increased cAMP are able to activate proteinkinase A (PKA) which phosphorylates 5-LO at Ser-523 thereby inhibiting 5-LO translocation [113].

Agents capable of activating 5-LO in the cell

Compounds leading to an elevation of the intracellular Ca^{2+} level are crucial for LT formation, for example ionophores, thapsigargin, platelet-activating factor (PAF), LTB_4, fMLP and complement component 5a (C5a). Among these compounds, Ca^{2+} ionophores mediate the strongest 5-LO product formation, whereas natural compounds are less efficient [114]. LT generation can be enhanced by “priming” with compounds, which do not increase 5-LO activity themselves. For example, priming with LPS followed by stimulation with fMLP strongly increases 5-LO product formation and elevates kinase activity phosphorylating $cPLA_2$ [115].

1.2.3.2 Subcellular translocation and the role of FLAP

In which cell compartment 5-LO is found in resting cells, is dependent on the cell type. In primary neutrophils, 5-LO is rather found in the cytoplasm, whereas in primary monocytes 5-LO is distributed between the nucleus and the cytosol [100, 116]. Independent of the cellular localization, upon cell stimulation 5-LO translocates in a Ca^{2+}-mediated manner to the outer or inner leaflet of the nucleus where membrane bound FLAP transfers AA to 5-LO to initiate leukotriene formation [117].

FLAP

FLAP is an 18-kDa integral nuclear membrane protein, a member of to the MAPEG family and was discovered as a target of MK886 [118]. FLAP forms active trimers anchored in the inner

as well as in the outer nuclear membrane partly associated with LTC_4-synthase (LTC_4S) and is necessary for the LT formation, although it lacks enzymatic activity. It is thought to act as a transfer protein, which enables conversion of AA to LTs, although the exact mechanism of AA transfer is currently unknown [7]. FLAP is required for the conversion of endogenous AA, but can enhance the transformation of exogenous AA as well [119, 120]. The expression coexists with 5-LO expression and upregulation is often observed coincidently as well [114].

1.2.3.3 Leukotriene formation

The 5-LO enzyme contains two distinct activities, dioxygenase activity and epoxide formation by the LTA_4S activity. 5-LO catalyzes the stereospecific insertion of molecular O_2 at C5 of AA forming 5(*S*)-hydroperoxy-6-*trans*-8,11,14-*cis*-eicosatetraenoic acid (5-HpETE) followed by immediate dehydration forming the unstable 5(*S*)-*trans*-5,6-oxido-7,9-*trans*-11,14-*cis*-eicosa-tetraenoic acid (LTA_4) [121]. For 5-LO catalytic activity the active site iron hast to be oxidized from the inactive ferrous to the active ferric state. Ferrous 5-LO reacts with hydroperoxides (e.g. 5-HpETE, 12-HpETE) creating an oxygen-substituted lipid radical and a hydroxide ion. The ferric form later reacts with a reducing agent to regenerate the ferrous form [104]. Lipid peroxides can also be generated for example via ROS formation. The first step in the generation of 5-HpETE is the abstraction of the pro-*S* hydrogen at C7. Radical rearrangement leads to the formation of a radical at C5, where molecular oxygen is inserted generating a peroxy radical. The iron is subsequently oxidized by electron transfer to the peroxy radical giving a peroxy anion, followed by protonation resulting in the hydroperoxide and the active ferric (Fe^{3+}) state [6]. The LTA_4S activity mediates abstraction of the pro-*R* hydrogen at C10 with radical migration to C6 and double bond rearrangement to form the unstable epoxide (LTA_4) with a conjugated triene system. 5-HpETE can alternatively be reduced by glutathione peroxidases to the corresponding alcohol 5(*S*)-hydroxy-6-*trans*-8,11,14-*cis*-eicosatetraenoic (5-HETE) [122]. 5-LO is additionally involved in the formation of 5-oxo-eicosatetraenoic acid (5-oxo-ETE) from 5-HETE [123] and together with 12-LO and 15-LO in the formation of anti-inflammatory lipoxins by transcellular mechanisms [124]. Subsequent hydrolysis by the soluble LTA_4-hydrolase (LTA_4H) yields the bioactive 5(*S*),12(*R*)-dihydroxy-6,14-*cis*-8,10-*trans*-eicosatetraenoid acid (LTB_4). In preparations of purified 5-LO enzyme, LTA_4 non-enzymatically degrades into two isomers (6-*trans*-LTB_4 and 6-*trans*-12-epi-LTB_4) [125]. In contrast, LTC_4S mediates conjugation of GSH to the epoxide moiety generating 5(*S*)-hydroxy-6(*R*)-S-glutathionyl-7,9-*trans*-11,14-*cis*-

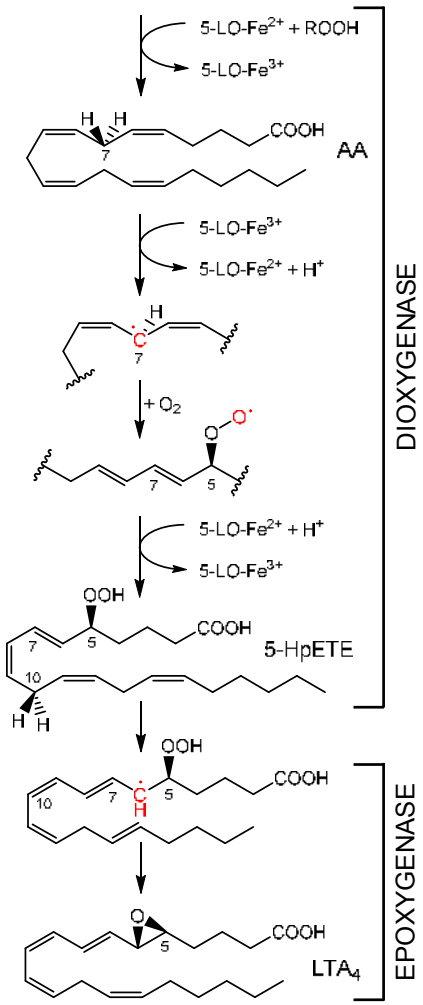

Figure 1.8: 5-LO catalytic formation of 5-HpETE and LTA_4, modified after Rådmark [104] and Haegstrom et al. [6].

eicosatetraenoic acid (LTC_4). LTC_4 is released from the cell and extracellular enzymes consecutively cleave the GSH tripeptide forming 5(*S*)-hydroxy-6(*R*)-S-cysteinylglycyl-7,9-*trans*-11,14-*cis*-eicosatetraenoic acid (LTD_4) and 5(*S*)-hydroxy-6(*R*)-cysteinyl-7,9-*trans*-11,14-*cis*-eicosatetraenoic acid (LTE_4). The γ-glutamyl transferase eliminates γ-glutamyl yielding LTD_4, whereas dipeptidases cleave glycine generating LTE_4 [126]. LTB_4 and LTC_4 can also be generated through transcellular mechanisms between two different cell types, like epithelial cells and platelets [127].

1.2.3.4 Other enzymes involved in the leukotriene biosynthesis

Cytosolic phospholipase A_2

The phospholipase family contains more than 30 different enzymes possessing PLA_2 or related activity, characterized by their structure, localization and requirement of Ca^{2+} [128]. The cytosolic PLA_2 group IV ($cPLA_2$)α is constitutively expressed in most cells and tissue and is responsible for the release of *sn*-2 bound AA from cellular membranes in the leukotriene pathway. $cPLA_2$ is an 85 kDa protein consisting of an N-terminal C2 domain and a C-terminal catalytic α/β hydrolase domain. Ca^{2+} binding at the C2 domain neutralizes negative charges, activates the enzyme and initiates translocation to the perinuclear membrane. The C2 domain anchors $cPLA_2$ in the membrane allowing hydrophobic interaction of the catalytic domain with membrane phospholipids preferentially with phosphocholine head groups [128-130].

LTA_4 hydrolase

LTA_4 hydrolase (LTA_4H) catalyzes the conversion from LTA_4 to LTB_4. LTA_4H is found in most cells and tissues, preferentially in neutrophils, however, with low levels in eosinophils and completely absent in basophils and platelets. The 68 kDa enzyme gets inactivated by its own substrate LTA_4, called a suicide inactivation [6]. LTA_4H is a zinc-dependent epoxide hydrolase and aminopeptidase containing an N-terminal, a catalytic and a C-terminal domain [131]. The opening of the epoxide of LTA_4 (C5 to C6) generates a carbocation delocalized over the conjugated triene system creating the essential *cis* double bond between C6 and C7 followed by insertion of the 12(*R*)-hydroxyl group [132].

LTC_4 synthase

Like FLAP, the LTC_4 synthase (LTC_4S) is an 18 kDa protein and a GSH-dependent member of the MAPEG family, expressed in leukocytes including eosinophils, mast cells and monocytes. LTC_4S is responsible for the conversion of LTA_4 to LTC_4, the parental compound of the cys-LTs [131]. LTC_4S is active as a heterotrimer, containing three transmembrane domains, situated at the nuclear membrane, partially colocalized with FLAP. LTA_4 binds in a hydrophobic gap, where it is in the optimal position for conjugation with GSH [133, 134]. Attack of the GSH anion leads to inversion and formation of the *R*-configuration followed by the formation of the 5(*S*)-hydroxyl group [135].

1.2.3.5 Biological and pathological effects of leukotrienes

Leukotrienes exert their biological activity via cognate GPCRs on target cells. They are predominantly produced by pro-inflammatory cells, like polymorphonuclear leukocytes, mast cells and macrophages and are involved in allergic reactions and inflammatory diseases.

LTB_4

LTB_4 is the most potent chemoattractant released by neutrophils mediating recruitment of inflammatory cells like eosinophils, monocytes, macrophages as well as T cells, linking the innate and the adaptive immune system. At the site of inflammation, LTB_4 promotes neutrophil activation and degranulation, is involved in enhancing phagocytic mechanisms and increases the production of inflammatory cytokines (IL-1, IL-2, IL-6) and chemokines [136], associating LTB_4 with atherosclerosis [137], rheumatoid arthritis and also with cancer [97, 138]. Furthermore, LTB_4 is released by alveolar macrophages, bronchial epithelial cells and fibroblasts, indicating a role in asthma and chronic obstructive pulmonary diseases (COPD) [139]. The effects of LTB_4 are mediated by 2 distinct GPCRs, BLT1 exclusively expressed in inflammatory cells and BLT2 ubiquitously expressed in various tissue. BLT2 functions as a low-affinity receptor for LTB_4, additionally binding 12-HETE, 15-HETE and with high affinity 12-HHT [6].

Cys-LTs

Cys-LTs are a group of lipid mediators composed of LTC_4, LTD_4 and LTE_4, known as the “slow reacting substance involved in anaphylaxis” (SRS-A). They are mainly produced by eosinophils, basophils, mast cells and macrophages and can additionally be generated by transcellular mechanisms together with platelets or endothelial cells [127]. The classical effects mediated by the cys-LTs are contraction of smooth muscle, increased vascular permeability and plasma leakage leading to oedema formation, mucus secretion and damage to the mucus layer in the lung [140]. Furthermore, cys-LTs enhance the production of chemokines (MCP-1) and mediate increased adhesion of neutrophils and eosinophils [141]. These effects associate the cys-LTs preferentially with asthma [142], but also with atopic dermatitis and cardiovascular diseases [141]. Cys-LTs mediate their effects via the two GPCRs $CysLT_1$ and $CysLT_2$ which preferably bind LTD_4 and LTC_4 and are widely expressed, e.g. in spleen, smooth muscle, lung and inflammatory cells [143, 144]. Since both CysLT receptors bind LTE_4 with low affinity it could be shown that LTE_4 mediates its pro-inflammatory activity via $P2Y_{12}$, a receptor for adenosine diphosphate [145].

1.2.3.6 12- and 15-lipoxygenases

The lipoxygenases are classified according to the position where they mediate the regioselective dioxygenation of AA, i.e. at C12 or C15 resulting primarily in 12-H(p)ETE and 15-H(p)ETE. 12-LO is preferentially expressed in platelets (platelet-type 12-LO), whereas 15-LO is expressed in leukocytes like eosinophils and epithelial cells [92]. Both 12-H(p)ETE and 15-H(p)ETE mediate inflammatory reactions: Together with LTB_4 12-H(p)ETE regulates platelet aggregation and is associated with cancer risk (colorectal cancer, breast cancer), 15-H(p)ETE plays a role in cardiovascular diseases like atherosclerosis and modulates cellular oxidative stress [96]. In contrast, cooperation of 5- and 12-LO, and 5- and 15-LO, respectively, leads to the generation of anti-inflammatory class of lipoxins [124].

1.2.3.7 5-LO inhibitors

In order to develop selective and potent drugs to interfere with the inflammatory effects of LTs, different approaches were made. Besides the use of LT receptor antagonists like montelukast, direct targeting of 5-LO is a promising therapeutic strategy to suppress leukotriene formation. Furthermore, the development of specific FLAP, LTA_4H or LTC_4S inhibitors are currently pursued. 5-LO inhibitors can be classified into four main groups based on their molecular mode of action: redox-type inhibitors, iron-ligand inhibitors, non-redox-type inhibitors and novel-type inhibitors acting at the C2-domain [121].

Redox-type inhibitors of 5-LO

Redox-type inhibitors are lipophilic substances, which interfere with intracellular peroxides (LOOH) [146], the intracellular oxidative tone or directly reduce the active site iron to the inactive ferrous (Fe^{2+}) state [147, 148]. Many of these compounds are plant-derived products like flavonoids, caffeic acid, coumarins, quinones and polyphenols [149]. Examples for synthetic compounds are BW-755C and L-656,224. However, due to low selectivity for 5-LO they lack efficacy *in vivo* and exert severe adverse effects like methemoglobin formation by interacting with other redox catalyzed enzymes or production of reactive superoxide anions [150]. Additionally, many of these natural compounds are insoluble and thus poorly bioavailable [151]. Regarding these negative properties. it is not surprising that no redox-type 5-LO inhibitor could be introduced into the market so far.

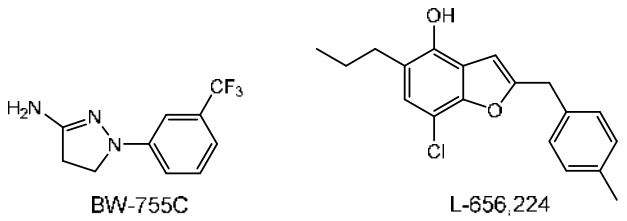

Figure 1.9: Synthetic redox-type inhibitors of human 5-LO.

Iron ligand inhibitors

Studies to improve the efficacy in vivo and to reduce the adverse effects revealed compounds with hydroxamic acids or related N-hydroxy urea structures as potent inhibitors. They chelate the active site iron thereby inhibiting the enzyme and stimulate peroxidase activity [152, 153]. BWA4C, a N-acylhydroxylamine compound showed selectivity for 5-LO and potent inhibitory potential (IC_{50} = 40 nM in intact cells), however, the essential hydroxamate group is rapidly metabolized to an inactive carboxylate form generating toxic nitride radicals [154, 155]. Further development yielded the more hydrolytically stable zileuton containing a N-hydroxy urea

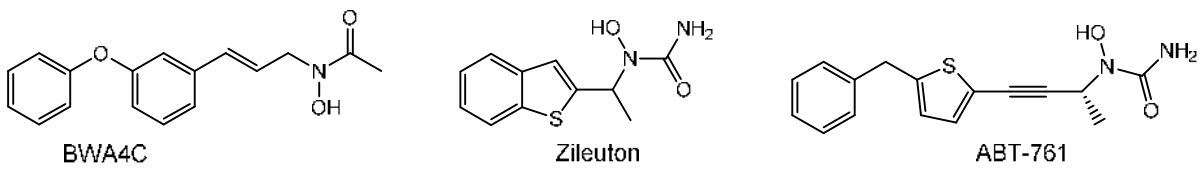

Figure 1.10: Iron ligand inhibitors.

structure (IC_{50} = 0.5 - 1 µM in intact cells). So far, zileuton is the only direct 5-LO inhibitor introduced to the market [156], of which the extended-release formulation is approved in the USA for the treatment of asthma (Zyflo®), whereas the immediate-release formulation was withdrawn in 2008. Based on zileuton, the thiophene analogue ABT-761 (atreleuton) was designed with promising efficacy blocking bronchoconstriction in asthma [157] but phase III clinical trials have been discontinued. For the treatment of acute coronary syndrome it is currently investigated in phase II trials [158].

Non-redox-type inhibitors

Promising structures like methoxytetrahydropyrans were identified to compete with AA or LOOH for the binding to 5-LO, probably in an allosteric mode of action [159, 160] and compounds like ZM-230487 and ZD-2138 showed promising selective oral activity (IC_{50} = 20 - 50 nM in human whole blood) [114, 161]. Their activity was impaired by increased peroxide levels, but could be potentiated by the addition of GSH or dithiothreitol (DTT) indicating the involvement of glutathione peroxidases [162]. Moreover, it could be shown that the inhibitory potency of these non-redox-type inhibitors is impaired by the activation of kinases phosphorylating the enzyme [163].

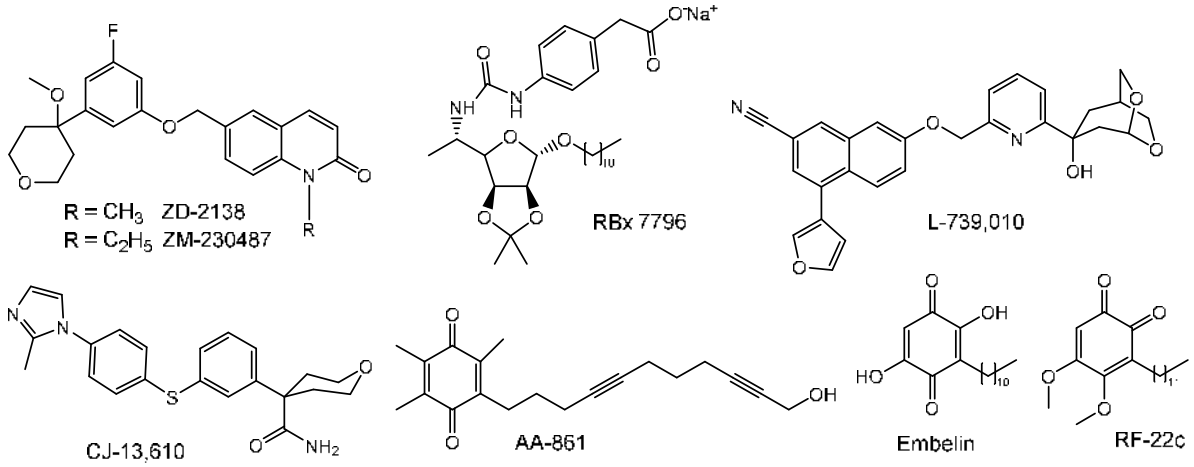

Figure 1.11: Non-redox-type inhibitors of 5-LO.

To date, numerous novel series with different basic structures were developed, for example urea derivatives with dodecyl chains (RBx 7796; IC_{50} = 5 µM in intact cells) [164], substituted coumarin structures and derivatives (L-739,010) [165], imidazoles and tetrahydropyran-carboxamides (CJ-13,610, IC_{50} = 70 nM in intact cells) [166] of which all exert promising anti-inflammatory effects *in vitro* and *in vivo* [121]. Recent findings show that compounds bearing a Michael acceptor structure potently inhibit 5-LO by binding to four cysteines (Cys-159, -300, -416 and -418) situated close to the catalytic center, e.g. AA-861 (IC_{50} = 0.2 µM in intact cells) [167]. Another promising approach to improve 5-LO inhibitors was pursued based on the potent inhibition of the plant-derived 1,4-benzoquinone embelin (IC_{50} = 60 nM in intact cells) [8]. Structural optimization yielded the compounds RF-Id [168, 169] and RF-22c (IC_{50} = 22 nM in intact cells) [170], both remarkably effective in cell-based assays as well as in inflammatory animal models of bronchoconstriction.

Novel type inhibitors

Additionally, there are inhibitors which cannot be classified by the three groups mentioned before. A possible mode of action is interference with the C2-like domain as described for 3-*O*-acetyl-11-keto-boswelic acid (AKBA) derived from *Boswellia* species and hyperforin from *Hypericum perforatum*. It is indicated that AKBA interacts with the PC binding site of the C2-like domain or with a second regulatory selective binding site different from the AA-binding site in a Ca^{2+}-dependent manner. Unfortunately, AKBA failed to inhibit LT generation in whole blood [171], whereas a *Boswellia serrata* extract has reached Phase II trial for osteoarthritis [172]. The compound hyperforin interferes with the 5-LO C2-like domain preventing the interaction of 5-LO with CLP and the translocation to the nuclear membrane and displays efficacy *in vivo* models like carrageenan-induced pleurisy [153].

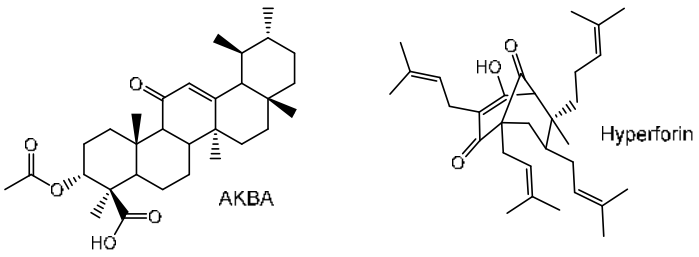

Figure 1.12: Novel type inhibitors.

Dual 5-LO/COX inhibitors

In order to provide a more efficient inhibition of eicosanoid formation, dual inhibitors of COX and 5-LO were designed. The prototype licofelone (ML3000) was found to interact with FLAP, COX-1 and mPGES-1 [163, 173] and is currently tested in Phase III clinical trials for osteoarthritis, though there is no development report for this study. Recently, new structures based on the COX-2 selective coxibes were designed, since celecoxib was shown to impair 5-LO activity as well [174]. Numerous novel structures like diaryl-dithiolane and isothiazole and series of phenylsulfonyl urenyl chalcone (e.g. Me-UCH 1) derivatives were identified as promising dual inhibitors [175] exerting anti-inflammatory effects in vitro as well as in vivo [176].

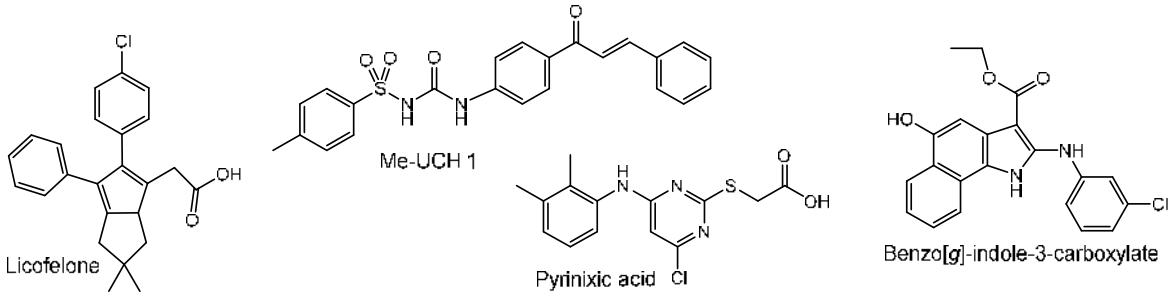

Figure 1.13: dual inhibitors of 5-LO/COX and 5-LO/mPGES-1.

Dual 5-LO/mPGES-1 inhibitors

Based on the dual 5-LO/COX inhibitors, more specialized compounds were designed to lower adverse effects. Thus, compounds like pirinixic acid derivatives interfering with 5-LO and mPGES-1 were introduced. They potently suppressed the formation of 5-LO products and the

generation of PGE_2 *in vitro* (IC_{50} = around 1 µM, for both enzymes) and *in vivo* [177, 178]. Another class of dual 5-LO/mPGES-1 inhibitors comprise the benzo[g]-indole-3-carboxylate structures. The lead compound of this series potently hampers 5-LO (IC_{50} = 0.23 µM in intact cells, 0.83 - 1.6 µM in human whole blood) and mPGES-1 activity (IC_{50} = 0.6 µM, isolated enzyme) and additionally showed efficacy in animal models of inflammation [179, 180].

1.2.3.8 Inhibition of other enzymes involved in LT formation

FLAP inhibitors

A novel strategy to circumvent direct inhibition of 5-LO activity but still block LT formation is interference with FLAP [181]. The first determined FLAP inhibitor was the indole MK886, with potent inhibitory properties (IC_{50} = 2.5 nM in intact cells) but was unfortunately about 50-fold less active in human whole blood (IC_{50} = 1.1 µM) [182]. Intensive research revealed novel compounds highly active also in human whole blood with additional confirmed efficacy in asthma patients as determined for GSK2190915 [183, 184]. Promising results were also obtained with the nonacidic benzimidazole BRP-7 and its structurally optimized derivatives regarding inhibition of 5-LO product synthesis in cell-based assays as well as zymosan-induced peritonitis in mice [185, 186]. Other indole derivatives like AM103 (IC_{50} = 4.2 nM, FLAP-binding assay) [187] and AM803 (IC_{50} = 76 – 506 nM, FLAP-binding assay) [188] displayed potent inhibition of 5-LO and both compounds were investigated in clinical trials. However, the current status for AM103 is not publicly known and for AM803 testicular toxicity in rats was reported.

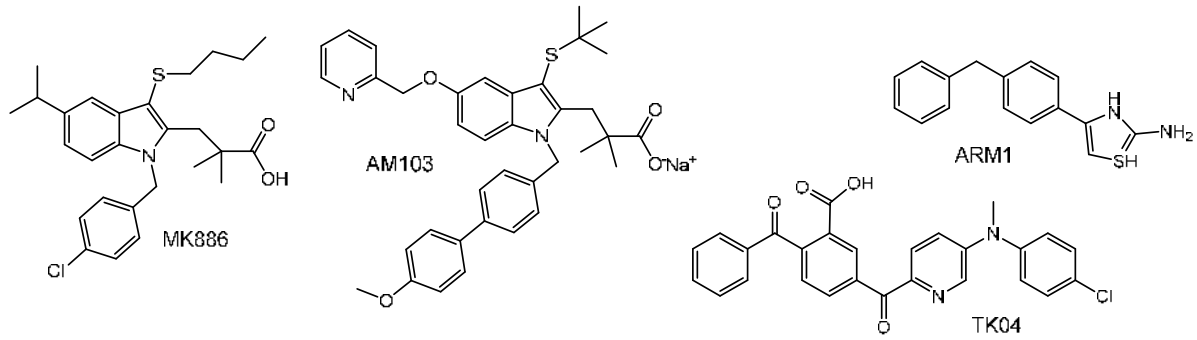

Figure 1.14: Inhibitors of FLAP, LTA_4 hydrolase and LTC_4 synthase.

LTA_4 hydrolase and LTC_4 synthase inhibitors

In contrast of classical 5-LO and FLAP inhibitors, the inhibition of LTA_4H and LTC_4S still allows the generation of LTA_4 necessary for the formation of anti-inflammatory lipoxins. Thus, intensive studies are made in this field and revealed azabenzthiazole [189] and substituted benzofurans [190] as potent LTA_4H inhibitors. With ARM1 the first inhibitor that selectively blocks the hydrolase activity and spares the aminopeptidase activity was reported [191]. The search for LTC_4S inhibitors yielded tandem benzophenone amine pyridines (TK04, TK04A, TK05), which apparently interact with the amino acids Arg-104 and Arg-36 in the active site and potently suppress LTC_4 formation *in vitro* and *in vivo* promoting the generation of lipoxins [192, 193].

2 AIM OF THE THESIS

In general, acute inflammation is an immune response exerted by the host organism to restore the healthy state [20]. However, acute inflammation can shade off into chronic inflammation escalating in diseases like atherosclerosis, rheumatoid arthritis, asthma and even cancer [28, 34]. It is known that female individuals undergo a stronger immune response, leading to a faster recovering but also to a higher susceptibility for autoimmune diseases like SLE or rheumatoid arthritis. In contrast, male individuals are more susceptible to infections and atherosclerosis [2]. In order to provide optimal pharmacological therapy, much effort has gone into the investigation of the sexual dimorphism in the past years, revealing several factors contributing to the gender disparity. Recently, the differential regulation of the 5-LO product formation in human neutrophils as well as *in vivo* could be detected [4, 194]. Like leukotrienes, prostaglandins are factors able to promote and sustain inflammation and evidence confirming a diverse production in male and female human neutrophils and in animal models of inflammation could be shown [5]. However, little is known about the role of prostaglandins and the COX pathway in the sexual dimorphism in healthy individuals and investigations of different research groups reported inconsistent results [85, 86]. The aim of the first part of the thesis was to reveal if there is a sex difference in prostanoid formation in human leukocytes and if so, to elucidate the underlying mechanisms. The prostanoid formation in each sex was analyzed upon stimulation with different agents in human whole blood and isolated leukocytes in short and long term incubations. To determine the observed difference in prostanoid formation in detail, processes influencing the amount of prostanoids like TLR4 protein expression, COX-1/2 protein and mRNA expression and the activity of the metabolizing enzyme 15-PGDH were evaluated. Furthermore, the effect of sex hormones in human whole blood and on freshly isolated PBMC was investigated regarding a modulation of the prostanoid biosynthesis.

The second part of this thesis was dedicated to small molecules that modulate 5-LO activity and LT formation. LTs play a pivotal role in inflammatory conditions and diseases, especially the cys-LTs in asthma [195]. Over the past years, numerous inhibitors were designed to interfere directly or indirectly with 5-LO aiming to suppress LT formation. However, only one direct 5-LO inhibitors, namely zileuton [196] and few indirect inhibitors like montelukast could be introduced to the market to date for the treatment of asthma [197]. A plethora of different structures were proposed as 5-LO inhibitors exerting different modes of action, involving redox activity, direct chelation of the catalytic iron or allosteric inhibition. Previous findings support the inhibitory potential of 1,4-benzoquinones [169] and consequent structurally modifications lead to a series of 1,2-benzoquinones and 1,2-benzohydroquinones highly effective in suppression of LT synthesis [198]. To evaluate the mechanism underlying the inhibition of the 5-LO product formation by small molecules, the efficacy in cell-free assays as well as in human leukocytes upon challenge with different stimuli and the detailed impact of the test compounds on the 5-LO activity was investigated. Biological data was verified by docking simulations and confirmed in animal models of inflammation. Furthermore, a special focus was placed on the selectivity for 5-LO as target.

3 MATERIALS AND METHODS

3.1 Materials

[^{3}H]-arachidonic acid	BIOTREND Chemikalien GmbH, Köln, Germany
11β-PGE_2	Cayman Chemical, Ann Arbor, MI, USA
17β-Estradiol	Sigma-Aldrich, Deisenhofen, Germany
5-LO primary antibody	Prof. Steinhilber, Goethe University of Frankfurt/Main, Germany
5α-DHT	Sigma-Aldrich, Deisenhofen, Germany
Acetic acid	Carl Roth GmbH Co. KG, Karlsruhe, Germany
Acetonitril	Thermo Fisher Scientific Inc., MA, USA
Acrylamide	Applichem GmbH, Darmstadt, Germany
Adenosine deaminase	Sigma-Aldrich, Deisenhofen, Germany
Ampicillin	Applichem GmbH, Darmstadt, Germany
Arachidonic acid	Cayman Chemical, Ann Arbor, MI, USA
AUDA	Cayman Chemical, Ann Arbor, MI, USA
B2M primer (forward and reverse)	TIB MOLBIOL Syntheselabor, Berlin, Germany
Biotase	Biochrom GmbH, Berlin, Germany
Bromophenol blue	Merck, KGaA, Darmstadt, Germany
BSA	Applichem GmbH, Darmstadt, Germany
BSA, fatty acid free	Sigma-Aldrich, Deisenhofen, Germany
BWA4C	Sigma-Aldrich, Deisenhofen, Germany
Ca^{2+} ionophore A23187	Cayman Chemical, Ann Arbor, MI, USA
$CaCl_2$	Applichem GmbH, Darmstadt, Germany
CD14 primer antibody, Cat#MHCD1427	Thermo Fisher Scientific Inc., MA, USA
CD19 primer antibody, Cat#302205	BioLegend, San Diego, CA, USA
CD3 primer antibody, Cat#317307	BioLegend, San Diego, CA, USA
Celecoxib	Sigma-Aldrich, Deisenhofen, Germany
Charcoal, dextran-coated	Sigma-Aldrich, Deisenhofen, Germany
Citric acid, monohydrate	Applichem GmbH, Darmstadt, Germany
COX-1, ovine	Cayman Chemical, Ann Arbor, MI, USA
COX-1 primary antibody, Cat#9896	Cell Signaling Technology Inc., MA, USA
COX-2 primer (forward and reverse)	TIB MOLBIOL Syntheselabor, Berlin, Germany
COX-2, human	Cayman Chemical, Ann Arbor, MI, USA
COX-2 primary antibody, Cat#4842	Cell Signaling Technology Inc., MA, USA
D'PBS	SERVA Electrophoreses GmbH, Heidelberg, Germany
d4-LTB_4	Cayman Chemical, Ann Arbor, MI, USA
d4-TxB_2	Cayman Chemical, Ann Arbor, MI, USA
d5-LXA_4	Cayman Chemical, Ann Arbor, MI, USA
d8-5S-HETE	Cayman Chemical, Ann Arbor, MI, USA
d9-PGE_2	Cayman Chemical, Ann Arbor, MI, USA
DAPI	Sigma-Aldrich, Deisenhofen, Germany

DCFH-DA	Sigma-Aldrich, Deisenhofen, Germany
Dexamethasone	Sigma-Aldrich, Deisenhofen, Germany
Dextran	Sigma-Aldrich, Deisenhofen, Germany
DMEM (high glucose)	Biochrom GmbH, Berlin Germany
DMSO	Merck, KGaA, Darmstadt, Germany
DPI	Sigma-Aldrich, Deisenhofen, Germany
DPPH	Cayman Chemical, Ann Arbor, MI, USA
EDTA	Applichem GmbH, Darmstadt, Germany
FCS	PAA/GE Healthcare Europe GmbH, Freiburg Germany
$FeCl_2$	Applichem GmbH, Darmstadt, Germany
$FeSO_4$ 7×H_2O	Applichem GmbH, Darmstadt, Germany
FLAP primary antibody, Cat#ab85227	Abcam plc, Cambridge, UK
fMLP	Sigma-Aldrich, Deisenhofen, Germany
Formic acid	Sigma-Aldrich, Deisenhofen, Germany
Fura-2-AM	Sigma-Aldrich, Deisenhofen, Germany
G-418 sulfate, Geneticin	Carl Roth GmbH Co. KG, Karlsruhe, Germany
Glucose	Applichem GmbH, Darmstadt, Germany
Glutathione, reduced	Applichem GmbH, Darmstadt, Germany
Glycerole	Caesar & Loretz GmbH, Hilden, Germany
Glycine	Carl Roth GmbH Co. KG, Karlsruhe, Germany
HCl	Grüssing GmbH, Filsum Germany
Hemoglobin	Sigma-Aldrich, Deisenhofen, Germany
Histopaque	Sigma-Aldrich
Human serum AB	Lonza Group Ltd, Basel, Switzerland
Hygromycin	Thermo Fisher Scientific Inc., MA, USA
IgG Alexa Fluor 488, Cat#A11034	Thermo Fisher Scientific Inc., MA, USA
IgG Alexa Fluor 555, Cat#A21424	Thermo Fisher Scientific Inc., MA, USA
IgG APC-Alexa Fluor 750, Cat#A-21006	Thermo Fisher Scientific Inc., MA, USA
IL-1β	ReproTech, Hamburg, Germany
Indomethacin	Sigma-Aldrich, Deisenhofen, Germany
IRDye 680LT secondary antibody Cat#925-68020 and -68021	LI-COR Bioscience Inc., Bad-Homburg, Germany
IRDye 800CW secondary antibody Cat#925-3221 and -32211	LI-COR Bioscience Inc., Bad-Homburg, Germany
KH_2PO_4	Sigma-Aldrich, Deisenhofen, Germany
Leupeptin hemisulfate salt	Sigma-Aldrich, Deisenhofen, Germany
L-glutamine	Biochrom GmbH, Berlin Germany
LPS	Sigma-Aldrich, Deisenhofen, Germany
LSC fluid Rotiszint eco plus	Carl Roth GmbH Co. KG, Karlsruhe, Germany
LTA_4-methyl ester	Cayman Chemical, Ann Arbor, MI, USA
LTC4-d5-methyl ester	Cayman Chemical, Ann Arbor, MI, USA
$MgCl_2$	Merck, KGaA, Darmstadt, Germany
$MgSO_4$	Applichem GmbH, Darmstadt, Germany
MK886	Cayman Chemical, Ann Arbor, MI, USA

MTT	Sigma-Aldrich, Deisenhofen, Germany
Na_3VO_4	Applichem GmbH, Darmstadt, Germany
$Na_4P_2O_7$	Sigma-Aldrich, Deisenhofen, Germany
NaCl	Carl Roth GmbH Co. KG, Karlsruhe, Germany
NADH	Applichem GmbH, Darmstadt, Germany
NaF	Applichem GmbH, Darmstadt, Germany
Nonidet P-40	Applichem GmbH, Darmstadt, Germany
p-38 MAPK primary antibody, Cat#8690	Cell Signaling Technology Inc., MA, USA
p-44/42 MAPK primary antib., Cat#4695	Cell Signaling Technology Inc., MA, USA
$Pam3CSK_4$	InvivoGen, San Diego, CA, USA
Paraformaldehyde	Carl Roth GmbH Co. KG, Karlsruhe, Germany
Penicillin/streptomycin solution	Biochrom GmbH, Berlin Germany
Peptone	Carl Roth GmbH Co. KG, Karlsruhe, Germany
PGB_1	Cayman Chemical, Ann Arbor, MI, USA
PGH_2	Larodan, Malmö, Sweden
PHOME	Cayman Chemical, Ann Arbor, MI, USA
Phospho-p-38 MAPK, primary antibody Cat#4631	Cell Signaling Technology Inc., MA, USA
Phospho-p44/42 MAPK, primary antibody Cat#5726	Cell Signaling Technology Inc., MA, USA
PMA	Applichem GmbH, Darmstadt, Germany
PMSF	Sigma-Aldrich, Deisenhofen, Germany
Ponceau	Sigma-Aldrich, Deisenhofen, Germany
Powdered milk, low fat	Carl Roth GmbH Co. KG, Karlsruhe, Germany
Progesterone	Sigma-Aldrich, Deisenhofen, Germany
Pyruvate	PAA/GE Healthcare Europe GmbH, Freiburg Germany
RPMI 1640	Sigma-Aldrich, Deisenhofen, Germany
RSC-3388	Cayman Chemical, Ann Arbor, MI, USA
SDS	Carl Roth GmbH Co. KG, Karlsruhe, Germany
Staurosporine	Merck, KGaA, Darmstadt, Germany
STI	Sigma-Aldrich, Deisenhofen, Germany
Sucrose	Applichem GmbH, Darmstadt, Germany
SW033291	Sigma-Aldrich, Deisenhofen, Germany
Testosterone	Sigma-Aldrich, Deisenhofen, Germany
TLR4 fluorescent antibody, Cat#564215	BD Bioscience, San Jose, CA, USA
Trifluoroacetic acid	Applichem GmbH, Darmstadt, Germany
Tris/HCl	Carl Roth GmbH Co. KG, Karlsruhe, Germany
Triton X-100	Carl Roth GmbH Co. KG, Karlsruhe, Germany
Trypan blue	Sigma-Aldrich, Deisenhofen, Germany
Trypsin-EDTA	Thermo Fisher Scientific Inc., MA, USA
Tween 20	Carl Roth GmbH Co. KG, Karlsruhe, Germany
U0126	Enzo Life Science Inc., NY, USA
Yeast extract	Carl Roth GmbH Co. KG, Karlsruhe, Germany
Zileuton	Sequoia Research Products, Oxford, UK

β-actin primer (forward and reverse)	TIB MOLBIOL Syntheselabor, Berlin, Germany
β-actin primary antibody, Cat#58169 and 4970	Cell Signaling Technology Inc., MA, USA
β-glycerophosphate	Sigma-Aldrich, Deisenhofen, Germany
β-mercaptoethanol	Carl Roth GmbH Co. KG, Karlsruhe, Germany

Compounds

Embelin, benzoquinones and hydroquinones were synthesized by the group of Dr. Rosanna Filosa, University of Salerno, Italy.

Buffer solutions

D'PBS: phosphate buffer containing 10 mM PO_4^{3-}, 137 mM NaCl, 2.7 mM KCl, pH 7.4

PG: D'PBS containing 0.1% glucose

PGC: PG containing 1 mM Ca^{2+}

D'PBS-C: D'PBS containing 1 mM Ca^{2+}

CCM-5% FCS: RPMI 1640 cell culture medium containing 5% (v/v) heat-inactivated fetal calf serum (FCS), L-glutamine (2 mM), penicillin (100 U/ml) and streptomycin (100 µg/ml)

CCM-10% FCS: RPMI 1640 cell culture medium containing 10% (v/v) heat-inactivated FCS, L-glutamine (2 mM), penicillin (100 U/ml) and streptomycin (100 µg/ml)

CCM-0.5% CSS: RPMI 1640 cell culture medium containing 0.5% (v/v) charcoal-stripped human serum (CSS), L-glutamine (2 mM), penicillin (100 U/ml) and streptomycin (100 µg/ml)

DMEM-10% FCS: Dulbecco's modified eagle medium (DMEM) containing 10% (v/v) heat-inactivated FCS, 100 U/ml penicillin, 100 µg/ml, 400 µg/ml Geneticin and 200 µg/ml hygromycin B

FACS buffer I: D'PBS containing 1% (m/v) bovine serum albumin (BSA), 0.1% (m/v) NaN_3, 2 mM EDTA

FACS buffer II: D'PBS containing 1% (m/v) BSA, 2 mM EDTA

3.2 Methods

3.2.1 Human whole blood

3.2.1.1 Complete blood count of human blood donations

Peripheral venous blood (30 - 50 ml) was taken from voluntary healthy donors by venipuncture at the Institute of Transfusion Medicine, Jena University Hospital. The blood was collected in heparinized monovettes (16 I.E. heparin/ml blood, Sarstedt, Nümbrecht, Germany). Subjects have not taken any anti-inflammatory drugs for at least ten days prior to blood donation. Freshly drawn blood was processed not later than within two hours. Counting of blood cells was done in the laboratories of the Jena University Hospital by flow cytometry (Sysmex, Norderstedt, Germany).

3.2.1.2 Isolation of plasma from human blood and sex hormone depletion

To obtain human plasma, heparinized peripheral venous blood was centrifuged at 600 × *g*, 10 min at 20 °C. The supernatant was additionally centrifuged again (800 × *g*, 15 min at 20 °C) and afterwards checked for cellular remnants. In order to eliminate sex hormones human plasma, fetal calf serum (FCS) or human serum was striped by continuous agitation (4 °C, overnight) with dextrane-coated charcoal (20 µg/ml) and centrifuged twice at 2000 × *g*, 15 min at 4 °C. The stripped plasma or serum was filtered, once through 45 µm pore-sized filter, with subsequent sterile filtration with 22 µm pore size (Carl Roth GmbH & Co. KG, Karlsruhe, Germany). Plasma was stored at -80 °C until use.

3.2.1.3 Determination of lipoxygenase and cyclooxygenase activity in human blood

For human whole blood assays, fresh peripheral venous blood was collected at the Jena University Hospital as described in 3.2.1.1. To determine lipoxygenase product formation, aliquots of 2 ml were preincubated with inhibitors or vehicle (0.1% DMSO) for 15 min at 37 °C, followed by stimulation with the A23187 or AA as indicated in the distinct experiments for 10 min at 37 °C. Alternatively, blood was primed with 1 µg/ml lipopolysaccharide from *E. coli* 0127:BS (LPS) for 30 min and 0.3 U/ml adenosine deaminase (ADA) for 20 min at 37 °C, followed by stimulation with 1 µM fMLP for 15 min at 37 °C. Test compounds, vehicle (1% DMSO) and control inhibitors were added 15 min prior fMLP stimulation. The reactions were stopped on ice and samples were centrifuged at 400 × *g*, 10 min at 4 °C. Collected plasma was mixed with 4 volumes of methanol, 200 ng prostaglandin B_1 (PGB_1) were added as internal standard and samples were frozen for 2 h at -20 °C. Denatured samples were centrifuged at 800 × *g*, 15 min at 4 °C and obtained supernatants were diluted with the equal amount of D'PBS and 25 µl/ml 1 N HCl. Lipoxygenase products were extracted by solid phase extraction (SPE) (3.2.6) and determined by liquid chromatography tandem mass spectrometry (LC-MS/MS) (3.2.7). To determine cyclooxygenase products, aliquots of 1 ml whole blood or whole blood homogenates (sonication: 3 × 10 s, 4 °C, cell disruption confirmed by light microscopy) were stimulated as indicated in the respective experiments. The reaction was stopped on ice and samples were centrifuged at 400 × *g*, 10 min at 4 °C. Prostanoids were determined by enzyme-linked immunosorbent assay (EIA, PGE_2 EIA Kit, Biotrend, Köln, Germany) following manufacturer's instructions or extracted by SPE (3.2.6) and determined by LC-MS/MS (3.2.7). For that, aliquots of 200 - 400 µl were mixed with 100 ng/ml PGB_1, 50 ng/ml deuterated prostaglandin E_2 (PGE_2-d9) and 50 ng/ml deuterated thromboxane B_2 (TxB_2-d4) as internal standards and 30 µl/ml 1 N HCl. Samples were frozen at -20 °C for at least 2 h and subsequently the denatured samples were centrifuged at 800 × *g*, 5 min at 4 °C.

3.2.2 Cells

3.2.2.1 Isolation of human primary cells from leukocyte concentrates

Human primary cells (PMNL, monocytes, platelets) were isolated from leukocyte concentrates generated at the Institute of Transfusion Medicine, Jena University Hospital. Blood was collected from adult healthy donors, which have not been taken any anti-inflammatory medication for at least ten days prior to blood donation. Cells for the gender study were isolated directly from heparinized whole blood whereby human plasma was separated prior to cell isolation for several experiments. Cells from the leucocyte concentrations were isolated by dextran sedimentation (5% (w/v) dextran from Leuconostoc spp. (Mr = 500,000 g/ml) in D'PBS) at room temperature (RT) with subsequent density gradient centrifugation on leucocyte separation medium (Histopaque-1077, Sigma Aldrich, Deisenhofen, Germany) at 800 × *g*, 10 min at 20 °C without brakes (Heraeus Multifuge X3R Centrifuge, Thermo Scientific, MA, USA). Density centrifugation results in different layers: platelet rich plasma (PRP) on top, followed by a layer of monocytes, T and B cells (PBMC) at the plasma/Histopaque®-1077 interface, and a pellet containing PMNL and remaining erythrocytes. To obtain platelets, PRP was diluted with cold D'PBS pH 5.9 (2:3) and centrifuged at 2100 × *g*, 15 min, at RT followed by washing with a mixture of 0.9% NaCl and D'PBS pH 5.9 (1:1; 1900 × *g* / 10 min / RT). Platelets were resuspended in cold D'PBS and immediately used for experiments. To purify PMNL, remaining erythrocytes in the obtained pellet were removed by hypotonic lysis with 10 ml cold H_2O for 45 s and subsequent dilution with D'PBS. After two additional washing steps (400 × *g* / 10 min / 4 °C) with D'PBS, PMNL were resuspended in PG buffer. PBMC were obtained by two washing steps (400 × *g* / 10 min / 4 °C) with D'PBS after density gradient centrifugation and resuspended in CCM-5% FCS or CCM-0.5% CSS. Monocytes were isolated from PBMC by adherence to cell culture flasks with a cell density of 2 × 10^7/ml in CCM-10% FCS for 1-1.5 h, 37 °C, 5% CO_2 (Heracell incubator, Heraeus, Hanau, Germany), as described in [4]. For gender studies, human serum or FCS was stripped as described in chapter 3.2.1.2. Before performing experiments, cells were counted by mixing with trypan blue solution (1:1, 0.2%) with a Vi-cell counter (Beckmann Coulter GmbH, Krefeld, Germany) or manually with a buerker haemocytometer under a light microscope.

3.2.2.2 HEK293 cells

HEK293 cells (human embryonic kidney cell line) were cultured in DMEM-10% FCS at 37 °C, 5% CO_2. HEK293 cells stably expressing FLAP and 5-LO_wt, or 5-LO_3W mutant or 5-LO_4C mutant, respectively, were selected using 400 µg/ml geneticin (for 5-LO) and 200 µg/ml hygromycin B (for FLAP). Cells were detached by trypsin-EDTA for 5 min at 37 °C, 5% CO_2 2-3 times per week, resuspended in DMEM-10% FCS and seeded in density of 0.25 × 10^6/ml at 37 °C, 5% CO_2. For determination of 5-LO products, cells (1 × 10^6/ml) were resuspended in PGC buffer, preincubated with compounds or vehicle (0.1% DMSO) for 15 min at 37 °C followed by stimulation with 2.5 µM A23187 with 3 µM AA. The reaction was stopped with 1 ml methanol, 500 µl D'PBS, 30 µl 1 N HCl and 200 ng PGB_1 as internal standard on ice. Lipoxygenase products were separated using solid phase extraction (SPE; 3.2.6) and determined using RP-HPLC (3.2.8).

3.2.3 Cellular assays

3.2.3.1 Determination of COX products in cellular test systems

To determine COX products, PBMC or monocytes (0.6 - 3 × 10^6/ml) were seeded in 12-well plates in CCM-0.5% CSS and stimulated with 10 µg/ml LPS for 24 h at 37 °C, 5% CO_2. Alternatively, freshly isolated PMNL (5 × 10^6/ml) were resuspended in PGC buffer and stimulated with 5 µM AA for 10 min. For inhibitor studies, freshly isolated monocytes (10^6/ml) seeded in 12-well plates in CCM-5% FCS were stimulated with 1 µg/ml LPS for 24 h at 37 °C, 5% CO_2. After 24 h, medium was replaced by D'PBS-C, cells were preincubated with compounds or vehicle (0.1% DMSO) for 15 min at 37 °C and stimulated with 1 µM AA for 30 min at 37 °C. The reactions were stopped on ice, supernatants were collected and centrifuged (400 × *g* / 10 min / 4 °C). Aliquots of 500 µl were mixed with 100 ng/ml PGB_1, 50 ng/ml PGE_2-d9 and 50 ng/ml TxB_2-d4 as internal standards and 30 µl/ml 1 N HCl. Samples were centrifuged (800 × *g* / 5 min / 4 °C) and COX products were extracted by SPE (3.2.6) and determined by LC-MS/MS (3.2.7). Alternatively, freshly isolated platelets (10^8/ml) resuspended in PGC buffer were preincubated with test compounds or vehicle (0.1% DMSO) for 15 min at RT followed by stimulation with 5 µM AA for 10 min at 37 °C. The reaction was stopped by addition of methanol and samples were treated as described for lipoxygenase product formation in cellular test systems (3.2.3.2). The formed COX-1 product 12-HHT was determined by RP-HPLC, according to [199].

3.2.3.2 Determination of lipoxygenase products in cellular test systems

PMNL or monocytes (2 - 3 × 10^6/ml) were resuspended in PGC buffer and preincubated with compounds or vehicle (0.1% DMSO) for 15 min at 37 °C followed by stimulation with either 2.5 µM A23187 alone or together with 20 µM AA for 10 min at 37 °C. Alternatively, cells were primed with 1 µg/ml LPS for 30 min and 0.3 U/ml ADA for 20 min at 37 °C, followed by stimulation with 1 µM fMLP for 5 min at 37 °C. Compounds or vehicle (1% DMSO) were added 15 min prior fMLP stimulation. The reactions were stopped by addition of 1 ml methanol together with 500 µl D'PBS and 30 µl 1 N HCl on ice. 200 ng PGB_1 were added as internal standard and samples were centrifuged (800 × *g* / 10 min / 4 °C). Eicosanoids were extracted by SPE (3.2.6) and determined by RP-HPLC (3.2.8). For lipid mediator profiling, 1.5 × 10^6 monocytes/ml seeded in 6-well plates in D'PBS-C were preincubated with compounds or vehicle (0.1% DMSO) for 15 min at 37 °C, followed by stimulation with 0.5 µM A23187 for 90 min at 37 °C. The reactions were stopped by addition of two volumes of methanol and addition of the internal standards (d4-PGE_2, d4-LTB_4, d5-LXA_4, d8-5S-HETE) on ice. Subsequently, samples were stored at -20 °C for at least 30 min. Afterwards, samples were centrifuged (1200 × *g* / 10 min / 4 °C), pH was adjusted to 3.5 by dilution with acidified H_2O and the content of methanol thereby was reduced to 25%. Samples were transferred to SPE (3.2.6) and lipid mediators were determined by LC-MS/MS (3.2.7). For cys-LT determination 3 × 10^6 monocytes/ml resuspended in PGC buffer were preincubated with compounds or vehicle (0.1% DMSO) for 15 min at 37°, followed by stimulation with 2.5 µM A23187 for 10 min at 37 °C. The reaction was stopped on ice, samples were centrifuged (400 × *g* / 10 min / 4 °C) and cys-LTs in the supernatants were determined by ELISA (cysteinyl leukotrienes ELISA kit,

Enzo Life Science Inc., NY, USA) following manufacturer's instructions. Leukotriene B_4 (LTB_4) was analyzed using RP-HPLC (3.2.8).

3.2.3.3 Determination of extracellular cytokine level

Freshly isolated monocytes (1.5 × 10^6/ml) were seeded in 96-well plates (200 µl cell suspension/well) in CCM-5% FCS. After 1 h at 37 °C, cells were preincubated with compounds or vehicle (0.5% DMSO) for 30 min at 37 °C, 5% CO_2, followed by stimulation with LPS 10 ng/ml for 4 h (determination of interleukin-8 (IL-8), tumor necrosis factor α (TNFα)), or 18 h (determination of IL-6, IL-1β) at 37 °C, 5% CO_2. Reaction was stopped on ice and cytokines in the supernatants were determined by in-house made ELISA.

3.2.3.4 Analysis of mRNA expression

PBMC (3 × 10^6) freshly isolated from heparinized whole blood resuspended in CCM-0.5% CSS were seeded in 12-well plates. After 1 h at 37 °C, cells were stimulated with 10 µg/ml LPS for 5 h or 18 h at 37 °C, 5% CO_2 or left untreated. Total RNA amount of PBMC was isolated using the E.N.Z.A. Total RNA Kit I (Omega Bio-tek Inc., GA, USA), following manufacturer's instructions. Total mRNA amount was detected by photometric measurement at 230 nm, 260 nm, 280 nm and 320 nm with a Nanodrop (Thermo Fisher Scientific Inc., MA, USA). Quality of isolated mRNA was confirmed by the ratios of A260 nm/A280 nm and A260 nm/A230 nm. cDNA was obtained from mRNA by reverse transcription using SuperScript® III First-Strand Synthesis SuperMix (Life technologies, MA, USA) with random hexamers incubated as follows: 5 - 10 min at 25 °C, followed by 50 min at 50 °C. The reaction was terminated at 85 °C for 5 min. cDNA was amplified by PCR (Mx3005P qPCR system, Agilent Technologies, CA, USA) with primers for COX-2, β-actin and beta-2-micoglobulin (B2M) (Table 3.2). PCR was conducted with the following protocol: Initial denaturation at 95 °C for 10 min (1 cycle), followed by 15 s denaturation at 95 °C, 30 s annealing at 60 °C and 30 s extension at 72 °C (45 cycles). The procedure was terminated with 60 s at 95 °C, 30 s at 55 °C and 30 s at 95 °C (1 cycle). To calculate the relative amount of COX-2 mRNA (normalized to β-actin), Maxima SYBR Green/ROX qPCR Master Mix (Fermentas, Darmstadt, Germany) was used in combination with the $2^{(-\Delta\Delta C(T))}$ method, according to [200]. Data was analyzed with the MxPro Software (Mx3005P/version 4.10, Agilent Technologies, CA, USA).

Table 3.1: Primer sequences.

Primer name	Strand	nucleotide sequence
COX-2	reverse	5'-AAAGGCGCAGTTTACGCTGTC-3'
	forward	5'-TGCATTCTTTGCCCAGCACT-3'
B-actin	reverse	5'- GAGCTGGAAGCAGCCGTGG-3'
	forward	5'-CTCACCGAGCGCGCTACGA-3'
B2M	reverse	5'-TTTGGAGTACGCTGGATAGCCT-3'
	forward	5'-CTCCGTGGCCTTAGCTGTG-3'

3.2.3.5 Determination of COX-2 protein expression, ERK1/2 and p-38 phosphorylation

For COX-2 protein expression, freshly isolated PBMC from human blood or PBMC or monocytes from leukocyte concentrates (1-3 × 10^6) seeded in 12-well plates in CCM- 0.5% CSS were incubated with 10 µg/ml LPS for 24 h at 37 °C, 5% CO_2. COX-2 expression was evaluated in whole cell lysates obtained according to 3.2.3.6 using SDS-polyacrylamide gel electrophoresis (SDS-PAGE; 3.2.9) with gels containing 10% acrylamide. Phosphorylation of ERK1/2 and p-38 MAPK was evaluated in freshly isolated PMNL (50 × 10^6/ml), resuspended in PGC buffer. Aliquots of 100 µl were preincubated with compounds or vehicle (1% DMSO) for 15 min at 37 °C, followed by stimulation with fMLP for 1.5 min at 37 °C. The reactions were stopped by addition of equal amounts of 2 × SDS-loading buffer (1 mM Tris/HCl (pH 8), 0.2 M EDTA, 10% (v/v) SDS, freshly added 10% (v/v) β-mercaptoethanol) on ice. To generate cell lysates, samples were treated as described in 3.2.3.6 and ERK1/2 and p-38 MAPK phosphorylation was determined as described in 3.2.9.

3.2.3.6 Generation of whole cell lysates

Cell lysates of PBMC and isolated monocytes were generated using NP-40 lysis buffer containing of 1% (v/v) NP-40, 1 mM sodium vanadate, 10 mM sodium fluoride, 5 mM sodium pyrophosphate, 25 mM β-glycerophosphate and 5 mM EDTA, 10 µg/ml leupeptin hemisulfate, 60 µg/ml soybean trypsin inhibitor (STI) and 1 mM phenylmethylsulfonyl fluoride (PMSF). Cells were lyzed for 30 min on ice with occasional agitation and cautious detachment of the cells from the culture plate. Lysates were centrifuged (10,000 × *g* / 5 min / 4 °C) and the protein amount in the supernatants was determined with a protein assay (Bio-Rad Laboratories, CA, USA). Subsequently, SDS-loading buffer I (50 mM Tris/HCl, pH 6.8, 2% (w/v) SDS, 10% (v/v) glycerol, 10% (v/v) β-mercaptoethanol, 12.5 mM EDTA, 0.02% (w/v) bromophenol blue) was added (loading buffer:supernatant = 1:4) and samples were boiled for 5 min at 96 °C. Protein expression was analyzed by SDS-PAGE (3.2.9).
Cell lysates of PMNL were generated by addition of the equal amount of SDS-loading buffer II (20 mM Tris/HCl, pH 8,5% (w/v) SDS, 10% (v/v) glycerol, 10% (v/v) β-mercaptoethanol, 20 mM EDTA) on ice followed by boiling for 5 min at 96 °C. Subsequently, samples were shattered by sonication (output 1, duty cycle 40%, 3 × 10 s on ice; SFX250, Branson, CT, US). After dilution with one fifth of bromophenol blue solution (33% (w/v) in glycerol), cell lysates were centrifuged (10,000 × *g* / 5 min / 4 °C) and analyzed by SDS-PAGE (3.2.9).

3.2.3.7 Fluorescence-activated cell sorting (FACS)

For evaluation of cell surface markers, freshly isolated monocytes (10^6/ml) seeded in 12-well plates in CCM-0.5% CSS were preincubated with 10 µg/ml LPS for 1 h at 37 °C, 5% CO_2 or left untreated. Monocytes were detached with biotase for 30 min at 37 °C, 5% CO_2 and centrifuged at 350 × *g*, for 6 min at 4 °C. The cells were resuspended in mouse serum (1:10) for 30 min at 4 °C followed by dilution with FACS buffer I (D'PBS containing 1% (m/v) BSA, 0.1% (m/v) NaN_3, 2 mM EDTA) and centrifugation (350 × *g* / 6 min / 4 °C). Subsequently, cells were mixed with the respective fluorescent antibodies (Table 3.5) for 15 min at 4 °C in the dark.

After centrifugation (350 × *g* / 6 min / 4 °C), cells were resuspended in FACS buffer I and cell surface markers were analyzed with the FACSCanto II (BD Bioscience, San Jose, CA, USA). Cell viability was monitored using 4',6-damidino-2-phenylindole (DAPI), IgG (mouse) was used as isotype control. For cell sorting, freshly isolated PBMC (50 × 10^6) were resuspended in FACS buffer II (D'PBS containing 1% (m/v) BSA, 2 mM EDTA) and mixed with the respective fluorescent antibodies (Table 3.5) for 20 min at 4 °C in the dark. After one washing step (350 × *g* / 6 min / 4 °C) cells were resuspended in FACS buffer II and sorted using the FACSAria™ Fusion (BD Bioscience, San Jose, CA, USA) at 4 °C by double cell exclusion. Cell viability was monitored by addition of DAPI. Cells were immediately used.

Table 3.2: Fluorescent antibodies used for FACS analysis.

Marker	Fluorochrome	Source
TLR4	PE	mouse
CD3	PE	mouse
CD19	FITC	mouse
CD14	APC-Alexa® Fluor 750	mouse
IgG	APC-Alexa® Fluor 750	mouse

3.2.3.8 Determination of [^{3}H]-AA-release and [^{3}H]-AA derived products in PMNL

To determine the release of AA and AA-derived products, freshly isolated PMNL (5 × 10^6) were resuspended in RPMI 1640 without additives and incubated with tritium-labelled AA (0.5 µCi/ml) for 2 h at 37 °C, 5% CO_2. Cells were washed twice with freshly prepared PG buffer containing 2 mg/ml fatty acid free BSA (600 × *g* / 10 min / 4 °C) and cell number was adjusted to 20 × 10^6/ml. The cell preparation was divided into aliquots of 0.5 ml, 1 mM Ca^{2+} was added and samples were incubated with the control inhibitor or vehicle (0.5% DMSO) for 10 min at 37 °C, followed by stimulation with A23187 for indicated times. The reaction was stopped on ice, samples were centrifuged (500 × *g* / 15 min / 4 °C) and 300 µl of obtained supernatants were mixed with 2 ml of liquid scintillation counting (LSC) fluid. Radioactivity was determined by scintillation counting (Micro Beta Trilux, Perkin Elmer, AM, USA).

3.2.3.9 Cell viability assay

MTT-assay

To evaluated the influence of the compounds on cell viability, a 3-(4,5-dimethylthiazol-2-yl)-2,5-diphenyltetrazolium bromide (MTT) assay was performed according to [201]. Freshly isolated monocytes (2 × 10^5/100 µl) were seeded in sterile 96-well plates CCM-5% FCS and after 1 h, cells were incubated with compounds or vehicle (0.3% DMSO) for 24 h at 37 °C, 5% CO_2. After addition of 20 µl MTT solution (5 mg/ml MTT in D'PBS, sterile filtered), samples were incubated for another 2-4 h at 37 °C, 5% CO_2 until blue formazan crystals appeared in the vehicle control due to reduction of MTT. To lyze the crystals, 100 µl SDS lysis buffer (10% (m/v) SDS in 20 mM HCl, pH 4.5) were administrated and samples were shaken for 20 h in the

dark at RT. Absorption was measured at 570 nm with a microplate reader (Thermo Fisher Scientific Inc., MA, USA).

LDH-assay

In order to determine the influence of test compounds on cell integrity, the lactate dehydrogenase (LDH) assay was performed. For this, 0.3 × 10^6 monocytes/200 µl were seeded in sterile 96-well plates in CCM-5% FCS. Cells were incubated with compounds or vehicle (0.3% DMSO) for 24 h at 37 °C, 5% CO_2, followed by collection of the supernatants by centrifugation at 600 × *g*, 5 min at 4 °C. To 100 µl of obtained supernatants 200 µl reaction mix (75 mM Tris, 1.5 mM pyruvate, 0.3 mM nicotinamide adenine dinucleotide (NADH) in H_2O) were added and absorbance of converted NADH was immediately assessed at 490 nm using a NOVOstar microplate reader (BMG Labtechnologies GmbH, Offenburg, Germany).

3.2.3.10 Immunofluorescence microscopy

To investigate subcellular 5-LO distribution, immunofluorescence microscopy was applied. Freshly isolated PMNL (3 × 10^6/ml) were seeded on poly-D-lysine-covered cover slips (Neuvitro Corp., Vancouver, WA, USA) in 12-well plates in PGC buffer. Cells were preincubated with compounds or vehicle (0.1% DMSO) for 15 min at 37 °C, followed by stimulation with 2.5 µM A23187 for 5 min at 37 °C. Subsequently, supernatant was removed and cells were fixed with paraformaldehyde (PFA, 4% (w/v)) solution for 20 min at RT. Autofluorescence of free formaldehyde was quenched with ammonium chloride (50 mM) for 20 min at RT. Cells were washed twice with D'PBS, permeabilized with ice cold acetone (100%) for 5 min at 4 °C and incubated with primary antibodies (5-LO, mouse, monoclonal, 1:100; FLAP, rabbit, polyclonal, 1:150) overnight at 4 °C in a humidity chamber. Samples were brought to RT and extensively washed with D'PBS, followed by incubation with fluorescent-labelled secondary antibodies Alexa Fluor 488 goat anti-rabbit IgG (1:1000) and Alexa Fluor 555 goat anti-mouse IgG (1:1000) for 30 min at RT. Samples were placed on microscope slides using ProLong® Diamond Antifade Mountant with DAPI (Thermo Fisher Scientific Inc., Waltham, MA, USA). The slides were stored at 4 °C in the dark until evaluation. For microscopic analysis of fluorescence an Axio Observer.Z1 inverted microscope and a LCI Plan-Neofluar 63x1.3 Imm Corr DIC M27 objective was used. Images were taken with an AxioCam MR3 camera and processed with AxioVision 4.8 software (all components from Carl Zeiss, Jena, Germany).

3.2.3.11 Determination of intracellular Ca^{2+}

Freshly isolated PMNL (50 × 10^6) were stained with the Ca^{2+}-sensitive dye Fura-2-acetoxymethyl ester (Fura-2-AM; 2 µM) for 45 min at 37 °C, 5% CO_2 in PG buffer in the dark, followed by a washing step (400 × *g* / 6min / 4 °C). Cells were resuspended in PG buffer containing 0.01% (m/v) BSA and the cell number was adjusted to 5 × 10^6/ml. Aliquots of 100 µl cell suspension were transferred to a 96-well plate and samples were preincubated with compounds or vehicle (1% DMSO) for 10 min at 37 °C. 2 min prior to stimulation with 1 µM fMLP, 1 mM Ca^{2+} was added. Fluorescence was monitored by excitation at 340 nm (Ca^{2+} bound Fura-2) and 380 nm (free Fura-2) and emission at 510 nm at 37 °C with a NOVOstar microplate reader (BMG Labtechnologies GmbH, Offenburg, Germany). After addition of triton

X-100 the maximal Ca^{2+} signals were detected at 340 nm, after addition of 10 mM EDTA the minimal Ca^{2+} signals at 380 nm. The amount of Ca^{2+} was calculated from the ratio of the signals at 340 and 380 nm, according to [202].

3.2.3.12 Determination of cellular reactive oxygen species formation

To determine cellular formation of reactive oxygen species (ROS) freshly isolated PMNL (0.5×10^6/100 µl, PG buffer) were pre-warmed in a 96-well plate for 3 min at 37 °C followed by pre-incubation with compounds or vehicle (0.3% DMSO) for 15 min at 37 °C. Oxidant-sensing fluorescent probe 2',7'-dichlorodihydrofluorescin diacetate (DCFH-DA) and 1 mM Ca^{2+} were added 2 min prior to stimulation with 1 µM fMLP or 0.1 µg/ml PMA. Fluorescence of the deacetylated dye (DCF) was monitored at an excitation of 485 nm and an emission of 535 nm using a NOVOstar microplate reader (BMG Labtechnologies GmbH, Offenburg, Germany).

3.2.3.13 Generation of cell homogenates

To generate cell homogenates, PMNL (50×10^6/ml) were resuspended in D'PBS containing 1 mM EDTA and kept at 4 °C for 5 min followed by sonication (3 × 10 s, 4 °C). After verifying cell disruption by light microscopy using trypan blue staining, homogenates were diluted 10-fold and inhibitor studies were performed as described for purified 5-LO enzyme (3.2.25).

3.2.4 *In vivo* evaluation of anti-inflammatory properties

The *in vivo* evaluation of the anti-inflammatory potential of the test compounds was performed at the laboratories of Dr. Lidia Sautebin at the Department of Pharmacy, University of Naples, Italy or the laboratories of Dr. Bruno D'Agostino, Department of Experimental Medicine, University of Naples. Male CD-1 mice (6-8 weeks, Charles River Laboratories, Calco, Italy) were housed in a controlled environment and provided with standard rodent chow and water. The experimental protocols were approved by the Animal Care Committee of the University of Naples, in compliance with Italian regulations on protection of animals used for experimental and other scientific purpose (Ministerial Decree 116/92) as well as with the European Economic Community regulations (Official Journal of E.C. L 358/1 12/18/1986). Compounds (10 mg/kg), zileuton (10 mg/kg) or vehicle (0.5 ml of 0.9% saline solution containing 2% DMSO) were given intraperitoneal (i.p.) 30 min before zymosan injection (0.5 ml of 2 mg/ml in 0.9% w/v saline). At specific time points after peritonitis induction (30 min and 4 h), mice were sacrificed by CO_2 inhalation and peritoneal exudates were collected by a lavage with D'PBS of the peritoneal cavity. Cells were counted using a light microscope in a Burker's chamber after vital trypan blue staining, exudates were centrifuged and stored at -80 °C for the determination of cys-LT formation. For carrageenan-induced paw oedema mice were lightly anaesthetized by inhalation of enflurane. Compounds (1 mg/kg) or vehicle (DMSO) were given i.p. 30 min before oedema was induced by subplantar injection of 50 µl carrageenan (1% (w/v)). Paw volume was measured with a hydroplethismometer (Ugo Basile, Milan, Italy) before and after indicated time points of carrageenan application.

3.2.5 Cell-free assays

3.2.5.1 Expression and purification of recombinant 5-LO

E. coli (BL21) was transformed with pT3-5-LO plasmid and recombinant 5-LO protein was expressed as described before with minor modifications [203]. Briefly, *E. coli* was cultured in LB-medium (5 g/l yeast extract, 10 g/l NaCl, 10 g/l peptone, pH 7.2) containing 100 µg/ml ampicillin, 5 µM iron(II) sulfate and 2 mM magnesium sulfate for 4 - 6 h at 30 °C. Once, an OD_{620} of 0.2-0.3 was reached, 190 µg/l isopropyl-β-D-thiogalactopyranoside was added to induce 5-LO expression at 30 °C, overnight. *E.coli* was collected by centrifugation at 7,700 × *g* for 15 min at 4 °C, resuspended in lysis buffer (50 mM triethanolamine (TEA)/HCl pH 8.0, 5 mM EDTA, 60 µg/ml STI, 1 mM PMSF, 2 mM DTT, 1 mg/ml lysozyme from chicken egg white) and kept on ice for 45 min. Cell lysis was completed by sonication (3 × 15 s, on ice) and the lysate was centrifuged at 40,000 × *g*, 20 min at 4 °C. The 5-LO enzyme protein was purified by affinity chromatography using an ATP-agarose column (Sigma A2767, Sigma-Aldrich, Taufkirchen, Germany), which was equilibrated with D'PBS containing 1 mM EDTA. After application of the supernatant the column was washed with 50 mM phosphate buffer containing 1 mM EDTA and 0.5 M NaCl, followed by phosphate buffer pH 7.4 with 1 mM EDTA. 5-LO protein was eluted with ATP solution (20 mM ATP, 50 mM phosphate buffer, 1 mM EDTA) [204].

3.2.5.2 Determination of lipoxygenase formation in cell-free systems

Semi-purified 5-LO was diluted with D'PBS/EDTA (1 mM). 3 µg aliquots were preincubated with compounds or vehicle (0.1% DMSO) for 15 min at 4 °C, followed by stimulation with 2 mM Ca^{2+} and 20 µM AA for 10 min at 37 °C. The reaction was stopped by addition of 1 ml methanol on ice. 500 µl D'PBS, 30 µl 1 N HCl, and 200 ng PGB_1 as internal standard were added and 5-LO products were subjected to SPE (3.2.6) and determined by RP-HPLC (3.2.8) as described before. For evaluations of reversible inhibition, partially purified 5-LO was preincubated with compounds at concentrations of 3 and 30 nM for 10 min at 4 °C. An aliquot of the 30 nM sample was diluted with the equal amount of assay buffer. After 10 min equilibration, both aliquots were stimulated with 2 mM Ca^{2+} and 20 µM AA for 10 min at 37 °C. Sample preparations and analysis was performed as described above.

3.2.5.3 Activity of isolated COX-1/2

To determine the influence of the compounds on isolated COX-1 and 2 [173], 50 U/ml ovine COX-1 and 20 U/ml human COX-2 were diluted in assay buffer (100 mM Tris, pH 8.0, 5 mM GSH, 5 µM hemoglobin, 100 µM EDTA) at 4 °C and aliquots of 1 ml were preincubated with compounds or vehicle (0.1% DMSO) for 5 min at RT. Samples were pre-warmed for 60 s at 37 °C, followed by stimulation with 5 µM AA (COX-1) or 2 µM AA (COX-2) for 5 min at 37 °C. The reaction was stopped with 1 ml methanol, 500 µl D'PBS, 30 ml 1 N HCl and 200 ng PGB_1 as internal standard on ice. The COX product 12-HHT was purified by SPE (3.2.6) and determined by RP-HPLC (3.2.8) as described before [199].

3.2.5.4 Induction of mPGES-1 expression in A549 cells, preparation of microsomes, and determination of mPGES-1 activity

Preparations of A549 cell microsomes and determination of mPGES-1 activity were performed as described before [177]. In brief, A549 cells (1×10^5/ml) were seeded in DMEM high glucose (4.5 g/l) supplemented with 10% (v/v) FCS, 2 mM L-glutamine, 100 U/ml penicillin and 100 µg/ml streptomycin for 20 h at 37 °C, 5% CO_2. After exchange of DMEM containing 2% (v/v) FCS cells were stimulated with 2 ng/ml IL-1β for 72 h at 37 °C, 5% CO_2. The cells were detached with trypsin/EDTA and washed with D'PBS (600 × *g* / 10 min / 20 °C). The obtained cell pellet was frozen in liquid nitrogen for 1 min, resuspended in homogenization buffer (0.1 M potassium phosphate buffer, pH 7.4, 1 mM PMSF, 60 µg/ml STI, 1 µg/ml leupeptin, 2.5 mM GSH and 250 mM sucrose) and sonicated (3 × 20 s). The homogenate was centrifuged (10,000 × *g* / 10 min / 4 °C) and microsomal fraction was extracted from obtained supernatant (174,000 × *g* / 1 h / 4 °C). Microsomal membranes were resuspended in homogenization buffer and the total protein concentration was determined with protein assay (Bio-Rad Laboratories, CA, USA). For determination of mPGES-1 activity, microsomal membranes (300 µg protein/ml) were diluted in homogenization buffer, preincubated with compounds or vehicle (1% DMSO) for 15 min at 4 °C, followed by initiation of product formation with 20 µM PGH_2 for 1 min at 4 °C. The reaction was stopped with 100 µl stop solution (40 mM iron(II) chloride, 80 mM citric acid, 10 µM 11β-PGE_2 as internal standard in H_2O) and samples were transferred to C_{18} columns (Clean-Up columns, UTC, Bristol, PA, USA) to extract PGE_2. Columns were preconditioned with 1 ml acetonitrile and 1 ml H_2O, samples were washed twice with 0.4 ml H_2O, eluted with 200 µl acetonitrile and extracts were diluted with 0.4 ml H_2O. PGE_2 formation was quantified by RP-HPLC using a C_{18} column (Nova-Pak cartridge, 5 × 100 mm, 4 µM particle size; Waters, Eschborn, Germany) with a mobile phase of acetonitrile/H_2O/TFA (30/70/0.007). PGE_2 was detected at 195 nm.

3.2.5.5 Preparation of microsomes from LTC_4S expressing HEK293 cells and determination of LTC_4S activity

Preparation of microsomes and determination of LTC_4S activity was performed as described before [193]. Briefly, 3×10^8 HEK293 cells expressing LTC_4S were harvested by trypsination, washed with D'PBS and frozen in liquid nitrogen. Afterwards, the cell pellet was resuspended in homogenization buffer (0.1 M potassium phosphate pH 7.4, 1 mM PMSF, 60 µg/ml STI, 1 µg/ml leupeptin, 2.5 mM glutathione, 250 mM sucrose). After incubation for 15 min, cell disruption was achieved by sonication (3 × 20 s, 4 °C) and the lysate was centrifuged twice (10,000 × *g* / 10 min / 4 C; 174,000 × *g* / 1 h / 4 °C). The microsomal fraction was resuspended in homogenization buffer and the protein amount was determined by a protein assay (Bio-Rad Laboratories, CA, USA). 2.5 µg/ml of protein was diluted in homogenization buffer containing 5 mM GSH and preincubated with compounds or vehicle (1% DMSO) for 10 min at 4 °C, with subsequent initiation of the product formation with 1 µM LTA_4-methyl ester. The reaction was stopped by addition of methanol, acidified D'PBS, and 5 ng LTC_4-d5-methyl ester as internal standard. The LTC_4S products were purified by SPE (3.2.6) and determined using LC-MS/MS (3.2.7).

3.2.5.6 Purification of soluble epoxide hydrolase and determination of activity

Human recombinant sEH was expressed in Sf9 cells and purified with affinity chromatography as described before [205, 206]. In brief, Sf9 insect cells were grown in suspension at 27 °C. Cells were infected with the recombinant baculovirus (kindly provided by Dr. B. Hammock, University of California, Davis, CA, USA) for 72 h, harvested and sEH was purified by affinity chromatography, dialyzed and concentrated using Amicon-ultra-15 centrifugal units (Merck Millipore, Darmstadt, Germany). To determine enzyme activity, the non-fluorescent substance 3-penyl-cyano(6-methox-2-naphthalenyl)-methyl ester-2-oxiraneaceic acid (PHOME) was used, based on conversion to the fluorescent 6-methoxy-naphtaldehyde by sEH. sEH was diluted in assay buffer (25 mM Tris/HCl, pH 7.0, 0.1 mg/ml BSA), preincubated with compounds or vehicle (1% DMSO) for 10 min at RT and to evaluate enzyme activity 50 µM PHOME were added for 60 min at RT in the dark. The reaction was stopped with zinc sulfate on ice and the fluorescence emission was monitored at 465 nm after excitation at 330 nm using a NOVOstar microplate reader (BMG Labtechnologies GmbH, Offenburg, Germany).

3.2.5.7 Evaluation of radical scavenging capacity

To evaluate the radical scavenging activity, reduction of the stable free radical 2,2-diphenyl-1-picrylhydrazyl (DPPH) was analyzed as described [207]. In brief, compounds were diluted to indicated concentrations and 100 µl were added to 100 µl DPPH solution (50 µM in ethanol, acetate buffered, pH 5-6.5) in a 96 well plate. Preparations were shaken for 30 min at RT in the dark following detection of the absorbance of the neutralized DPPH at 520 nm with a microplate reader (Thermo Fisher Scientific Inc., MA, USA).

3.2.6 Solid phase extraction

For solid phase extraction, sample preparations were centrifuged (800 × *g* / 10 min / 4 °C) and transferred to C_{18} SPE columns (Clean-Up columns, UTC, Bristol, PA, USA), which were washed with 1 ml methanol (100%) and preconditioned with 1 ml H_2O. To extract lipid mediators, columns were washed with 1 ml H_2O and 1 ml methanol (25%) and eluted from the column with 300 µl methanol (100%). Extracts were diluted with 120 µl H_2O, centrifuged (15,000 × *g* / 5 min / 4 °C) and lipid mediators were either determined with RP-HPLC (3.2.8) or LC-MS/MS (3.2.7). To extract prostanoids, columns were washed twice with 0.5 ml H_2O and eluted with 250 µl methanol (100%). After centrifuging twice (15,000 × *g* / 5 min / 4 °C) prostanoids were determined using LC-MS/MS (3.2.7). To extract eicosanoids for lipid mediator profiling in monocytes, obtained sample preparations were transferred to C_{18} columns (SepPak Vac C_{18} 6cc, Waters, Milford, MA, USA), which were washed with 6 ml methanol (100%) and preconditioned with 2 ml H_2O. Columns were washed with 6 ml H_2O and 6 ml hexane followed by elution with 6 ml methyl formate. Samples were evaporated until dryness using a TurboVap (TurboVap LV, Biotage, Uppsala, Sweden) with 5 - 10 PSI (N_2). Subsequently, samples were reconstituted in 100 µl Methanol/H_2O (1:1) and centrifuged twice (15,000 × *g* / 5 min / 4 °C). Lipid mediators were determined using LC-MS/MS (3.2.7).

3.2.7 UPLC-MS/MS analysis

Liquid chromatography tandem mass spectrometry (LC-MS/MS) analysis was conducted with an Aquity UPLC BEH C_{18} column (1.7 µm, 2.1 × 50 mm, Waters, Milford, MA, USA) for eicosanoid evaluation or an Aquity UPLC BEH C_{18} column (1.7 µM, 2.1 × 100 mm, Waters, Miford, MA, USA) for the lipid mediator profiling in monocytes using an Aquity^{TM} UPLC system (Waters, Milford, MA, USA). For Eicosanoid evaluation, chromatography was performed with a mobile phase composed of H_2O/acetonitrile (90/10, A) and acetonitrile (B), both acidified with 0.07% (v/v) formic acid, with a flow rate of 0.8 ml/min at 45 °C column temperature. Isocratic elution at A/B = 70/30 was performed for 2 min and followed by a linear gradient to A/B = 30/70 within 5 min. For the lipid mediator profiling in monocytes, chromatography was performed with a mobile phase composed of H_2O (A) and methanol (B), both acidified with 0.01% acetic acid, with a flow rate of 0.3 ml/min at 50 °C (column temperature). Elution by a linear gradient starting at A/B = 58/42 to 2/98 within 12.5 min, followed by isocratic elution performed for 3 min. The UPLC was coupled to a QTRAP 5500 mass spectrometer (AB Sciex, Darmstadt, Germany) equipped with a Turbo V^{TM} source and electrospray ionisation (ESI) probe. All lipid mediators were detected by multiple reaction monitoring (MRM) using the negative ion mode, based on specific ion fragmentation (Table 3.1) with following parameters: The ions spray voltage was -4000 to -4500 V, the declustering potential -30 to -120 eV, the entrance potential -5 to -10 eV and the collision cell exit potential -11 to -17 eV at a heater temperature of 500 °C. The curtain gas pressure was 35 psi, the nebulizer gas pressure 50 psi and the Turbo V gas pressure 80 psi. Detected eicosanoids were quantified using Analyst 1.6 software (AB Sciex, Darmstadt, Germany) with automatic peak integration using IntelliQuan default settings. Data were normalized to the internal standards PGB_1 given as relative intensities or d9-PGE_2 or d4-TxB_2, given as ng/ml.

Table 3.3.1: specific fragment ions and conditions used in MRM. Q1, first quadrupole; Q3, third quadrupole; Part 1.

	transitions 1			transition 2			
mediator	Q1 $(m/z)^2$	Q3 $(m/z)^3$	collision energy (eV)	Q1 $(m/z)^2$	Q3 $(m/z)^3$	collision energy (eV)	retention time (min)
Eicosanoid evaluation; column: 2.1 × 50 mm							
PGB_1	335.2	113.2	-31	335.2	221.2	-28	1.7
d9-PGE_2	360.2	189.0	-22	360.2	280.0	-20	0.6
d4-TxB_2	373.2	199.0	-38	-	-	-	0.4
PGE_2	351.2	189.0	-22	351.2	271.0	-20	0.6
TxB_2	369.2	195.0	-18	369.2	169.1	-25	0.4
$PGF_{2\alpha}$	353.2	193.0	-35	-	-	-	0.6
12-HHT	279.0	163.0	-30	-	-	-	3.3
Epi- trans LTB_4	335.2	195.0	-22	-	-	-	2.6
LTB_4	353.2	129.1	-26	353.2	195.0	-22	2.7
5-HETE	319.2	115.0	-20	319.2	203.0	-20	5.0
12-HETE	319.2	179.0	-18	-	-	-	4.8
15-HETE	319.2	219.0	-18	-	-	-	4.5
d5-LTC_4-ME	643.0	272.0	-30				3.1
LTC_4	624.0	272.0	-30				1.6

Table 3.3.2: specific fragment ions and conditions used in MRM. Q1, first quadrupole; Q3, third quadrupole; Part 2.

	transitions 1			transition 2			
mediator	Q1 $(m/z)^2$	Q3 $(m/z)^3$	collision energy (eV)	Q1 $(m/z)^2$	Q3 $(m/z)^3$	collision energy (eV)	retention time (min)
Lipid mediator profiling; column: 2.1 × 100 mm							
d8-5S-HETE	327.3	116.1	-17	-	-	-	10.9
d4-PGE_2	355.3	193.2	-25	-	-	-	5.1
d4-LTB_4	339.3	197.2	-22	-	-	-	8.1
d5-LXA_4	356.3	115.2	-19	-	-	-	5.8
PGE_2	351.3	189.1	-25	351.2	271.0	-20	5.1
PGD_2	351.3	233.1	-16	-	-	-	5.2
PGE_1/PGD_1	353.2	317.4	-18	335.2	273.4	-28	5.4
$PGF_{2\alpha}$	353.3	193.1	-34	-	-	-	5.4
TxB_2	369.3	169.1	-22	-	-	-	4.7
12-HHT	279.0	163.1	-30	-	-	-	8.7
ep/t-LTB_4	335.2	195.1	-22	-	-	-	7.6
LTB_4	335.2	195.1	-22	-	-	-	8.1
20-OH-LTB_4	351.3	195.1	-24	-	-	-	3.8
5-HEPE	317.2	115.2	-18	-	-	-	10.1
5-HETE	319.2	115.1	-21	-	-	-	11
11-HEPE	317.2	167.1	-19	-	-	-	9.6
11-HETE	319.2	167.1	-21	-	-	-	10.5
12-HEPE	317.2	179.1	-19	-	-	-	9.7
12-HETE	319.2	179.1	-21	-	-	-	10.6
14-HDHA	343.2	205.1	-17	-	-	-	10.6
15-HEPE	317.2	219.1	-18	-	-	-	9.6
15-HETE	319.2	219.1	-19	-	-	-	10.3
5,15-diHEPE	333.3	115.1	-22	333.3	235.1	-22	6.8
5,15-diHETE	335.3	201.0	-22	335.3	235.1	-30	7.8
RvD5	359.2	199.1	-21	359.2	261.1	-20	7.8

3.2.8 Reversed phase-HPLC

To determine 5-, 12- and 15-LO products, samples were centrifuged twice (15,000 × *g* / 5 min / 4 °C) after SPE to remove all solid particles. Chromatography was conducted with 50 µl of sample preparation on a C_{18} column (Nova-Pak cartridge, 5 × 100 mm, 4 µM particle size, Waters, Eschborn, Germany) using methanol/H_2O/trifluoroacetic acid (TFA) (73/27/0.007) as mobile phase with a flow rate of 1.2 ml/min at RT and isocratic elution [208]. The chromatographic system was coupled to an UV detector and leukotrienes (e.g. LTB_4 and its all-trans isomers) were detected at 280 nm, whereas metabolites with two conjugated double bonds (e.g. 5-H(p)ETE, 12-H(p)ETE, 12-HHT, 15-H(p)ETE) were detected as 235 nm. Based on PGB_1 as internal standard, metabolites were quantified by peak area integration.

3.2.9 SDS-PAGE and Western blot

Proteins from cell lysate preparations were separated using SDS-PAGE. A Mini-Protean electrophoresis system (Mini-PROTEAN® Tetra Cell, Bio-Rad Laboratories Inc., Hercules, CA, USA) was used. Cell lysates were added on a 10% or 12% polyacrylamide gel and vertically segregated immersed in running buffer (192 mM glycine, 25 mM Tris, 3.5 mM SDS). Using a

pre-stained marker (Protein-Marker IV, VWR Peqlab, Erlangen, Germany) size analysis could be conducted in a range between 10 to 170 kDa. For Western Blot analysis, proteins were electroblotted on nitrocellulose membranes (Amersham Bioscience, Little Chalfont, UK) with a tank blotting method (Bio-Rad Mini Trans-Blot® cell, Bio-Rad Powerpac™ Basic, Bio-Rad Laboratories Inc., Hercules, CA, USA) at 90 V for 90 min performed in a transfer buffer (48 mM Tris, 40 mM glycine, 20% (v/v) methanol). In order to verify appropriate protein transfer, membranes were stained by Ponceau (5% (w/v) Ponceau S in 5% (v/v) acetic acid). After blotting, membranes were washed and blocked in 5% BSA or 5% low fat powdered milk in TBS for 1 h at RT, followed by incubation with the primary antibody in TBS-Tween (TBS-T, 0,1% (v/v) Tween®20) containing 5% BSA overnight at 4 °C (antibodies see table 3.3). Afterwards, membranes were washed three times in TBS-T and incubated with fluorescent-labelled secondary antibodies IRDye 800 CW (dilution 1:10,000) and IRDye 680 LT (dilution 1:80,000) for 1 h at RT. Membranes were washed three times with TBS-T and once with TBS before drying at 37 °C in the dark. Proteins were detected using the Odyssey Infrared Imaging System (LI.COR Bioscience, Bad Homburg, Germany) and analyzed with Odyssey application software.

Table 3.4: Primary antibodies. Antibodies were diluted as indicated in 5% BSA or 5% low fat powdered milk in TBS-T.

antibody	source	dilution
COX-1	mouse, polyclonal	1:200, 5% BSA
COX-2	rabbit, polyclonal	1:1000, 5% milk
β-actin	mouse or rabbit, monoclonal	1:1000, 5% BSA or 5% milk
ERK1/2	rabbit, polyclonal	1:1000, 5% BSA
Phosphorylated-ERK1/2	mouse, monoclonal	1:1000, 5% BSA
p-38	rabbit, monoclonal	1:1000, 5% BSA
phosphorylated-p38	rabbit, monoclonal	1:1000, 5% BSA

3.2.10 Docking simulations with 5-LO

Docking simulations were performed in collaboration with Dr. Daniela Schuster (University of Innsbruck, Austria). The target protein was based on the 5-LO crystal structure 3o8y. To return the stable 5-LO [102] to wild type, four residues were exchanged *in silico* (Glu13Trp, His14Phe, Gly75Trp, Ser76Leu). Subsequently, the structure was energetically minimized in DS version 4.0. The binding site was defined in a 10 Å radius around Ile167. All ligands were drawn in ChemDraw version 14.0, converted to sd files with pipeline pilot version 9.1 and energetically minimized with OMEGA version 2.2.1. Simulations were conducted in GOLD version 5.2.

3.2.11 Statistics

Results are given as means ± standard error of the mean (SEM) of n observations, where n represents the number of different experiments at different days. Statistical evaluation was performed using GraphPad Prism 4 Software (San Diego, CA, USA). For paired observations, the Student's t-test was used with Welch's correction if variances were significantly different, for multiple comparison one-way ANOVA followed by a Bonferroni (≤ 5 groups) or Tukey-Kramer (> 5 groups) post-hoc test was applied. To determine normal distribution, the D'Agostino-Pearson omnibus test was performed. Paired observations which were not distributed normally were evaluated with the Mann-Whitney *U* test. A p value of 0.05 was considered significant (*). IC_{50} values were calculated by nonlinear regression (sigmoidal dose response/four-parameter logistic) with GraphPad Prism 4 Software.

4 RESULTS

4.1 The influence of sex on prostanoid formation

4.1.1 Difference in cell numbers of male and female whole blood

Recently published data by our group showed a sex-dependent difference in PGE_2 formation in zymosan-induced peritonitis in mice and carrageenan induced pleurisy in rats [5]. To investigate whether this sex difference appears also in human, fresh human whole blood (HWB), randomly collected from healthy volunteers, was used for experiments.

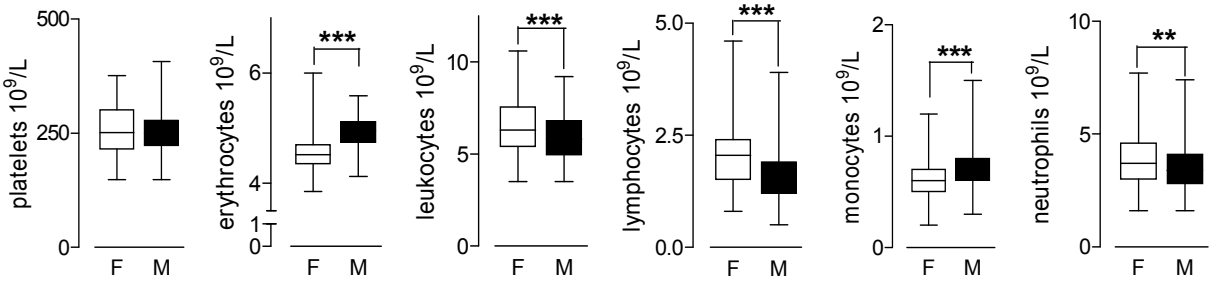

Figure 4.1: Blood cell population counts of human whole blood differ between sexes. F, female; M, male. Cell numbers of HWB were detected via flow cytometry at the laboratories of the blood donation centre of the Jena University Hospital. Data are shown as 25th, 50th, 75th percentiles and range; n = 174. Data for PLT, RBC, WBC and PMNL passed normality D'Agostino-Pearson omnibus test; **p < 0.01, ***p < 0.001, female vs. male, paired t-test. Data for lymphocytes and monocytes did not pass normality test; ***p < 0.001, female vs. male, Mann-Whitney *U* test.

Evaluation of cell numbers of HWB samples, revealed sex differences in the amount of different cell types in male and female HWB, which is consistent with other studies [209, 210]. Except for platelets, all blood cell types (erythrocytes, all leukocytes) revealed significant sex differences in the cell number (Figure 4.1). There were higher amounts of white blood cells in female HWB, which arise from higher counts of lymphocytes and neutrophils. Only monocytes and red blood cells showed significant higher cell numbers in male HWB. Given that monocytes together with neutrophils are the main producers of prostanoids in HWB [48, 211], this study focused on these cell types in the subsequent investigations and related data of HWB was always normalized to the cell number of monocytes plus PMNL.

4.1.2 Evaluation of prostanoid formation in male and female whole blood

The first step was to investigate effects of different physiological and non-physiological stimuli on the prostanoid formation in male and female blood. After stimulation for 24 h with various agents (Figure 4.2 and 4.3), the amounts of biosynthesized prostanoids were detected via liquid chromatography-tandem mass spectrometry (LC-MS/MS) or enzyme-linked immunosorbent assays (ELISA). In order to elucidate a COX-related group effect, three prostanoids were chosen for investigations: prostaglandin E_2 (PGE_2), thromboxane B_2 (TxB_2)

and prostaglandin $F_{2\alpha}$ ($PGF_{2\alpha}$). For physiological cell stimulation, two distinct toll-like receptor (TLR) activating ligands were applied, first LPS a TLR4 agonist and second Pam3CSK4, a TLR2/TLR1 agonist. Stimulation of HWB for 24 h with LPS (Figure 4.2 A) led to a significant higher biosynthesis of PGE_2 and $PGF_{2\alpha}$ in male blood compared to female. For $PGF_{2\alpha}$, there was already a sex-related difference in unstimulated conditions evident. However, TxB_2 showed the same tendency, but was not significant. Stimulation with the TLR2/TLR1 agonist Pam3CSK4 revealed a similar pattern (Figure 4.2 B). There was a tendency for higher amounts of PGE_2 and TxB_2 in male HWB. Furthermore, it seemed Pam3CSK4 had no stimulating effect on TxB_2 formation in female HWB in general.

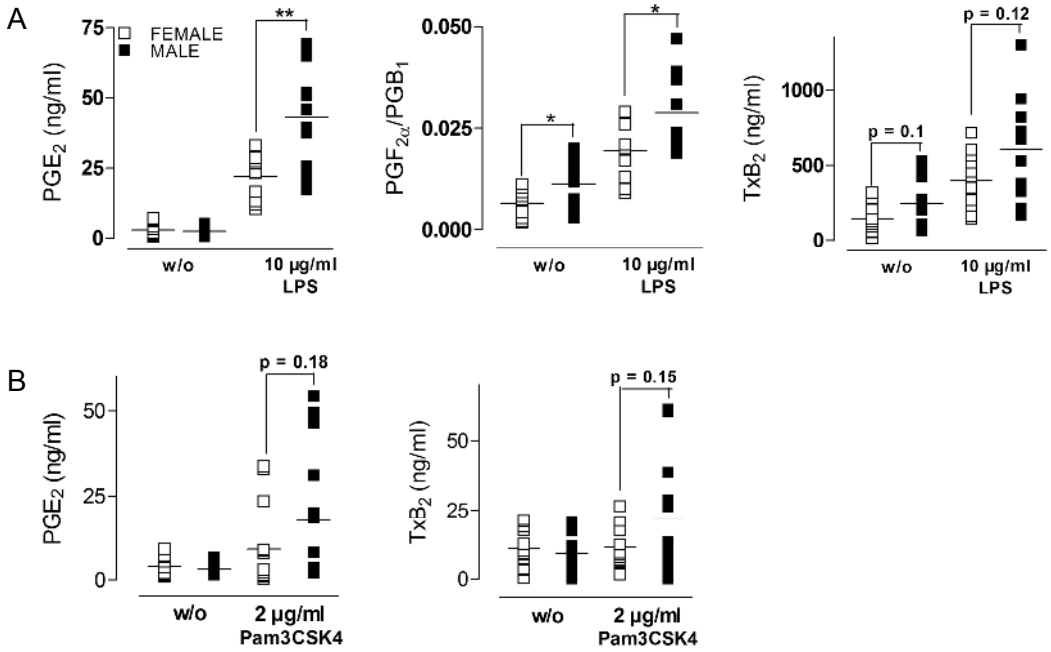

Figure 4.2: Prostanoid formation after TLR activation is higher in male versus female HWB. (A) 1 ml of HWB was either treated with vehicle (w/o; 0.5% PBS) or 10 µg/ml LPS for 24 h at 37 °C. Prostanoids were detected in the supernatant via LC-MS/MS. Data is shown as means ± SEM; (B) 1 ml of HWB was either treated with vehicle (w/o; 0.2% H_2O) or 2 µg/ml Pam3CSK4 for 24 h at 37 °C. Prostanoids were detected via ELISA following manufacturer's instructions. Data is shown as means ± SEM; (A) n = 11-13 (PGE_2), n = 10-12 ($PGF_{2\alpha}$), n = 10-13 (TxB_2); (B) n = 10-14 (PGE_2), n = 11-13 (TxB_2); data passed normality D'Agostino-Pearson omnibus test; *p < 0.05, **p< 0.01, female vs. male, unpaired t-test with Welch's correction if variances were significantly different. Data of HWB is normalized to number of monocytes plus PMNL.

To evaluate if this sex difference was related to a sex dimorphism in the TLR biology, HWB was challenged with arachidonic acid (AA; Figure 4.3 A), the Ca^{2+} ionophore A23187 (Figure 4.3 B), the bacteria-derived peptide fMLP (Figure 4.3 C) and the protein kinase C activator phorbol-12-myristat 13-acetate (PMA; Figure 4.3 D). Similar as for the incubation with TLR agonists, AA and A23187 led to a higher prostanoid formation in blood from males compared to females, either significantly or with a tendency. Following stimulation with fMLP (10 µM), there was a strong increase of PGE_2 in male but there was no stimulating effect in female HWB. The formation of both TxB_2 and $PGF_{2\alpha}$ increased in male and female following fMLP stimulation but more efficiently in males.

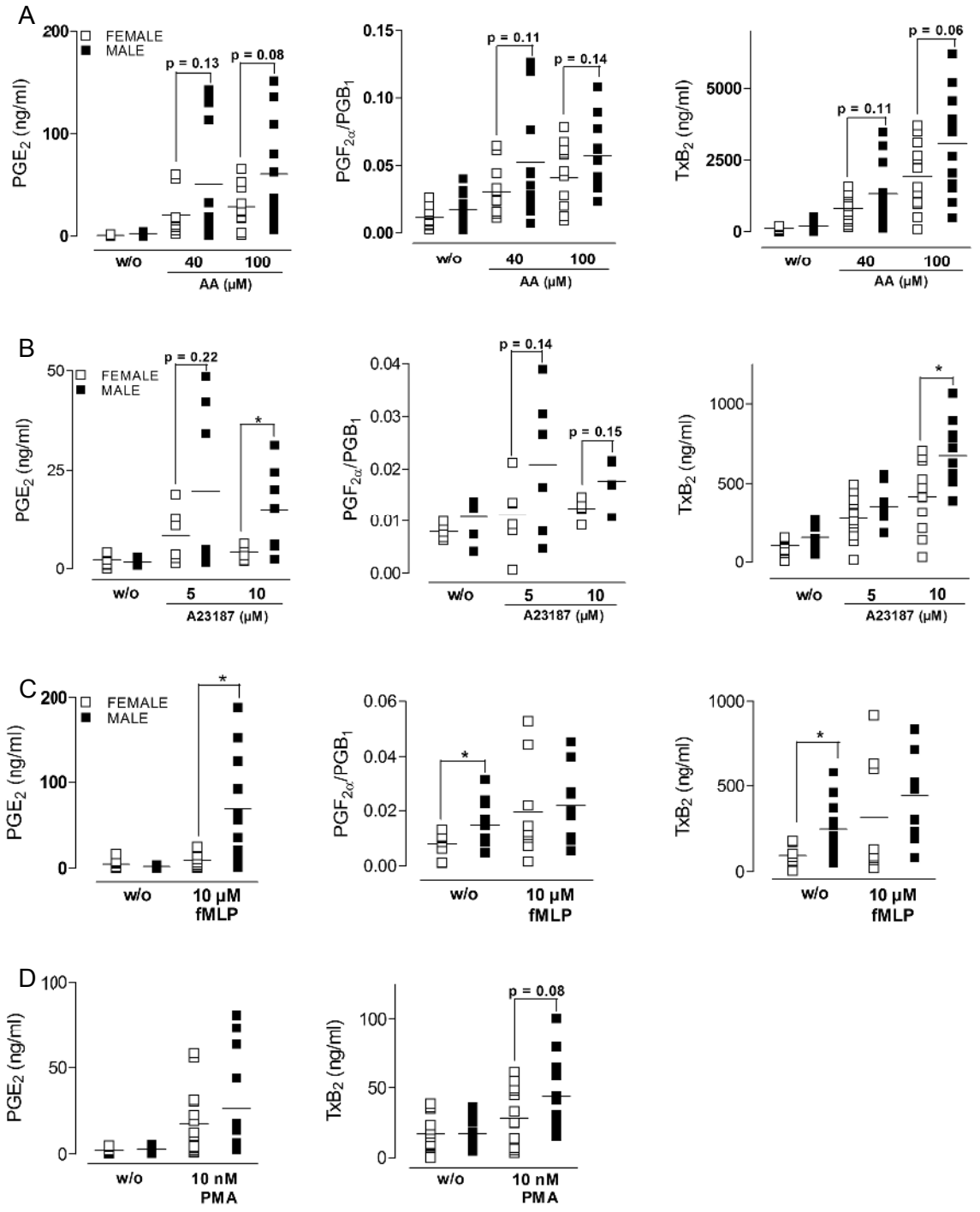

Figure 4.3: A tendency for higher prostanoid formation in male HWB samples verus samples from females. 1 ml of HWB was either treated with (A) vehicle (w/o; 0.25% EtOH) or AA at indicated concentrations, (B) vehicle (w/o; 0.5% MeOH) or A23187 at indicated concentrations, (C) vehicle (w/o; 0.1% DMSO) or 10 µM fMLP for 24 h at 37 °C. Prostanoids were detected in supernatants via LC-MS/MS. (D) 1 ml of HWB was either treated with vehicle (w/o; 0.1% DMSO) or 10 nM PMA for 24 h at 37 °C. Prostanoids were detected by ELISA following manufacturer's protocol. Data is shown as means ± SEM; (A) n = 8-12 (PGE_2), n = 11-13 ($PGF_{2\alpha}$ and TxB_2); (B) n = 6-7 (PGE_2), n = 4-6 ($PGF_{2\alpha}$), n = 9-12 (TxB_2); (C) n = 7-11 (PGE_2), n = 9-11 ($PGF_{2\alpha}$), n = 7-12 (TxB_2), (D) n = 11-13 (PGE_2), n = 13-14 (TxB_2) data passed normality D'Agostino-Pearson omnibus test; *p < 0.05, female vs. male, unpaired t-test with Welch's correction if variances were significantly different. Data of HWB is normalized to number of monocytes plus PMNL.

Note, the formation of $PGF_{2\alpha}$ and TxB_2 significantly differed between male and female already in unstimulated blood, which equalized after fMLP treatment. Stimulating the blood with 10 nM PMA, PGE_2 and TxB_2 levels increased after 24 h with no significant sex difference. Incubation of human whole blood with various stimuli generated higher levels of prostanoids, mainly PGE_2, in male samples compared to female. Even after normalization to the same cell number of monocytes plus PMNL the sex difference was evident.

4.1.3 Evaluation of prostanoid formation in male and female PBMC isolated from HWB

Amongst other cell types, monocytes are responsible for the immune response during inflammatory conditions [15]. They can be isolated from HWB together with T- and B-cells as mixed PBMC fraction. To investigate the sex-related prostanoid formation in PBMC, they were isolated from HWB, seeded in 12-well plates in cell culture medium containing human serum (sex hormones were removed by charcoal treatment) and stimulated for 24 h with LPS. The formed prostanoids were detected in the supernatant using LC-MS/MS (Figure 4.4 A). Due to the fact that male and female PBMC fractions contain different numbers of monocytes, data were normalized to the number of monocytes.

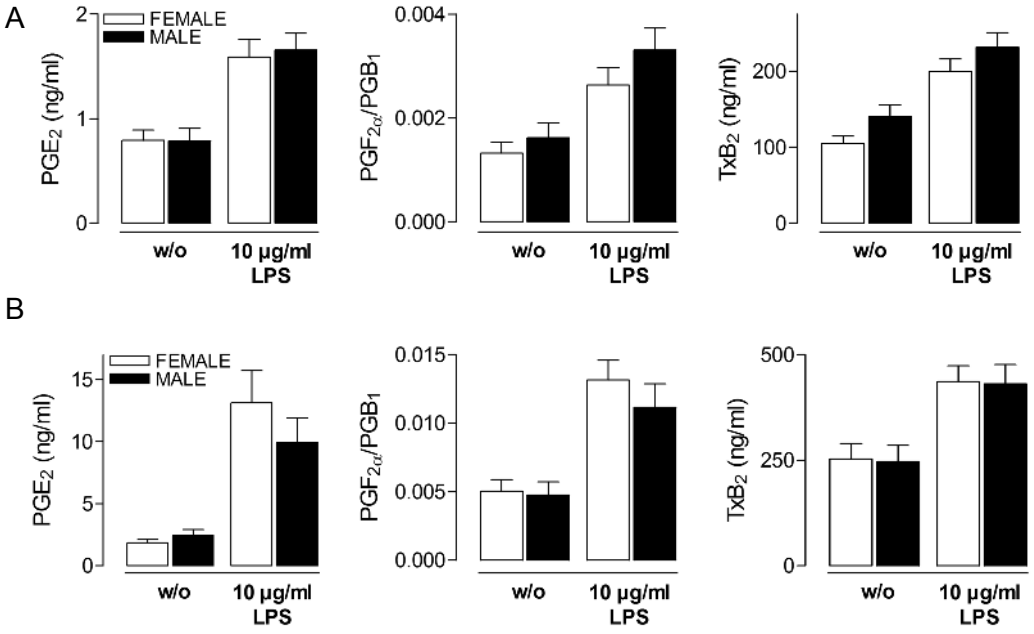

Figure 4.4: Sex differences in prostanoid formation in PBMC following stimulation with LPS are not apparent. 1×10^6 male and female PBMC isolated from HWB were seeded in (A) cell culture medium containing 0.5% of sex hormone free human serum (0.5% CSS) or (B) non-autologous human plasma, treated with either vehicle (w/o; 0.5% PBS) or 10 µg/ml LPS for 24 h at 37 °C. Supernatant was analyzed using LC-MS/MS. Data is shown as means ± SEM; (A) n = 14-15 (PGE_2), n = 13 ($PGF_{2\alpha}$), n = 11-15 (TxB_2); (B) n = 12-14 (PGE_2), n = 12-13 ($PGF_{2\alpha}$ and TxB_2); data passed normality D'Agostino-Pearson omnibus test; female vs. male, unpaired t-test with Welch's correction if variances were significantly different. Data is normalized to number of monocytes.

After incubation in cell culture medium and LPS stimulation for 24 h (Figure 4.4 A) no sex difference was evident regarding the PGE_2, $PGF_{2\alpha}$ and TxB_2 levels. Note, the total amount of prostanoids detected in stimulated PBMC was clearly below levels quantified in HWB. On one hand this could be due to missing factors out of the HWB for example the LPS binding protein (LBP), which is necessary for the activation of the TLR4 by LPS [212] or on the other hand due to lack of sex hormones [213, 214]. Therefore, female PBMC were seeded in non-autologous female plasma and male PBMC in non-autologous male plasma, respectively, to overcome this discrepancy (Figure 4.4 B). Interestingly, incubation of PBMC in human plasma could increase the overall prostanoid levels but could not restore the sex difference found in HWB, i.e. higher levels for male cells. In contrast, PGE_2 and $PGF_{2\alpha}$ levels were slightly higher in female PBMC, whereas there was no difference in TxB_2 formation.

4.1.4 Cyclooxygenase-2 gene expression and protein biosynthesis in isolated cells

During inflammation, the inducible cyclooxygenase-2 (COX-2) determines prostanoid formation [60] after LPS stimulation and is abundantly found in monocytes. To investigate if a diverse COX-2 expression was responsible for the sex difference in prostanoid formation in HWB, PBMC were isolated and mRNA levels were analyzed. Cells were either stimulated with vehicle or with LPS for 5 and 18 h. Total mRNA was extracted using a RNA Kit following manufacturer's instructions, cDNA was generated by reverse transcription and amplified by RT-qPCR. Figure 4.5 A shows the amounts of COX-2 mRNA expressed in female PBMC relative to male, where male data was set to 1 arbitrary. Independent of LPS stimulation female COX-2 mRNA levels were similar to male levels, indicating that in both healthy and inflammatory conditions no sex difference was evident in COX-2 mRNA expression.

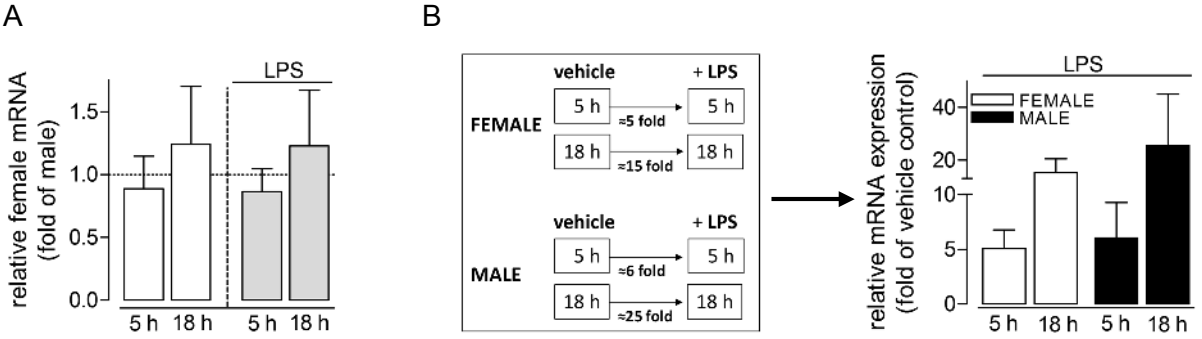

Figure 4.5: Sex differences in COX-2 mRNA expression in PBMC are not apparent. (A) 3×10^6 male and female PBMC were seeded in medium (0.5% CSS) and either incubated with vehicle (0.5% PBS) or 10 µg/ml LPS for 5 or 18 h at 37 °C. mRNA was extracted and determined using RT-qPCR. mRNA was normalized to β-actin. Data is shown as (A) fold of male samples (male mRNA level set to 1 arbitrary) or as fold of unstimulated controls at 5 h and 18 h of each sex (B), means ± SEM, (A)/(B) n = 3.

Additionally, the relative fold change in mRNA expression of stimulated to corresponding unstimulated samples was determined. Upon 5 h stimulation, the fold change in male and female PBMC was similar, whereas after 18 h stimulation a stronger increase occurred in male COX-2 mRNA expression.

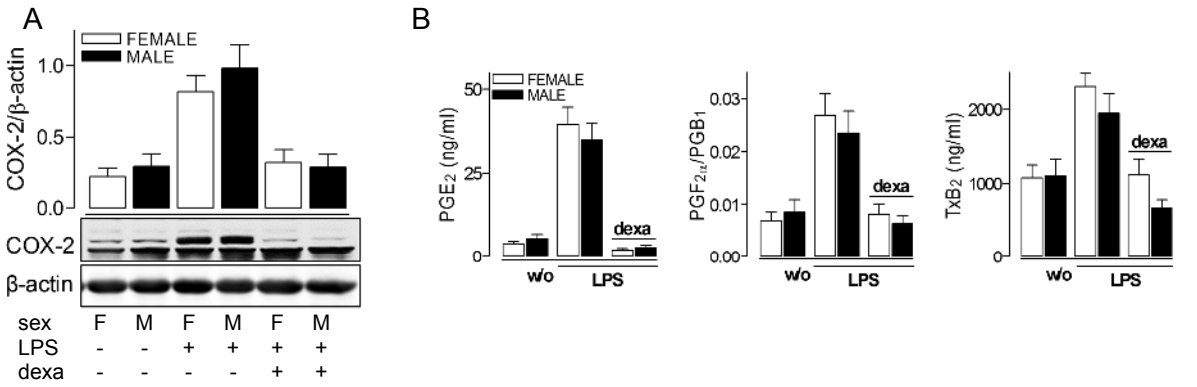

Figure 4.6: Sex differences in COX-2 protein expression and prostanoid formation after LPS stimulation in PBMC are not apparent. 3×10^6 PBMC were seeded in medium (0.5% CSS) and preincubated with 1 µM dexamethasone (dexa) or vehicle (w/o; 0.5% PBS) for 30 min, followed by stimulation with 10 µg/ml LPS for 24 h at 37 °C. (A) Cell lysates were obtained using NP-40 lysis buffer. COX-2 protein expression was determined via Western blot analysis; β-actin was used as control. Image represents 1 out of 13 independent experiments (dexa: n = 5). Data is presented as ratio of densitometry. (B) Prostanoids were determined in supernatant of cells used for Western blot analysis by LC-MS/MS. Data is shown as means ± SEM; n = 5-12; data passed normality D'Agostino-Pearson omnibus test; female vs. male, unpaired t-test. Data is normalized to number of monocytes.

However, mRNA-levels do not necessarily reflect protein biosynthesis. Therefore, the actual amount of COX-2 protein was evaluated using immunoblotting analysis. PBMC isolated from HWB were stimulated for 24 h with LPS and dexamethasone was used as negative control, since it is a well-known inhibitor of COX-2 expression [215]. COX-2 protein levels were determined as well as the formation of prostanoids in corresponding supernatants (Figure 4.6 A and B). In response to LPS the COX-2 protein biosynthesis in PBMC from HWB increased as expected, but with no sex difference. In parallel, the prostanoid formation, was evaluated upon LPS stimulation but with no difference either. It is important to mention that male and female donors show different numbers of monocytes within the mixed PBMC fractions. In this case, only for the prostanoid formation in the supernatants normalization could be performed, but is not possible for the Western blot data.

Table 4.1: Percentage of monocytes within PBMC fractions of male and female donors on different experimental days. LYM, lymphocytes; mono, monocytes; similar amounts of monocytes marked in bold.

	female			**male**		
	LYM 10^9/L	mono 10^9/L	mono %	LYM 10^9/L	mono 10^9/L	mono %
day 1	2.2	0.6	21.4%	2.7	1.1	28.9%
day 2	**2.9**	**0.9**	**23.7%**	**2.8**	**0.7**	**20.0%**
day 3	**1.3**	**0.5**	**27.8%**	**1.8**	**0.7**	**28.0%**
day 4	2.1	0.7	25.0%	1.0	0.7	41.2%
day 5	2.2	0.4	15.4%	1.1	0.7	38.9%
day 6	2.1	0.7	25.0%	1.2	1.1	47.8%
day 7	2.4	0.5	17.2%	1.3	0.9	40.9%
day 8	**2.2**	**0.6**	**21.4%**	**2.0**	**0.6**	**23.1%**
day 9	**2.0**	**0.8**	**28.6%**	**1.6**	**0.8**	**33.3%**
day 10	**1.6**	**0.6**	**27.3%**	**1.1**	**0.4**	**26.7%**
day 11	1.6	0.3	15.8%	0.9	0.9	50.0%
day 12	**1.2**	**0.6**	**33.3%**	**2.5**	**0.9**	**26.5%**
day 13	2.5	0.6	19.4%	1.9	1.1	36.7%

Table 4.1 shows the percentage of monocytes in different PBMC fractions of the blood samples used for Western blot analysis. Only on few experimental days, the number of monocytes were comparable (bold font). Taken together, male PBMC distinctly contained more monocytes what in turn did not lead to a higher COX-2 protein synthesis or a higher prostanoids formation. In fact, COX-2 protein and prostanoid levels were similar in males and females, indicating a higher COX-2 expression in female monocytes. Therefore, COX-2 protein expression was investigated additionally in monocytes isolated from leukocyte concentrates (buffy coats). Unexpectedly, after 24 h treatment with LPS no sex difference in COX-2 protein expression and no difference in prostanoid formation was evident, as seen before (Figure 4.7 A and B).

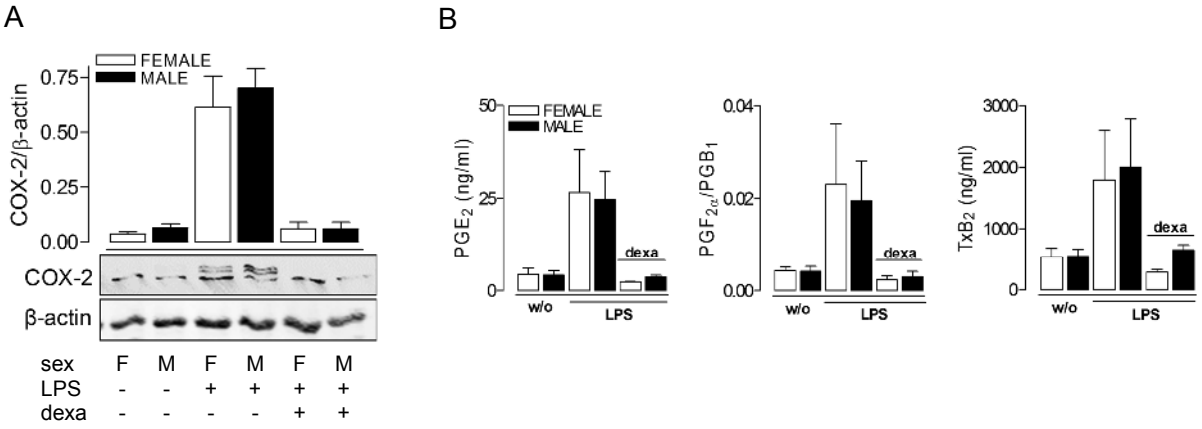

Figure 4.7: Sex differences in COX-2 protein expression and prostanoid formation after LPS stimulation in monocytes isolated from leukocyte concentrates are not apparent. 1×10^6 monocytes from leukocyte concentrates were seeded in medium (0.5% CSS) and preincubated with 1 µM dexamethasone (dexa) or vehicle (w/o; 0.5% PBS) for 30 min, followed by stimulation with 10 µg/ml LPS for 24 h at 37 °C. (A) Cell lysates were obtained using NP-40 lysis buffer. COX-2 protein expression was determined via Western blot analysis; β-actin was used as control. Image represents 1 out of 5 independent experiments. Data is presented as ratio of densitometry. (B) Prostanoids were determined in supernatant from cells used for Western blot by LC-MS/MS. Data is shown as means ± SEM; n = 5; data passed normality D'Agostino-Pearson omnibus test; female vs. male, unpaired t-test. Data is normalized to number of monocytes.

However, monocytes isolated following the standard protocol (Methods 3.2.2.1) still show impurities of lymphocytes (T-/B-cells). To prevent the influence of these cells, PBMC were separated using fluorescence-activated cell sorting (FACS). Therefore, PBMC isolated from leukocyte concentrates were incubated with appropriate antibodies (monocytes: CD14, APC-labelled; T-cells: CD3, PE-labelled; B-cells: CD19, FITC-labelled), separated by FACS analysis and stimulated with vehicle (0.5% PBS) or LPS for 24 h (Figure 4.8 A). COX-2 protein expression and prostanoid formation in the respective supernatants were analyzed. The results clearly show that (I) COX-2 was only expressed in monocytes and (II) when 99% pure monocytes were used, higher amounts of COX-2 protein were evident in females compared to males. However, prostanoid formation showed no significant sex difference (Figure 4.8 B). Taken together, neither the COX-2 mRNA expression nor the COX-2 protein biosynthesis was higher in male monocytes after LPS stimulation. Therefore, the COX-2 enzyme does not seem to be the cause for the determined difference in prostanoid levels in male HWB versus female.

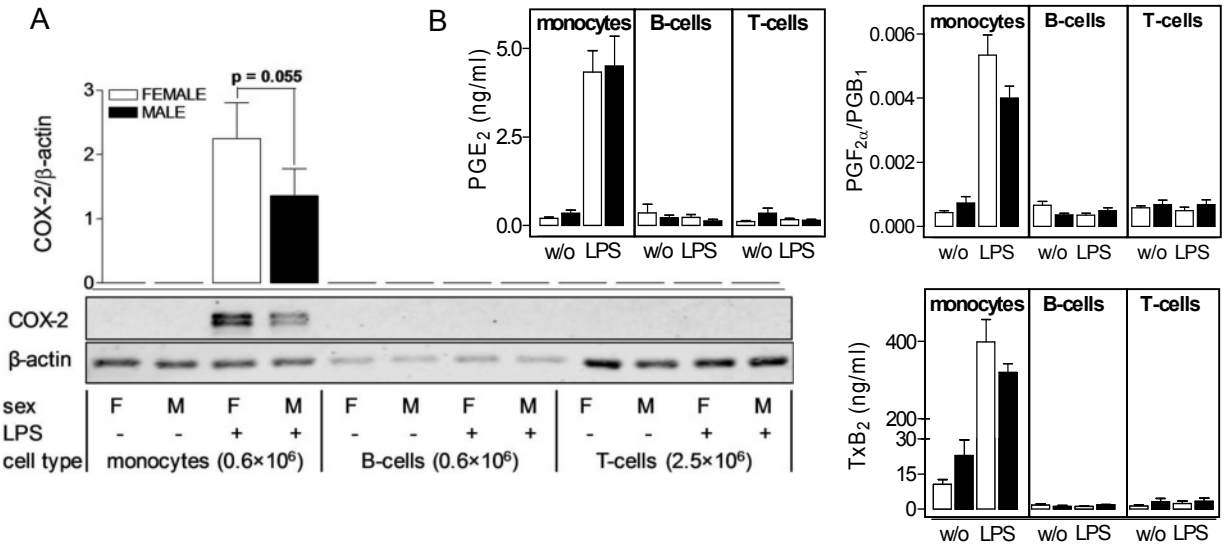

Figure 4.8: Higher COX-2 protein expression in female monocytes but no sex difference in prostanoid formation. (A) 50×10^6 PBMC isolated from leukocyte concentrates were treated with antibodies for 15 min on ice (monocytes, CD14, APC; B-cells: CD19, FITC; T-cells: CD3, PE). After cell separation by FACS, 0.6×10^6 monocytes, 0.6×10^6 B-cells and 2.5×10^6 T-cells were seeded in medium (0.5% CSS) and incubated with vehicle (w/o; 0.5% PBS) or 10 µg/ml LPS for 24 h at 37 °C. Cell lysates were obtained using NP-40 lysis buffer. COX-2 protein expression was determined via Western blot analysis; β-actin was used as control. Image represents 1 out of 5 (T-/B-cells) - 8 (monocytes) independent experiments. Data is presented as ratio of densitometry and passed normality D'Agostino-Pearson omnibus test; female vs. male, paired t-test. (B) Prostanoids were determined in supernatants from cells used for Western blot by LC-MS/MS. Data is shown as means ± SEM; n = 5-7 (PGE_2), n = 4-6 ($PGF_{2\alpha}$), n = 4-7 (TxB_2); data passed normality D'Agostino-Pearson omnibus test; female vs. male, unpaired t-test with Welch's correction if variances were significantly different.

4.1.5 Influence of TLR4 expression on the monocyte cell surface

An initial step of the LPS-mediated COX-2 expression is the binding and thus activation of TLR4 on the cell surface. Hence, the presence of TLR4 on male and female monocytes was evaluated. Monocytes were isolated from leukocyte concentrates and TLR4 expression was analyzed by flow cytometry in untreated conditions and after 1 h stimulation with LPS. In untreated cells TLR4 expression was elevated on female monocytes compared to male and after 1 h incubation the TLR4/LPS complex got internalized to equal proportions, leaving a higher amount of TLR4 on the cell membrane of female monocytes.

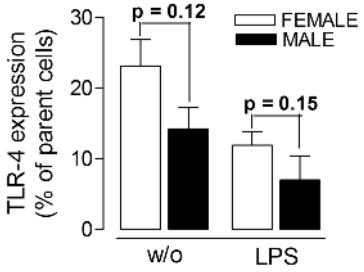

Figure 4.9: Higher TLR4 expression on the cell surface of female monocytes. 1×10^6 monocytes isolated from leukocyte concentrates were left untreated (w/o) or stimulated with 10 µg/ml LPS for 1 h at 37 °C. Afterwards cells were incubated with fluorescent antibodies for flow cytometry (monocytes: CD14, APC; TLR4, PE). Data is shown as percentage of monocytes expressing TLR4 (parental monocytes = 100%), n = 3; female vs. male paired t-test.

4.1.6 Influence of exogenously provided sex hormones in HWB and isolated cells

Sex hormones could play a role in the sex-related difference of prostanoid formation in blood, since there are several reports that sex hormones are involved in immune reactions [76, 216]. Therefore, HWB was preincubated with different sex hormones, followed by stimulation with LPS for 24 h. Unfortunately, in this set of experiments no sex difference in prostanoid formation was evident following LPS stimulation for 24 h in HWB (Figure 4.10 A). As a result, it could not be answered whether male sex hormones are able to increase prostanoid formation in female HWB to levels detected in males, or the other way around, if female sex hormones are able to decrease prostanoid formation in male HWB down to levels seen in female HWB. Nonetheless, none of the sex hormones appeared to affect prostanoid formation in female blood, whereas all hormones independent of sex marginally increased prostanoid formation in male HWB. To exclude the influence of other cell types and plasma proteins like albumin, which can bind the sex hormones, PBMC were isolated from HWB and seeded in cell culture medium, additionally (Figure 4.10 B). Male and female PBMC were preincubated with sex hormones and stimulated with LPS for 24 h. As seen before, if PMBC were isolated from the HWB, there was nearly no difference in prostanoid formation between males and females.

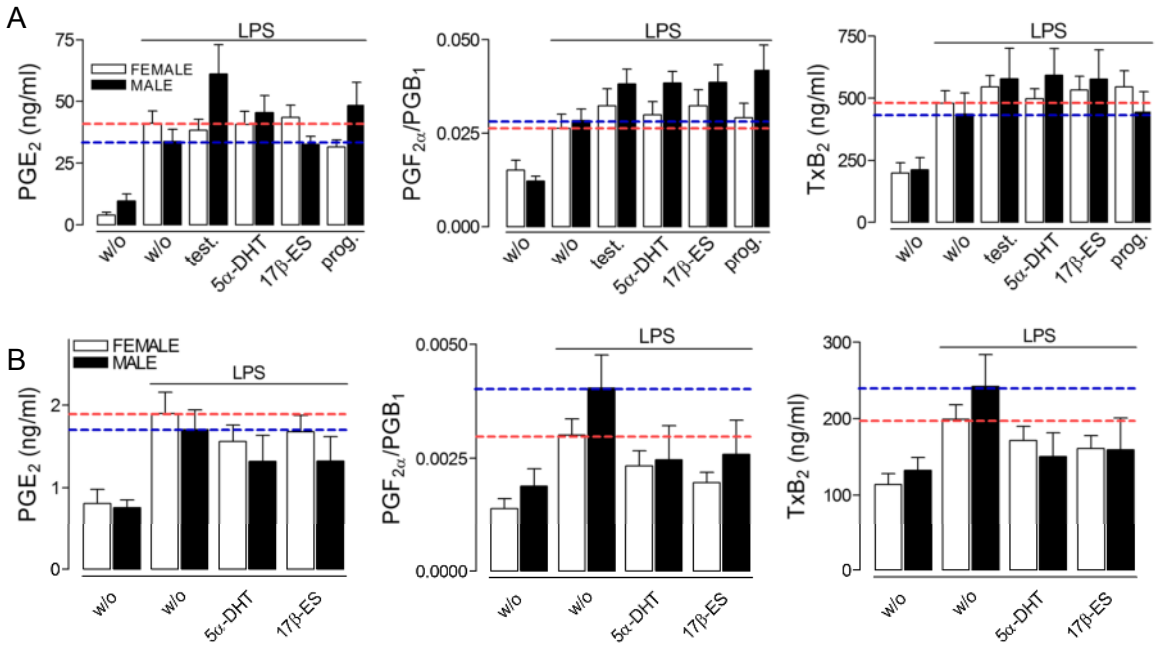

Figure 4.10: Lack of influence of sex hormones on prostanoid formation in HWB and isolated PBMC. (A) 1 ml of HWB or (B) 3×10^6 male and female PBMC isolated from HWB, seeded in their distinct plasma, were preincubated for 30 min at 37 °C with sex hormones as follows (HWB): test. = 300 nM testosterone, 5α-DHT = 300 nM 5α-dihydrotestosterone, 17β-ES = 300 nM 17β-estradiol, prog. = 3 µM progesterone; or in PBMC as follows: 30 nM 5α-DHT or 30 nM 17β-ES. Upon preincubation HWB or PBMC were treated with vehicle (w/o; 0.5% PBS) or 10 µg/ml LPS for 24 h at 37 °C. Prostanoid formation was determined in supernatants by LC/MS-MS. Data is shown as means ± SEM; (A) n = 7-11 (PGE_2), n = 8-11 ($PGF_{2\alpha}$), n = 9-10 (TxB_2); (B) n = 4-6 (PGE_2, TxB_2), n = 4-7 ($PGF_{2\alpha}$); data passed normality D'Agostino-Pearson omnibus test; female vs. male, unpaired t-test with Welch's correction if variances were significantly different. Data of HWB is normalized to number of monocytes plus PMNL, data of PBMC is normalized to number of monocytes.

In contrast to the findings of HWB pre-treated with sex hormones where the exogenous hormones exerted rather stimulating effects, they showed a moderately decreasing effect in both male and female PBMC, regarding all three prostanoids.

4.1.7 Prostanoid formation in HWB and cyclooxygenase-1 in short-term incubations

In long term incubations, e.g. for 24 h, prostanoid formation is mainly mediated by inducible COX-2. Additionally, there exists also the constitutively expressed COX-1, which mediates prostanoid formation within shorter incubation periods. To determine if the sex difference discovered in HWB was mediated rather by COX-1 activity than COX-2, short time stimulations were performed (Figure 4.11). Male and female HWB was incubated with AA (40 µM and 100 µM) for 10 min or with A23187 (30 µM) for 10 and 30 min at 37 °C.

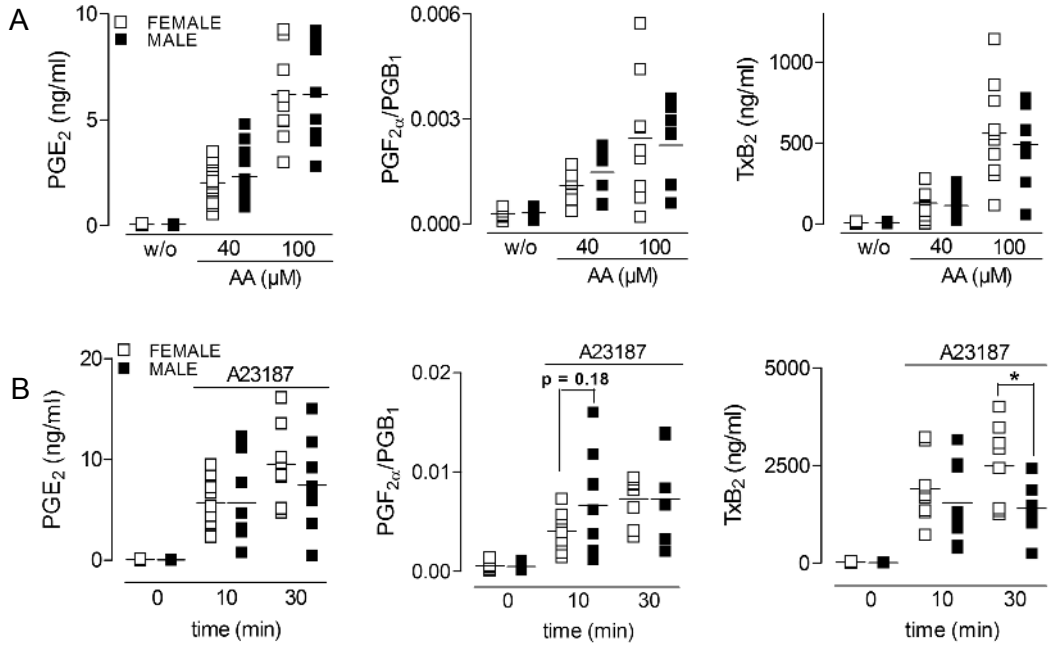

Figure 4.11: Sex differences in short term incubations of HWB following stimulation with A23187 but not with AA. (A) 1 ml of HWB was treated with (A) vehicle (w/o; 0.5% EtOH) or 40 µM or 100 µM AA for 10 min at 37 °C, or (B) with vehicle (w/o; 0.5% MeOH) or 30 µM A23187 for 10 and 30 min. Prostanoid formation was analyzed by LC-MS/MS in supernatants. Data is shown as means ± SEM; (A) n = 10-15 (PGE_2), n = 7-10 ($PGF_{2\alpha}$), n = 8-14 (TxB_2); (B) n = 7-9 (PGE_2, TxB_2), n = 8-9 ($PGF_{2\alpha}$); data passed normality D'Agostino-Pearson omnibus test; female vs. male, unpaired t-test with Welch's correction if variances were significantly different. Data is normalized to number of monocytes plus PMNL.

In contrast to incubations for 24 h with AA, in short time incubations there was no significant sex difference in prostanoid formation for all three mediators derived from AA (Figure 4.11 A). In treatment of HWB with A23187 all three prostanoids appeared to increase stronger in female blood over time compared to male (Figure 4.11 B), showing a significant difference in TxB_2 formation after 30 min.

Furthermore, the COX-1 protein levels were investigated in PBMC isolated from HWB (Figure 4.12). Only male and female samples with comparable amounts of monocytes were used (Table 4.2). Western blot analysis revealed a tendency to higher COX-1 expression in female PBMC from HWB. This finding might explain the results of prostanoid formation obtained in incubations with AA and A23187 for 10 or 30 min in male and female HWB but otherwise COX-1 does not contribute to the sex difference in prostanoids in HWB after 24 h.

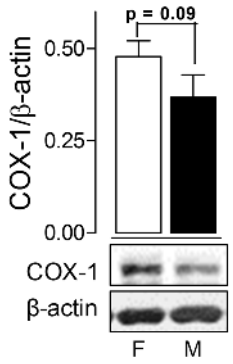

Figure 4.12: COX-1 protein expression in male and female PBMC isolated from HWB. 3×10^6 PBMC isolated from male and female HWB were used untreated. Cell lysates were obtained using lysis buffer. COX-1 protein expression was determined via Western blot analysis; β-actin was used as control. Image represents 1 out of 5 independent experiments. Data is presented as ratio of densitometry and passed normality D'Agostino-Pearson omnibus test. Female vs. male, paired t-test.

Table 4.2: Percentage of monocytes within PBMC fractions.

	female	male
	mono (%)	mono (%)
day 1	16.7	22.7
day 2	26.1	33.3
day 3	21.1	27.8
day 4	21.2	25.0
day 5	31.3	24.1

4.1.8 Evaluation of prostanoid formation in male and female PMNL isolated from HWB

PMNL are responsible for the early immune response but display a shorter lifetime compared to monocytes [217]. To investigate whether these cells contribute to the sex difference in prostanoid formation in HWB, they were isolated from male and female HWB and incubated for 10 min with 5 µM AA (Figure 4.13 A). In general, PMNL produced only little amounts of prostanoids and showed no difference in prostanoid formation between males and females. Under these conditions, $PGF_{2\alpha}$ formation was below detection limit. Additionally, in PMNL isolated from leukocyte concentrates the release of AA was investigated (Figure 4.13 B).

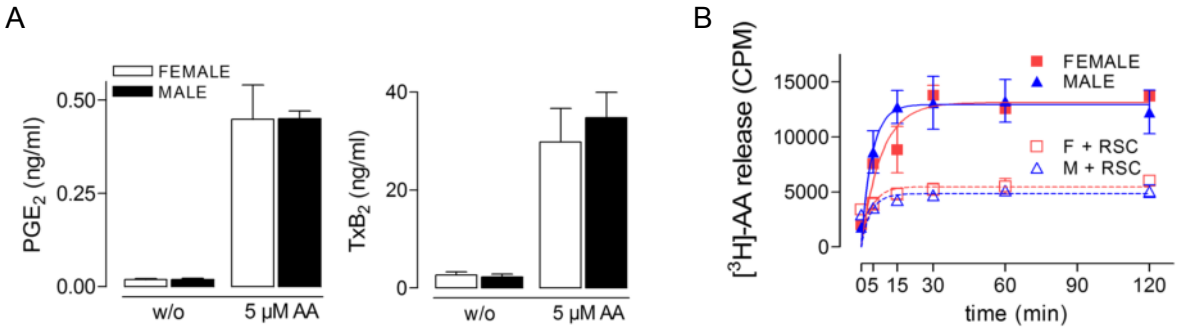

Figure 4.13: Sex differences in prostanoid formation and AA-release in isolated PMNL are not apparent. (A) 5×10^6 PMNL isolated from male and female HWB were treated with vehicle (w/o; 0.5% EtOH) or 5 µM AA for 10 min at 37 °C in PBS-glucose. Prostanoid formation was determined in supernatants using LC-MS/MS. Data is shown as means ± SEM; n = 5-8 (PGE_2), n = 7-8 (TxB_2); data passed normality D'Agostino-Pearson omnibus test female vs. male, unpaired t-test. (B) PMNL isolated from leukocyte concentrates were treated with 0.5 µCi/ml tritium labelled AA ([^{3}H]-AA) for 2 h at 37 °C. Afterwards, cells were pre-treated with 2 µM RSC-3388 (RSC) or vehicle (0.5% MeOH) for 10 min and stimulated with 0.5 µM A23187. Radioactivity was measured with scintillation counter in supernatants at indicated time points. Data is shown as counts per minute (CPM); means ± SEM, n = 2; curve fitted with one side exponential association.

PMNL were incubated with [^{3}H]-AA for 2 h to incorporate the fatty acid in their cell membranes. Upon cell stimulation by 0.5 µM A23187, [^{3}H]-AA was released from the membranes and converted into lipid mediators. The well-known cPLA$_2$ inhibitor RSC-3388 was used as control. With detection of scintillation not only free [^{3}H] labelled AA but also all mediators derived from the labelled AA were determined. After 15 to 30 min, the A23187-induced AA release/AA-product formation in male and female cells reached a plateau, stable up to 2 h, with no sex difference, comparable with the prostanoid formation in PMNL after 10 min. This indicates that PMNL do not contribute to the sex specific difference in prostanoid formation in HWB.

4.1.9 Differences in the time-dependent degradation of prostanoids

Levels of prostanoids in the blood not only depend upon the rate of synthesis, but also on the rate of degradation. Therefore, the prostanoid catabolism is another point to consider, regarding the difference in prostanoid levels. The enzyme responsible for PGE$_2$ degradation and in parts also for other prostanoids is the 15-hydroxyprostaglandin dehydrogenase (15-PGDH) [218] and several studies showed sex-dependent effects in its expression and activity [219, 220]. To test whether the catabolism was responsible for the different prostanoid formation in HWB, a high-affinity and non-competitive 15-PGDH inhibitor (SW033291) was used [221]. HWB was preincubated with the inhibitor followed by stimulation.

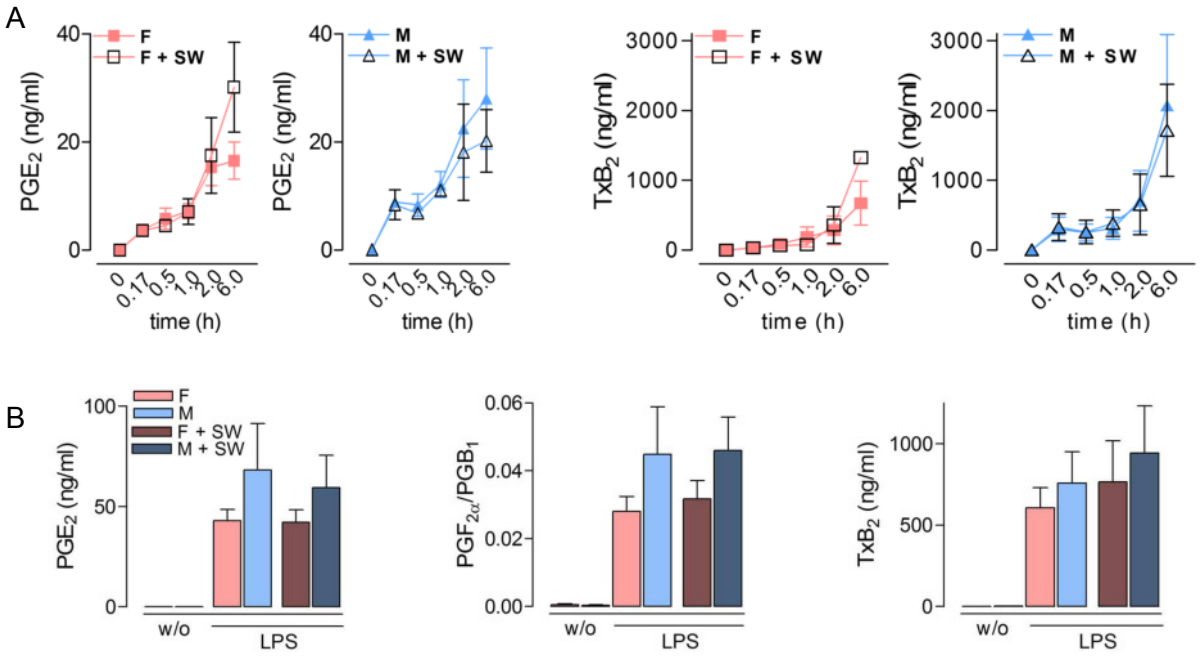

Figure 4.14: Evaluation of the 15-PGDH inhibitor SW033291 in HWB in short-and long-term incubations. (A) 1 ml of HWB was pre-incubated with 10 µM SW033291 for 30 min at 37 °C, followed by stimulation with 40 µM AA. Prostanoid formation was analyzed at indicated time points using LC-MS/MS. Data is shown as means ± SEM; n = 2 (6 h)-3. Data is normalized to number of monocytes plus PMNL. (B) 1 ml of HWB was pre-incubated with 10 µM SW033291 or vehicle (w/o; 0.5% PBS) for 30 min at 37 °C, followed by stimulation with 10 µg/ml LPS for 24 h at 37 °C. Prostanoid formation was analyzed in supernatants by LC-MS/MS. Data passed normality D'Agostino-Pearson omnibus test female vs. male, unpaired t-test. Data is shown as means ± SEM; n = 5. Data is normalized to number of monocytes plus PMNL.

For early time points up to 6 h AA was used as stimulus (Figure 4.14 A), for long term incubation (24 h) LPS (Figure 4.14 B). To verify whether initially higher prostanoid formation in male individuals in HWB was mediated due to a higher activity or expression of 15-PGDH in females, the prostanoid levels should be equalized after pre-treatment with the inhibitor. After short-term incubations up to 2 hours with AA, no difference in female blood between samples with and without pre-treatment appeared. Only at 6 h AA incubation, the inhibitor increased the PGE_2 formation in female HWB up to the level obtained in males (M w/o SW: 28.0 ± 9.3 ng/ml; F plus SW: 30.1 ± 8.3 mg/ml). The same effect was visible in TxB_2 formation, though the higher PGE_2 level detected in female samples treated with SW033291 could not entirely reach the level in males (M w/o SW: 2073.0 ± 1016.2 ng/ml; F plus SW: 1326.3 ± 39.32 ng/ml). In contrast, the inhibitor had no effect in male blood on TxB_2 formation, PGE_2 formation appeared to be even lower compared to untreated samples. Amounts of $PGF_{2\alpha}$ were not influenced in both sexes by the inhibitor (data not shown). Even though, after 24 h incubations with LPS, the inhibitor did not longer influence the prostanoid biosynthesis (Figure 4.14 B), 15-PGDH seems to play a role in the sex-biased prostanoid formation in blood.

4.1.10 Involvement of cell-cell interactions in sex related differences of prostanoid formation

So far, a concrete cause leading to the sex difference in prostanoid formation in HWB could not be identified. Interactions between platelets and immune cells forming heterogeneous aggregates are known to play an important role in inflammation, e.g. in cardiovascular diseases [222-224]. Therefore, the cross talk between PMNL and PBMC was evaluated in more detail. One part of HWB was used to obtain plasma, as well as PBMC and PMNL, the other part was left untreated. Then, PMNL and PBMC were added in autologous plasma alone or together to investigate the effect of a cell-cell interplay. Afterwards, blood, cells and cell mixtures of PMNL and PBMC were stimulated with LPS (Figure 4.15) or AA (Figure 4.16) for 24 h. After LPS stimulation, only in PMNL formation of PGE_2 was higher in female cells, whereas in PBMC, PBMC plus PMNL and HWB itself, prostanoid formation was higher in males. Cell interactions seemed to push the formation in male cells, overcoming the higher amount of PGE_2 formed by female PMNL. TxB_2 formation showed a similar pattern, though the higher formation in female PMNL lowered the TxB_2 difference in the cell mixture consisting of PBMC plus PMNL, compared to PBMC alone. In whole blood, there was the previous determined tendency to higher prostanoid levels in males. In contrast, $PGF_{2\alpha}$ formation in unstimulated PMNL was substantially higher in female cells and rather equal after LPS treatment, which resulted in same $PGF_{2\alpha}$ levels in both sexes. In PBMC alone, there was a tendency to a higher $PGF_{2\alpha}$ formation in male cells, but in the cell mixture of PBMC plus PMNL to higher levels in female cells. Nevertheless, in HWB the difference in prostanoid formation was restored to higher levels in male blood, as seen before.

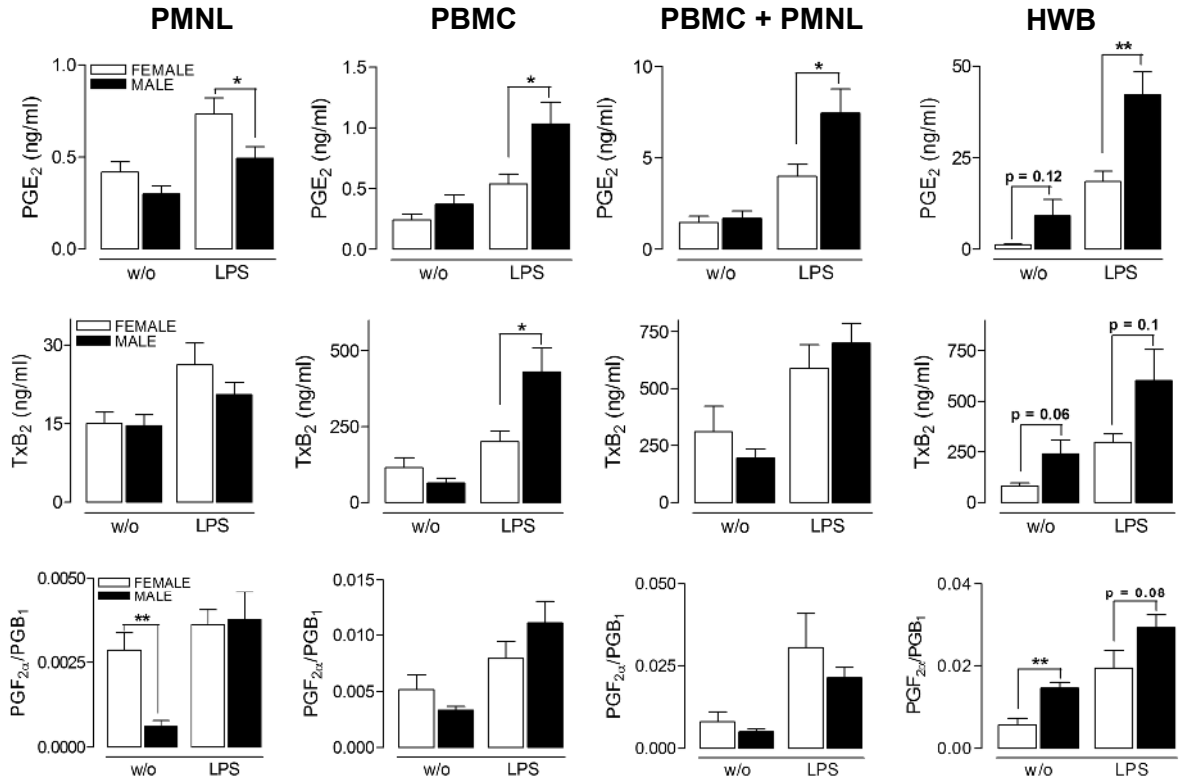

Figure 4.15: Cell-cell cross talk and sex differences in the prostanoid formation following LPS stimulation. PMNL and PBMC were isolated from HWB. 3.5×10^6 PMNL, 2.5×10^6 PBMC were seeded in autologous plasma, alone or together. Cells or 1 ml of the same HWB were stimulated with 10 µg/ml LPS for 24 h at 37 °C. Prostanoid formation was analyzed by LC-MS/MS in supernatants. Data is shown as means ± SEM; (A) n = 4-12 (PGE_2, $PGF_{2\alpha}$), n = 7-12 (TxB_2); data passed normality D'Agostino-Pearson omnibus test; *p < 0.05, **p < 0.01, female vs. male, unpaired t-test with Welch's correction if variances were significantly different. Data of PBMC is normalized to number of monocytes, data of PMNL plus PBMC and of HWB is normalized to number of monocytes plus PMNL.

Stimulation with AA for 24 h revealed somewhat different results (Figure 4.16). PMNL showed no sex difference in PGE_2 formation, whereas a tendency to higher level in PBMC alone, in PBMC plus PMNL and in HWB in male was detected. This indicated that cell interactions could push the formation to higher level in male samples. TxB_2 and $PGF_{2\alpha}$ did not show a different formation in isolated PMNL and PBMC alone, but in the combination of both cell types there was a tendency to higher prostanoid levels in male cells, also seen in male whole blood. This indicated again that cell interactions could play an important role in sex-related differences in prostanoid formation, depending on the stimulus and the mediator analyzed. Furthermore, these experiments show that the combination of cells led to higher amounts of prostanoids as the single cell types formed by itself, stimulating each other.

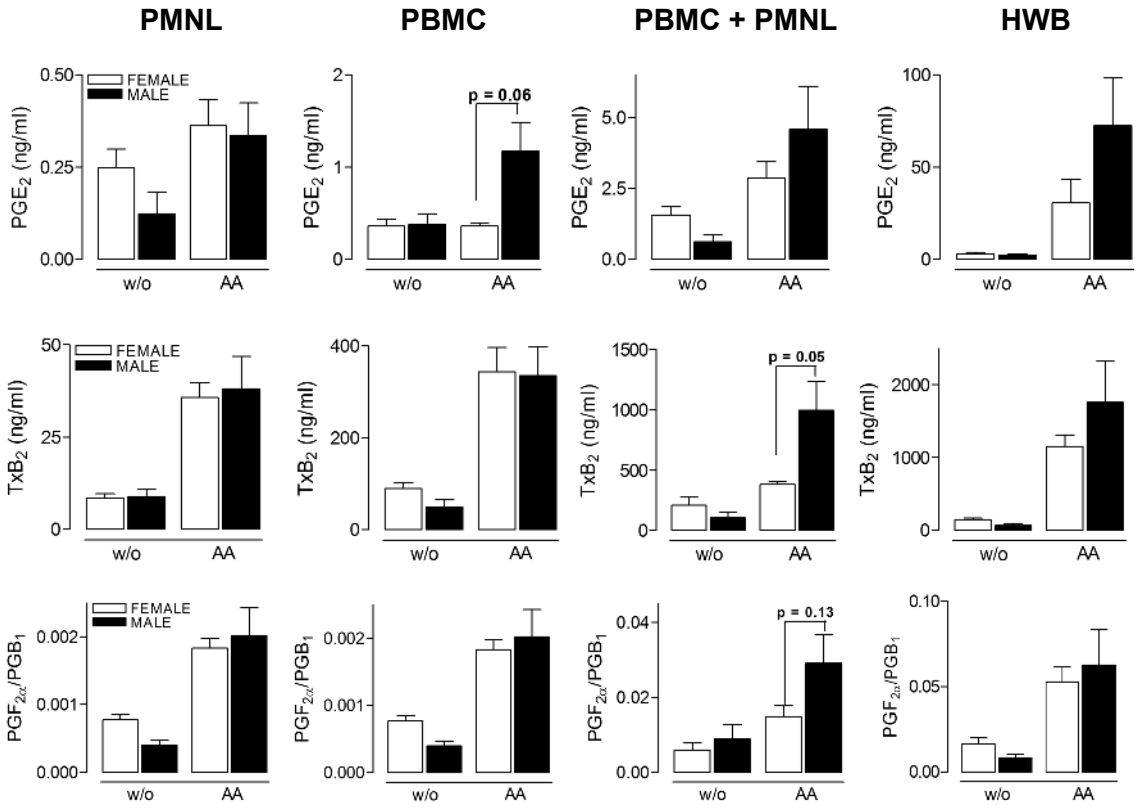

Figure 4.16 ell-cell cross talk and sex differences in the prostanoid formation following AA stimulation. PMNL and PBMC were isolated from HWB. 3.5×10^6 PMNL, 2.5×10^6 PBMC were seeded in autologous plasma, alone or together. Cells or 1 ml of the same HWB were stimulated with 40 µM AA for 24 h at 37 °C. Prostanoid formation was analyzed by LC-MS/MS in supernatants. Data is shown as means ± SEM; (A) n =3-6; data passed normality D'Agostino-Pearson omnibus test; *p < 0.05, **p < 0.01, female vs. male, unpaired t-test with Welch's correction if variances were significantly different. Data of PBMC is normalized to number of monocytes, data of PMNL plus PBMC and of HWB is normalized to number of monocytes plus PMNL.

4.2 Modulation of the inflammatory response by benzoquinones and benzohydroquinones

4.2.1 Inhibitory potential of 1,2- and 1,4-benzoquinones on 5-LO

Previous data by our group revealed a potent dual inhibitory effect of the 1,4-benzoquinone embelin on 5-LO and mPGES-1, indicating a modulation of the inflammatory response [8]. Starting from embelin as parental compound additional benzoquinone derivatives were systematically synthesized. First, the *n*-alkyl chain in 3-position was modified, introducing residues varying in the number of carbon atoms. Next, the 1,4-benzoquinone core was altered to a 1,2-benzoquinone and the free hydroxy groups were partially methylated. Four different series, namely 2,5-methoxy-1,4-benzoquinones (series A), 2-hydroxy-5-methoxy-1,4-benzoquinones (series B), 4,5-dimethoxy-1,2-benzoquinones (series C) and 2,5-dihydroxy-1,4-benzoquinones (series D), in total 48 compounds, were synthesized and biologically evaluated. The synthesis was performed by collaboration partners (Prof. Rosanna Filosa, Univeristy of Naples, Italy) and the compounds were provided to us. 16 of these compounds are part of this thesis and published in [225]. To evaluate the pharmacological relevance, the inhibition of 5-LO product formation was analyzed. Direct effects on 5-LO were determined in a cell-free assay with the partially purified enzyme incubated with exogenous AA. Intact human neutrophils (PMNL) and monocytes were used to evaluate the potency of the compounds in a cellular environment and on other lipoxygenases, when challenged with the Ca^{2+} ionophore A23187 with or without exogenous AA. The functionality of the assays was monitored with the reference control inhibitor *N*-[1-(1-benzothien-2-yl)ethyl]-*N*-hydroxyurea (zileuton) [196], which is the only 5-LO inhibitor on the market for asthma therapy so far. Furthermore, the ability to affect mPGES-1 was evaluated in an established cell-free assay, using microsomes from interleukin-1β-stimulated A549 cells with PGH_2 as substrate and 3-[3-(tert-butylsulfanyl)-1-[(4-chlorophenyl)methyl]-5-(propan-2-yl)-1H-indol-2-yl]-2,2-dimethyl-propanoic acid (MK886) as control inhibitor.

Table 4.3 - 4.6 show the effects of all four series on 5-LO, as well as on 12- and 15-LO and mPGES-1. Regarding 5-LO, the results clearly revealed the most potent effects for the 1,2-benzoquinones (series C, Table 4.5) in cell-free as well as in cell-based settings, except for EA-112C. Regardless of the chain length, *ortho*-quinones were superior over *para*-quinones in all three assays. EA-110C was identified as the most promising compound (IC_{50} cell-free: 0.08 ± 0.01 µM; cell-based with A23187:0.12 ± 0.01 µM; cell-based with A23187 plus AA: 0.05 ± 0.03 µM) revealing a 1,2-benzoquinone core substituted with a C13-*n*-alkyl residue in 3-position as the optimal structure to suppress 5-LO activity. Regarding mPGES-1, the potency depended on both, the free hydroxy groups and the length of the alkyl chain in 3-position. Combination of the two free hydroxy groups with a C8-*n*-alkyl chain, EA-109D, exerted the most pronounced effect with an IC_{50} of 0.8 ± 0.2 µM. In contrast, compounds from other 1,4-benzoquinone series showed highest inhibitory potential when bearing a C13-*n*-alkyl residue. Derivatives of the 1,2-quinone series were not able to interfere with mPGES-1 catalytic activity at all. Furthermore, none of these 16 compounds affected 12- and 15-LO, indicating that especially the 1,2-benzoquinones were highly active and specific for 5-LO.

Table 4.3: Effects of 2,5-methoxy-1,4-benzoquinones (series A) on the activity of 5-, 12- and 15-LO and mPGES-1. IC_{50} values are presented as means ± SEM of two to three independent experiments. Values given in parentheses: remaining activity in % at 10 µM. Cmpd., compound.

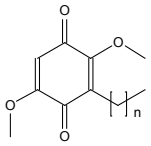

		5-LO activity IC_{50} (µM) or (remaining activity in %) at 10 µM			**12-LO activity**	**15-LO activity**	**mPGES-1 activity**
		cell-free	**cell-based**		**cell-based**		**cell-free**
cmpd.	residue	AA	A23187	A23187 + AA	A23187 + AA		PGH_2
EA-109A	n = $(CH_2)_7$	1.2±0.29	0.32±0.01	0.57±0.17	> 10 (89.6±13.1%)	>10 (123.0±26.9%)	> 10 (63.0±8.2%)
EA-110A	n = $(CH_2)_{12}$	0.26±0.01	0.23±0.04	0.31±0.05	> 10 (58.8±15.5%)	> 10 (84.1±17%)	1.8±0.4
EA-111A	n = $(CH_2)_{13}$	0.21±0.03	0.29±0.09	1.4±0.75	> 10 (84.5±6.7%)	> 10 (115.6±8.5%)	4.4±1.3
EA-112A	n = $(CH_2)_{14}$	0.27±0.1	0.39±0.14	0.86±0.27	>10 (87.3±5.7%)	>10 (115.4±3.2%)	7.2±1.1

Table 4.4: Effects of 2-hydroxy-5-methoxy-1,4-benzoquinones (series B) on the activity of 5-, 12- and 15-LO and mPGES-1. IC_{50} values are presented as means ± SEM of two to three independent experiments. Values given in parentheses: remaining activity in % at 10 µM. Cmpd., compound.

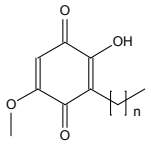

		5-LO activity IC_{50} (µM) or (remaining activity in %) at 10 µM			**12-LO activity**	**15-LO activity**	**mPGES-1 activity**
		cell-free	**cell-based**		**cell-based**		**cell-free**
cmpd.	residue	AA	A23187	A23187 + AA	A23187 + AA		PGH_2
EA-109B	n = $(CH_2)_7$	3.01±0.38	> 10 (73.5±8.6%)	> 10 (72.9±12%)	> 10 (86.8±13.7%)	> 10 (104.9±27.1%)	> 10 (81.4±11.2%)
EA-110B	n = $(CH_2)_{12}$	0.92±0.47	0.77±0.26	2.3±1.10	> 10 (73.2±15.7%)	> 10 (88.1±20.7%)	6.1±1.2
EA-111B	n = $(CH_2)_{13}$	0.42±0.01	0.27±0.04	0.49±0.1	> 10 (113.5±8.3%)	> 10 (115.8±8.8%)	> 10 (52.1±2.9%)
EA-112B	n = $(CH_2)_{14}$	0.34±0.04	0.76±0.13	1.51±0.46	> 10 (92.8±3.7%)	> 10 (103.2±3.2%)	9.3±0.8

Table 4.5: Effects of 4,5-methoxy-1,2-benzoquinones (series C) on the activity of 5-, 12- and 15-LO and mPGES-1. IC_{50} values are presented as means ± SEM of two to three independent experiments. Values given in parentheses: remaining activity in % at 10 µM. Cmpd., = compound.

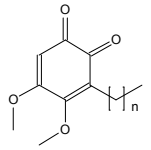

		5-LO activity IC_{50} (µM) or (remaining activity in %) at 10 µM			**12-LO activity**	**15-LO activity**	**mPGES-1 activity**
		cell-free	**cell-based**		**cell-based**		**cell-free**
cmpd.	residue	AA	A23187	A23187 + AA	A23187 + AA		PGH_2
EA-109C	n = $(CH_2)_7$	0.33±0.05	0.38±0.07	0.82±0.38	> 10 (59.3±15.8%)	> 10 (101.7±24%)	> 10 (51.1±3.4%)
EA-110C	n = $(CH_2)_{12}$	0.08±0.01	0.12±0.01	0.05±0.03	> 10 (78.5±28.8%)	> 10 (137.1±36.9%)	> 10 (77.5±4.4%)
EA-111C	n = $(CH_2)_{13}$	0.04±0.02	0.12±0.0	0.13±0.0	> 10 (87.3±11.6%)	> 10 (138.9±8.9%)	> 10 (84.0±3.6%)
EA-112C	n = $(CH_2)_{14}$	0.6±0.1	> 10 (57.6±3.2%)	> 10 (66.8±3.5%)	> 10 (88.9±6.8%)	> 10 (114.8±9.5%)	> 10 (97.3±11%)

Table 4.6: Effects of 2,5-hydroxy-1,4-benzoquinones (series D) on the activity of 5-, 12- and 15-LO and mPGES-1. IC_{50} values are presented as means ± SEM of two to three independent experiments. Values given in parentheses: remaining activity in % at 10 µM. Cmpd., compound.

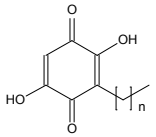

		5-LO activity			**12-LO activity**	**15-LO activity**	**mPGES-1 activity**
		IC_{50} (µM) or (remaining activity in %) at 10 µM					
		cell-free	**cell-based**		**cell-based**		**cell-free**
cmpd.	residue	AA	A23187	A23187 + AA	A23187 + AA		PGH_2
EA-109D	n = $(CH_2)_7$	0.38±0.04	> 10 (53.6±4.8%)	> 10 (80.1±8%)	> 10 (75.7±11.3%)	> 10 (88.9±18.4%)	0.8±0.2
EA-110D	n = $(CH_2)_{12}$	0.22±0.0	2.52±0.38	4.65±0.24	> 10 (84.3±2.9%)	> 10 (123.6±11.7%)	0.9±0.2
EA-111D	n = $(CH_2)_{13}$	0.17±0.01	3.14±0.45	5.12±0.57	> 10 (101.2±11%)	> 10 (138.9±12.1%)	1.6±0.3
EA-112D	n = $(CH_2)_{14}$	0.23±0.08	4.3±0.52	> 10 (61.7±2.1%)	> 10 (87.7±17.8%)	> 10 (103.4±6.8%)	2.1±0.4

4.2.2 Variation of the 1,2-benzoquinone to a 1,2-benzohydroquinone core improves the inhibitory potency against 5-LO

Based on the results obtained from the previous series, further structural optimizations were made to improve the inhibitory potential of the 1,2-benzoquinones to intervene with 5-LO product formation. There are many active hydroquinone compounds known so far by literature [226, 227]. Therefore, the quinone moiety was reduced, resulting in a 1,2-benzohydroquinone (RED). Out of the overall 48 structures tested, two other promising compounds emerged besides EA-110C, namely EA-107C and EA-100C with a C11- and C12-*n*-alkyl residue, respectively (Table 4.7) published in [168]. Additionally, the reduced forms of these two derivatives were synthesized as well as different hydroquinone derivatives of EA-110C.

Table 4.7: Effect of the 4,5-dimethoxy-1,2-benzoquinone EA-107C and EA-100C on 5-LO activity. IC_{50} values are presented as means ± SEM of three to four independent experiments. Cmpd., compound [168].

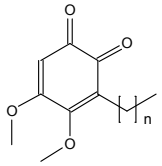

		5-LO activity	
		IC_{50} (µM)	IC_{50} (µM)
		cell-free	**cell-based**
cmpd.	residue	AA	A23187 + AA
EA-107C	n = $(CH_2)_{10}$	0.94±0.40	0.10±0.03
EA-100C	n = $(CH_2)_{11}$	0.26±0.02	0.15±0.03

The new series was analyzed in cell-free and cell-based assays (Figure 4.17 A and B) and compared with their oxidized analogues to evaluate the benefit of the reduction to the hydroquinone core, regarding the inhibitory capacity on 5-LO product formation, also published in [198]. Figure 4.17 A shows that only the hydroquinone EA-107C RED was about 10-fold superior over the parental quinone structure in cell-free conditions (EA-107C IC_{50} = 0.94 ± 0.4 µM; EA-107C RED IC_{50} = 0.11 ± 0.05). In agreement with the literature, this indicated that the hydroquinone moiety is the active form in cellular environments [228], where components like GSH create reducing conditions [229]. Two other hydroquinones with a different *O*-methylation pattern were synthesized, one with a *tri*-hydroxylated core and one with a *para*-hydroxy moiety (Table 4.8). All three EA-110C hydroquinones contained a C13-*n*-alkyl chain in 3-position. In cell-free, as well as in cell-based assays (Figure 4.17 A

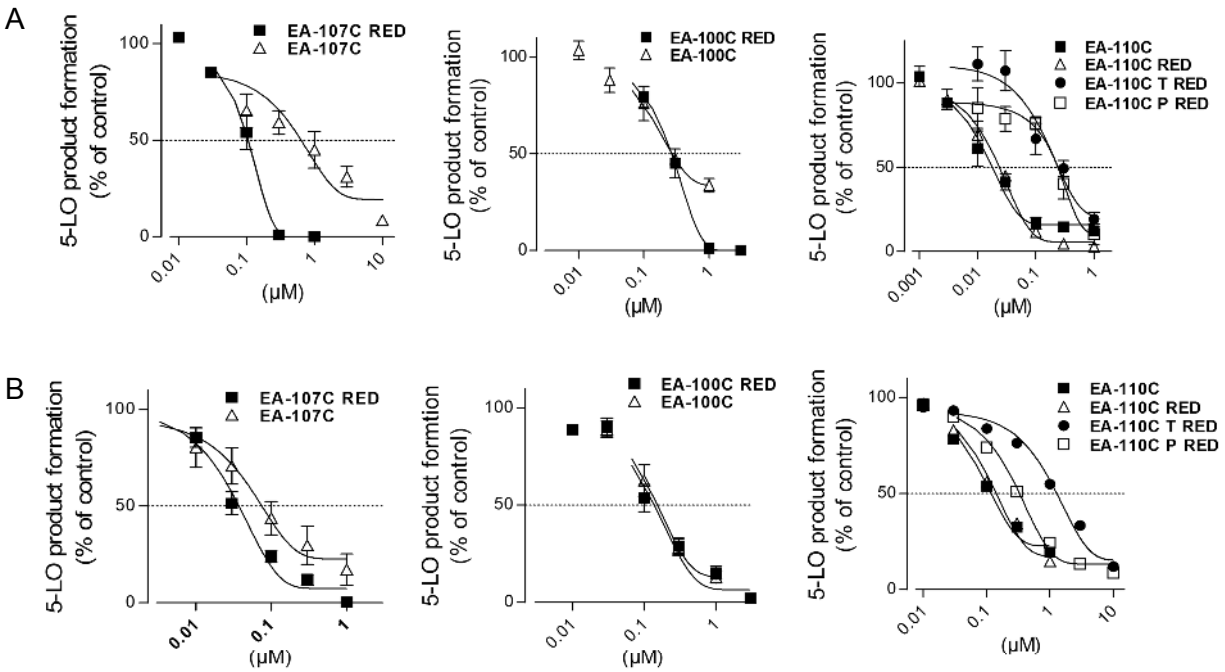

Figure 4.17: Inhibition of 5-LO product formation by EA-107C, EA-100C and EA-110C and by their reduced analogues. (A) Partially purified recombinant 5-LO was preincubated with compounds or vehicle (0.1% DMSO) at the indicated concentrations for 10 min at 4 °C, followed by stimulation with 20 µM AA plus 2 mM Ca^{2+} for 10 min at 37 °C. (B) PMNL were preincubated with compounds at the indicated concentrations or vehicle (0.1% DMSO) for 15 min at 37 °C, followed by stimulation with 2.5 µM A23187 plus 20 µM AA for 10 min at 37 °C. 5-LO product formation was detected by RP-HPLC. Data is shown as percentage of control (100%); means ± SEM, n = 3-7.

and B), altered *O*-methylation reduced the ability to intervene with 5-LO product formation. Interestingly, the 1,2-quinone/-hydroquinone core combined with a C13-*n*-alkyl residue (EA-110C/RED) appeared to be the most effective compound of the entire series in cell-free as well as in cell-based experiments (Table 4.8).

Based on this result, further studies were performed to characterize the mechanism of 5-LO inhibition and to analyze the physiological relevance in animal models of the two most promising compounds. First, the mode of inhibition was analyzed.

Table 4.8: Effect of the different benzohydroquinones on 5-LO activity. IC_{50} values are presented as means ± SEM of three to four independent experiments. Cmpd., compound. See also [198].

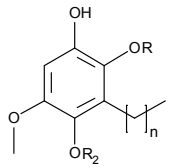

				5-LO activity IC_{50} (µM) or (remaining activity in %) at 10 µM	
				cell-free	**cell-based**
cmpd.	residue	R	R_2	AA	A23187 + AA
EA-107C RED	n = $(CH_2)_{10}$	-H	$-CH_3$	0.11±0.05	0.04±0.04
EA-100C RED	n = $(CH_2)_{11}$	-H	$-CH_3$	0.24±0.03	0.09±0.06
EA-110C RED	n = $(CH_2)_{12}$	-H	$-CH_3$	0.06±0.02	0.03±0.02
EA-110C T RED	n = $(CH_2)_{12}$	-H	-H	0.29±0.05	0.16±0.58
EA-110C P RED	n = $(CH_2)_{12}$	$-CH_3$	-H	0.26±0.07	0.31±0.03

Therefore, partially purified 5-LO was preincubated with the compounds and stimulated with AA at varying concentrations. Although these compounds showing a fatty acid like structure, results (Figure 4.18) revealed a non-competitive mode of EA-110C and EA-110C RED with AA. This suggested that the compounds did not compete with AA for the binding site.

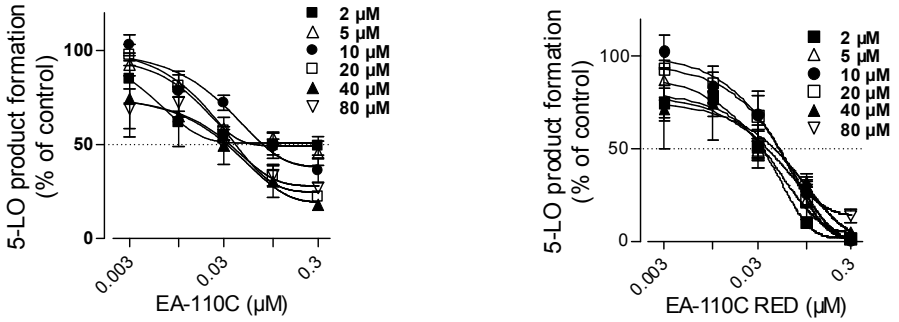

Figure 4.18: Effect of variation of the substrate concentration on inhibition of 5-LO activity by EA-110C and EA-110C RED. Partially purified recombinant 5-LO was preincubated with compounds at the indicated concentration or vehicle (0.1% DMSO) for 10 min at 4 °C, followed by stimulation with 20 µM AA plus 2 mM Ca^{2+} for 10 min at 37 °C. 5-LO products were detected by RP-HPLC. Data are given as percentage of control (100%); means ± SEM, n = 3.

To assess the exact binding mode, docking simulations were performed, using Pocket-Finder software. Two binding sites were identified, one cavity on the opposite side of the substrate channel and one located between the membrane binding C2 domain and the catalytic domain. The docking simulation was conducted in collaboration with Dr. Daniela Schuster (University of Innsbruck, Austria) and suggested a possible positioning of the substituted benzene moiety in a region of the binding pocket also accessible for polar solvents. At this location, hydrogen bonds with Tyr-383, Tyr-81, Trp-102 and Glu-622 were most likely. Docking simulations of EA-110C and EA-110C RED revealed a similar binding mode at the 5-LO binding site opening. The quinone interacted with Tyr-81 and Tyr-383 whereas the hydroquinone formed hydrogen bonds with Tyr-81 and Glu-622 (Figure 4.19 A, B). According to the simulation, the hydroquinone did not directly interact with the active site iron.

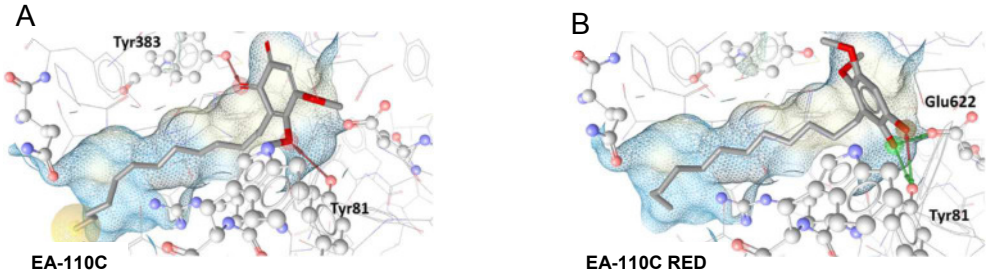

Figure 4.19: Docking simulations of EA-110C and EA-110C RED at the 5-LO binding site. Both, the quinone (A) and hydroquinone ring (B) were located at the binding site opening, allowing the *n*-alkyl chain to fill the hydrophobic ion channel. Binding to 5-LO is mediated through hydrogen bonds with Tyr-81 and Tyr-383 (A) or Tyr-81 and Glu-622 (B). Red arrow – hydrogen bond acceptor, green arrow – hydrogen bond donor, yellow spheres – hydrophobic interaction. See also [198].

Next, the pharmacological relevance in treatment of inflammatory conditions was analyzed in two different *in vivo* models of acute inflammation performed in the lab of Prof. Bruno D'Agostino, University of Naples, Italy. Carrageenan-induced paw oedema in mice was induced by intraplantar injection of carrageenan in the hind paw. This led to a massive swelling and oedema formation. Both EA-110C and EA-110C RED could significantly reduce paw swelling during the early (4 h) as well as the late (48 h) time points, in a concentration of 1 mg/kg given i.p. 30 min prior carrageenan injection (data not shown, published in [198]). Peritonitis in mice was generated by intraperitoneal injection of zymosan. Pre-application of the two EA-compounds (1 mg/kg i.p.) 30 min prior zymosan injection showed a marked repression of cys-LT formation and migration of inflammatory cells into the peritoneal cavity for both compounds, equally effective as the control inhibitor zileuton (data not shown, published in [198]).

4.2.3 Lipophilic catechols exhibit inhibitory capacity on 5-LO product formation

Encouraged by the results obtained with the previous 1,2-hydroquinone series, which potently modulated the inflammatory response, another set of 15 compounds was synthesized to further improve the inhibitory capacity (synthesized by Prof. Rosanna Filosa, University of Naples, Italy). The novel structures were substituted with various rather bulky aromatic residues in 4-position, in contrast to the linear *n*-alkyl chains in 3-position used in the previous studies. A screening on 5-LO activity revealed highly active compounds (Table 4.9), especially in cell-free assays where IC_{50} values were in a range from 7 to 210 nM.

Table 4.9.1: Effect on 5-LO activity in cell-free and cell-based assays by 1,2-hydroquinones; part 1.

		5-LO activity		
		IC_{50} (µM) cell-free	IC_{50}(µM) cell-based	
cmpd	**STRUCTURE**	AA	A23187 + AA	A23187
F-I	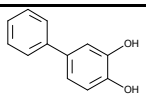	0.05 ± 0.01	0.93 ± 0.11	0.37 ± 0.11
F-III	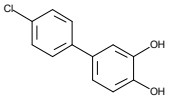	0.02 ± 0.002	0.44 ± 0.0	0.26 ± 0.07
F-IV	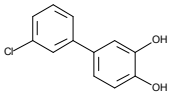	0.02 ± 0.005	0.36 ± 0.11	0.21 ± 0.02
F-V	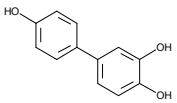	0.21 ± 0.0	2.31 ± 0.02	1.33 ± 0.47
F-XI	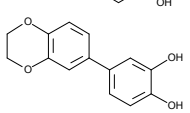	0.04 ± 0.01	0.62 ± 0.25	0.24 ± 0.03
F-XII	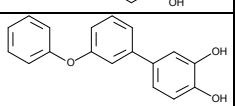	0.02 ± 0.01	0.07 ± 0.03	0.07 ± 0.004

Table 4.9.2: Effect on 5-LO activity in cell-free and cell-based assays by 1,2-hydroquinones; part 2.
*data published in [225].

		5-LO activity		
		IC_{50} (µM) cell-free	IC_{50}(µM) cell-based	
cmpd	**structure**	AA	A23187 + AA	A23187
F-XIII	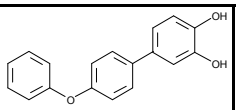	0.01 ± 0.002	0.23 ± 0.05	0.17 ± 0.11
F-XV	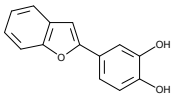	0.03 ± 0.005	0.43 ± 0,04	1.11 ± 0.54
F-XVI	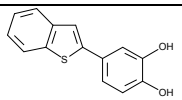	0.02 ± 0.031	0.11 ±0.03	0.06 ± 0.004
F-XVII	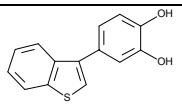	0.02 ± 0.006	1.14 ±0.08	1.21 ± 0.51
F-XVIII	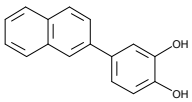	0.007 ± 0.001	0.30 ±0.03	0.22 ± 0.05
F-XIX	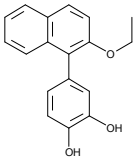	0.01± 0.005	0.40 ± 0.01	0.27 ± 0.02
F-XXII	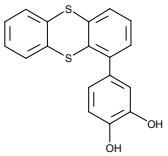	0.008 ± 0.001	0.19 ± 0.04	0.22 ± 0.04
F-XXIII	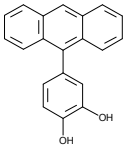	0.01 ± 0.001	0.40 ± 0.14	2.34 ±0.49
F-XXIV	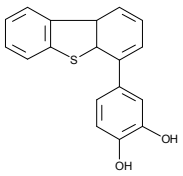	0.007 ± 0.001	0.25 ± 0.06	0.31 ± 0.11
Zileuton*	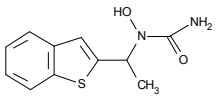	0.59 ± 0.10	2.5 ± 1.2	0.9 ± 0.3

Inhibition of cellular activity in PMNL stimulated with A23187 displayed IC_{50} values in a range of 0.07 to 2.31 µM, whereas in cells stimulated with A23187 plus exogenous AA, the IC_{50} values were between 0.07 and 2.34 µM. To exert intracellular inhibition, it seemed rather linear structures with lipophilic residues were favored, e.g. compounds F-III, F-XII or F-XVI. Interestingly, linear structures bearing an inflexible or an additional hydrophilic substituted aromatic residue led to reduction of activity, e.g. compounds F-XXIII or F-V.

4.3 Inhibitory potential of F-XII and F-XVI on 5-LO activity

4.3.1 Interaction of F-XII and F-XVI with 5-LO in cell based assays

Encouraged by this positive outcome, pharmacological relevance and the possibility to apply such compounds in the therapy of inflammatory disorders were assessed. The mechanism of 5-LO product formation was characterized in detail using the two most promising compounds F-XII, containing a benzothiophene residue in 4-position and F-XVI bearing a diphenyl ether. First, the effect on 5-LO activity in human leukocytes was analyzed (Figure 4.20 A).

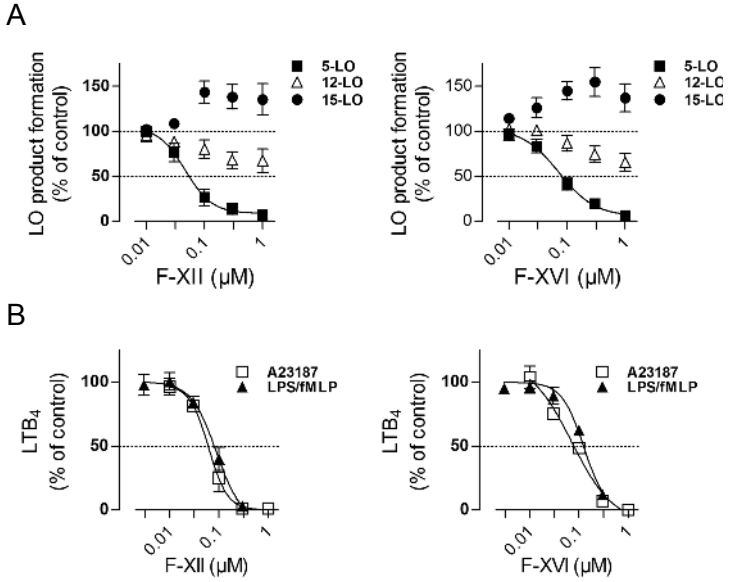

Figure 4.20: Effect of F-XII and F-XVI on 5-LO activity in cellular assays. (A) PMNL were preincubated with compounds at the indicated concentrations or vehicle (0.1% DMSO) for 15 min, followed by stimulation with 2.5 µM A23187 plus 20 µM AA for 10 min. (B) PMNL were preincubated with compounds at the indicated concentrations or vehicle (0.1% DMSO) for 15 min, followed by stimulation with 2.5 µM A23187 for 10 min. Alternatively, PMNL were primed with 1 µg/ml LPS for 30 min and 0.3 U/ml for 20 min, followed by stimulation with 1 µM fMLP for 5 min. Compounds were added 15 min prior fMLP stimulation. 5-LO product formation was determined by RP-HPLC. Data are given as percentage of control (100%), means ± SEM, n= 3-7.

In PMNL stimulated with A23187 plus AA, F-XII and F-XVI were equally active in suppressing 5-LO product biosynthesis (F-XII: IC_{50} = 0.07 ± 0.03 µM; F-XVI: IC_{50} = 0.11 ± 0.03 µM, see also table 4.9). Of note, they were able to outperform the control inhibitor zileuton (PMNL stimulated with A23187 IC_{50} = 2.5 ± 1.2 µM, see also [225]). Up to a concentration of 1 µM both hydroquinones had no effect on the related 12- and 15-LO. Remaining activity regarding 15-LO was 135.4 ± 17.4% for F-XII and 137.0 ± 15.5% for F-XVI, respectively. Inhibitory potency on 12-LO activity was more pronounced but was not reduced below 65% (F-XII: remaining activity = 67.2 ± 13.2%; F-XVI: remaining activity = 65.5 ± 9.7%).

Next, PMNL were stimulated either with A23187 alone or by priming with the bacterial product LPS, followed by stimulation with fMLP (Figure 4.20 B). The latter is a pathophysiological means to induce leukotriene biosynthesis in immune cells. Regardless of the stimulus used, F-XII and F-XVI were equally potent in decreasing LTB_4 formation (F-XII: A23187 IC_{50} = 0.07 ± 0.004 µM, LPS/fMLP IC_{50} = 0.1 ± 0.01 µM; F-XVI: A23187 IC_{50} = 0.06 ± 0.004 µM, LPS/fMLP IC_{50} = 0.12 ± 0.01 µM). Stimulation with A23187 alone or LPS/fMLP leads to AA release from nuclear membranes by $cPLA_2$ and to leukotriene formation in concert with 5-LO and FLAP. Since stimulation in the presence of exogenous AA did not change the potency of F-XII and F-XVI, this indicated that $cPLA_2$ is not a primary target of these hydroquinones.

The instable epoxide Leukotriene A_4 (LTA_4) can either be converted to LTB_4 via the LTA_4-hydrolase, or to the cys-LTs by the LTC_4-synthase. Therefore, the formation of cys-LTs in monocytes was explored with parallel detection of LTB_4 (Figure 4.21). The hydroquinones showed a likewise influence on the formation of both LTB_4 and the cys-LTs, suggesting no additional inhibition of the LTC_4-synthase.

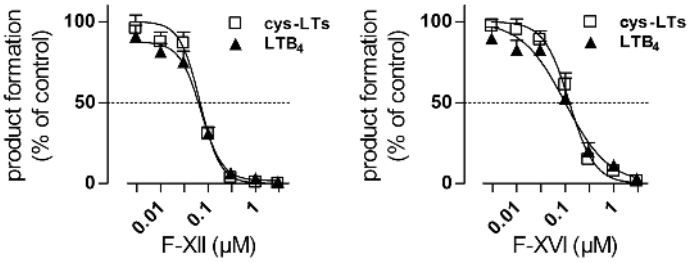

Figure 4.21: Influence of F-XII and F-XVI on cys-LT and LTB_4 formation in human monocytes. Monocytes were preincubated with compounds at the indicated concentrations or vehicle (0.1% DMSO) for 15 min, followed by stimulation with 2.5 µM A23187 for 10 min. LTB_4 formation was determined using RP-HPLC analysis, cys-LTs were analyzed using ELISA. Data are presented as percentage of control (100%), means ± SEM, n = 4-6.

In order to verify that the ability to interfere with 5-LO was due to the hydroquinone moiety, *O*-methylated analogues of F-XII (AF-06) and F-XVI (AF-13) were used as control compounds (Figure 4.22 A and B). Apparently, masking the hydroxy groups substantially decreased the inhibitory potency of AF-06 (stimulation with A23187: IC_{50} = 2.7 ± 0.2 µM; stimulation with A23187 plus AA: IC_{50} = 2.9 ± 0.5 µM) and led to a complete loss of activity of AF-13 (stimulation with A23187: remaining activity at 10 µM = 63.8 ± 19.4%; stimulation with A23187 plus AA: remaining activity at 10 µM = 84.5 ± 3.5%).

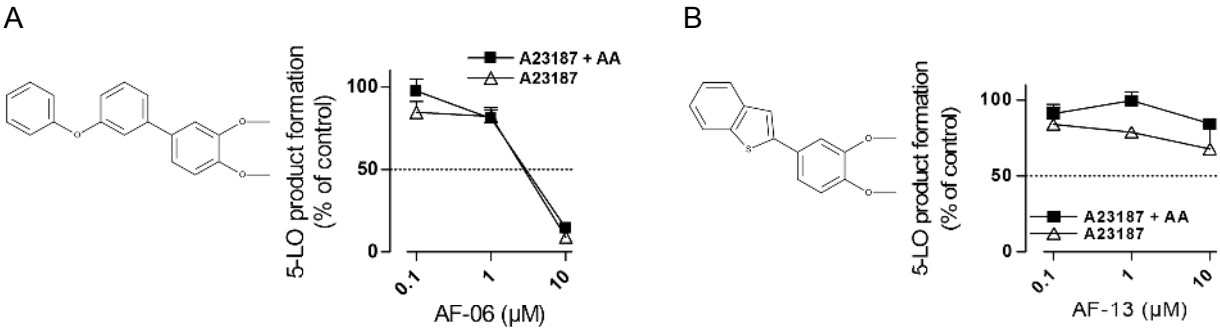

Figure 4.22: Chemical structures of AF-06 and AF-13 and their effect on 5-LO activity in PMNL. PMNL were preincubated with (A) AF-06 or (B) AF-13 at the indicated concentrations or vehicle (0.1% DMSO) for 15 min, followed by stimulation with 2.5 µM A23187 with or without 20 µM AA for 10 min. 5-LO product formation was determined using RP-HPLC. Data is given as percentage of control (100%); means ± SEM, n = 3.

Nevertheless, high efficiency of 5-LO inhibition was not due to cytotoxic effects. Monocytes challenged by F-XII or F-XVI for 24 h did not show detrimental effects on cells as shown by MTT as well as LDH assays (Figure 4.23). Staurosporine (stsp), a well-known apoptosis inducer was used as positive control.

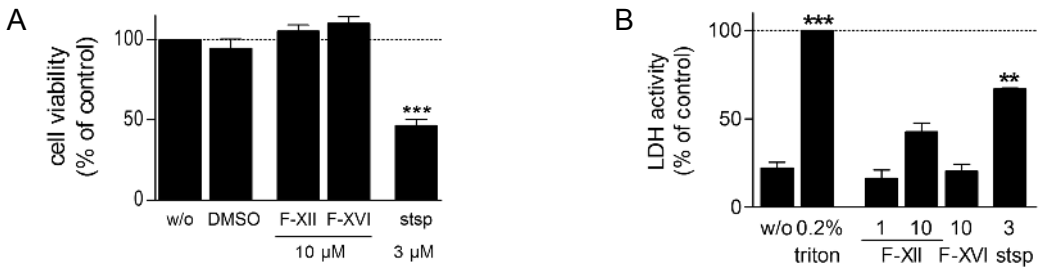

Figure 4.23: Effect of F-XII and F-XVI on cell viability. (A) Monocytes were preincubated with compounds at the indicated concentrations, 3 µM staurosporine (stsp), or vehicle (0.3% DMSO) for 24 h. Afterwards cell viability was monitored by addition of MTT and photometric measurement at 570 nm. Data are presented as percentage of untreated control (100%). (B) Monocytes were preincubated with compounds at indicated concentrations, 3 µM staurosporine, 0.2% triton X-100 or vehicle (0.5% DMSO) for 24 h. Afterwards, cell viability was monitored by LDH activity at 340 nm. Data are given as percentage of triton X-100 control (100%); means ± SEM, n = 3-6. **p < 0.01***p < 0.001 vs. untreated sample, repeated measures ANOVA followed by Bonferroni (MTT) or Tukey (LDH) post hoc test applied to absolute values.

4.3.2 Effect of F-XII and F-XVI on 5-LO activity in cell-free assays

Next, the ability to interact with the isolated 5-LO in cell-free conditions was investigated. Therefore, partially purified 5-LO was preincubated with the test compounds followed by incubation with AA. The capacity of 5-LO inhibition was higher as compared to cellular settings. (IC_{50} values: F-XII = 0.02 ± 0.01 µM, F-XVI = 0.02 ± 0.03 µM; Figure 4.24 A) and again superior over zileuton (IC_{50} = 0.59 ± 0.01 µM).

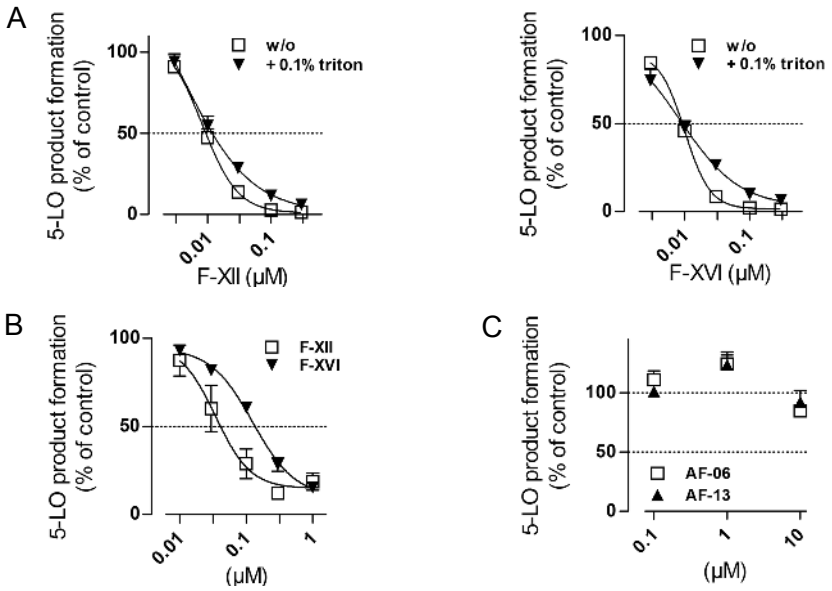

Figure 4.24: Effects of hydroquinones and methylated analogous on 5-LO activity in cell-free assays. (A) Partially purified recombinant 5-LO was preincubated with F-XII or F-XVI, (C) AF-06 or AF-13 at the indicated concentrations or vehicle (0.1% DMSO) for 10 min at 4 °C followed by stimulation with 20 µM AA and 2 mM Ca^{2+} for 10 min at 37 °C. Triton X-100 was added as indicated. (B) PMNL were homogenized by sonication at 4 °C. Homogenates (corresponding to 2×10^6 cells) were preincubated with F-XII or F-XVI at the indicated concentrations or vehicle (0.1% DMSO), followed by stimulation with 20 µM AA and 2 mM Ca^{2+} for 10 min at 37 °C. 5-LO product formation was determined by RP-HPLC. Data are given as percentage of control (100%); means ± SEM, n = 3.

One possibility of 5-LO inhibition could be the formation of compound aggregates. Compounds executing this mechanism are called nuisance inhibitors [230]. They form colloid like aggregates with the enzyme protein without target specificity. These aggregates can be prevented by non-ionic detergents like triton X-100. After pre-treatment of the partially purified 5-LO with triton X-100 at a concentration of 0.1% the potency of F-XII and F-XVI was not decreased, excluding nuisance inhibition (F-XII with triton: IC_{50} = 0.01 ±0.001 µM, F-XVI with triton: IC_{50} = 0.01 ± 0.001 µM) (Figure 4.24 A). In PMNL homogenates F-XII and F-XVI were less effective compared to purified 5-LO preparations (Figure 4.24 B). The IC_{50} value of F-XII shifted only slightly to 0.04 ± 0.01 µM, whereas the value of F-XVI shifted to 0.13 ± 0.02 µM, similar to the value seen in intact cells. As well as in PMNL, AF-06 and AF-13 were used in cell-free conditions to confirm that he inhibitory activity relies on the hydroquinone structure (Figure 4.24 C). Both molecules lost their ability to interfere with 5-LO (F-XII: remaining activity at 10 µM = 84.6 ± 5.3%, F-XVI: remaining activity at 10 µM 92.2 ± 9.8%).

4.3.3 Detailed investigations of the binding mode of F-XII and F-XVI to 5-LO

Next we studied the binding mode of the compounds to the 5-LO enzyme. First, reversibility of inhibition was evaluated. Partially purified 5-LO preparation was preincubated with F-XII or F-XVI at a concentration of 30 nM. One aliquot was diluted 10-fold with assay buffer, the other was not altered. Following incubation of both aliquots with AA neither F-XII nor F-XVI showed an irreversible inhibition (Figure 4.25 A). Second, competition of the compounds with AA was analyzed by incubation of 5-LO with varying AA concentrations (Figure 4.25 B). The results indicated no competitive inhibition for both F-XII and F-XVI.

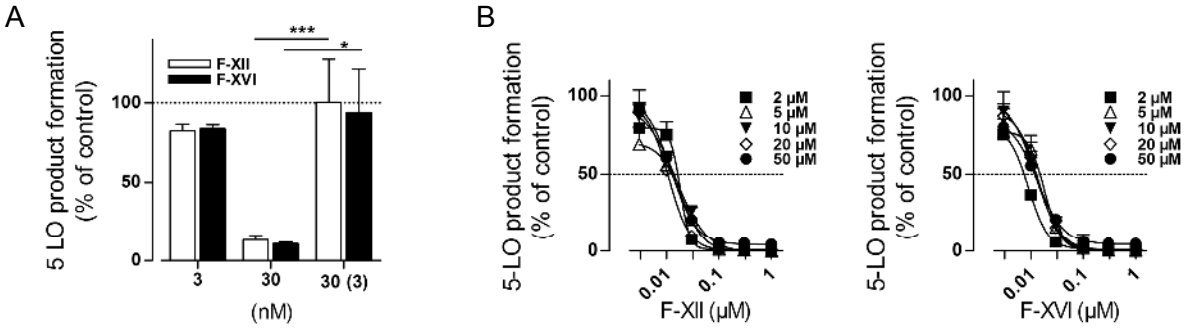

Figure 4.25: Investigation of the reversibility and substrate competitive mode of inhibition of 5-LO by F-XII and F-XVI. (A) Partially purified recombinant 5-LO was preincubated with F-XII or F-XVI at 3 and 30 nM for 10 min at 4 °C. An aliquot of the 30 nM sample was diluted 1:10 with assay buffer to give 3 nM. After another 10 min samples were stimulated with 20 µM AA and 2 mM Ca^{2+} for 10 min at 37 °C. (B) Partially purified recombinant 5-LO was preincubated with compounds at the indicated concentrations or vehicle (0.1% DMSO), followed by stimulation with varying concentrations of AA plus 2 mM Ca^{2+} as described in (A). Data are given as percentage of control (100%), means ± SEM, n = 3-4. *p < 0.05, ***p < 0.001 vs. not diluted sample (30 nM), paired t-test applied to absolute values.

For some benzoquinones e.g. AA-861 containing a Michael acceptor function an interaction with some of the cysteines Cys-159, Cys-300, Cys-416 and Cys-418 located on the surface of the catalytic C-terminal domain, in close proximity to the substrate entrance, could be shown [167]. To evaluate the possible interference of F-XII and F-XVI with these specific amino acids, HEK293 cells stably expressing the mutant 5-LO_4C, where Cys-159, Cys-300, Cys-416 and Cys-418 are replaced by serines (kindly provided by Dr. Steinhilber, University of Frankfurt) were used (Figure 4.26). Interestingly, both hydroquinones were equally active on wild type and mutant 5-LO, with even lower IC_{50} values for the mutated 5-LO (F-XII: 5-LO_wt IC_{50} = 0.11 ± 0.01 µM vs. 5-LO_4D IC_{50} = 0.08 ± 0.03 µM; F-XVI: 5-LO_wt IC_{50} = 0.14 ± 0.05 µM vs. 5-LO_4D IC_{50} = 0.12 ± 0.01 µM). Thus, the four critical cysteines that are targeted by 5-LO inhibitors with Michael acceptor functions are not required for 5-LO inhibition by F-XII and F-XVI.

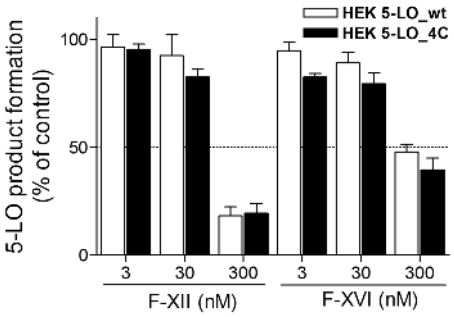

Figure 4.26: Impact of F-XII and F-XVI on HEK293 cells stably expressing FLAP and 5-LO_wt or 5-LO_4C, respectively. Cells were preincubated with F-XII or F-XVI at the indicated concentrations or vehicle (0.1% DMSO) for 15 min, followed by stimulation with 2.5 µM A23187 and 3 µM AA for 10 min. LT formation was detected by RP-HPLC. Data are given as percentage of control (100%); means ± SEM, n = 4.

To get a more detailed insight into the binding mode, docking simulations with the 5-LO ("Stable-5-LO") were performed in collaboration with Dr. Daniela Schuster (University of Innsbruck, Austria). Docking simulation revealed a similar binding mode for both compounds. The *ortho*-hydroquinone ring was coordinated by three amino acids (F-XII; Arg-138, Tyr-142, Asp-166) or two amino acids (F-XVI; Tyr-142, Asp-166) on the C-terminal catalytic domain (Figure 4.27 A). Interestingly, Asp-166 on the catalytic domain is considered to interact intramolecular with Arg-101 on the regulatory N-terminal C2 like domain. It is also part of a short α2 helix, which is proposed to control access to the active site [101]. In the compounds AF-06 and AF-13, the hydroxy groups were replaced with methoxy groups, hence making it difficult to form stabilizing hydrogen bonds due to a displacement of the molecules within the binding pocket. Although methoxy groups are capable to form hydrogen bonds, they are considered very weak. Figure 4.27 B clearly shows the different docking positions in the binding site compared to the hydroquinones, displacing the oxygens of forming the ideal interactions.

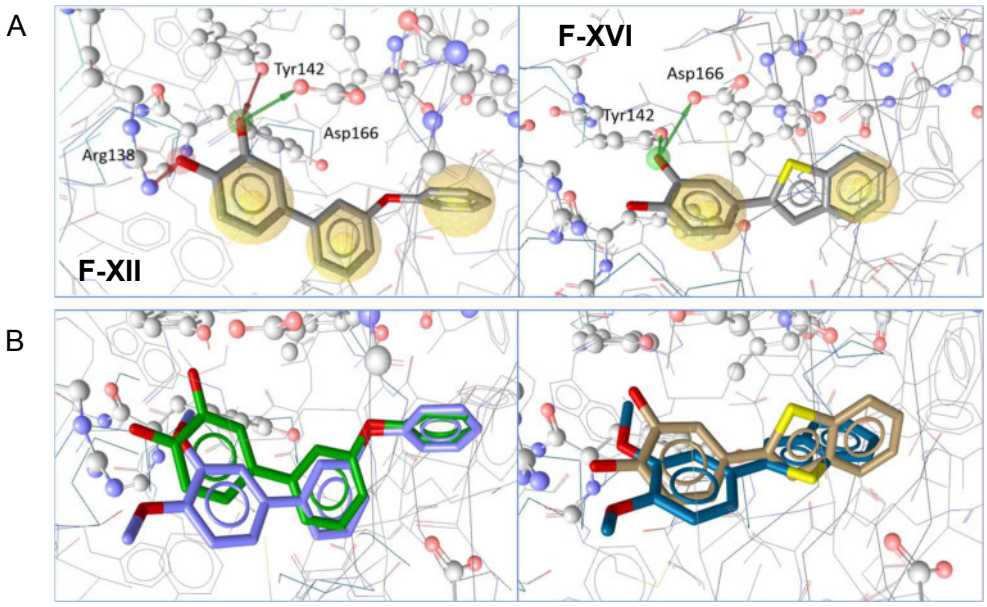

Figure 4.27: Molecular docking simulations with F-XII, F-XVI and the methylated analogous into the "Stable-5-LO". Exemplary docking poses are shown. (A) Molecular docking poses of F-XII (left) and F-XVI (right). The location of the hydroquinone ring is stabilized through hydrogen bonds formed by the amino acids Arg-138, Tyr-142 and Asp-166. (B) comparison between docking poses of F-XII (green) and AF-06 (purple) on the left and F-XVI (brown) and AF-13 (dark blue) on the right. Interactions are displayed colored. Red arrow – hydrogen bond acceptor, green arrow – hydrogen bond donor, yellow spheres – hydrophobic interaction.

4.3.4 Interference with 5-LO translocation and activation

Inhibitors of LT formation can not only interfere with 5-LO itself, they may also intervene with the cellular 5-LO redistribution as well. Hyperforin [231] for example is known to hamper the intracellular translocation of 5-LO to the nuclear membrane, where interaction with FLAP and LT formation takes place. In order to evaluate the possible inhibition of subcellular redistribution of 5-LO by hydroquinones, PMNL were preincubated with F-XII or F-XVI, followed by stimulation with A23187. Subsequent incubation with fluorescent antibodies enabled to visualize the translocation of 5-LO by immunofluorescence microscopy (Figure 4.28 A). Independent of cell stimulation, the helper protein FLAP was permanently located at the nuclear envelope (green fluorescence signal), presented in Figure 4.29 A in the top row. In unstimulated conditions 5-LO was located within the nucleus, appearing as diffuse red fluorescence signals (Figure 4.28 A, left column). Upon cell stimulation with A23187 5-LO translocated to the nuclear membrane, visible as yellow signals in the overlay with FLAP, (Figure 4.28 A third row). F-XII failed to affect 5-LO translocation but F-XVI seemed to impair the redistribution of 5-LO to some extent. In contrast, pre-incubation with hyperforin led to a complete inhibition of the 5-LO translocation.

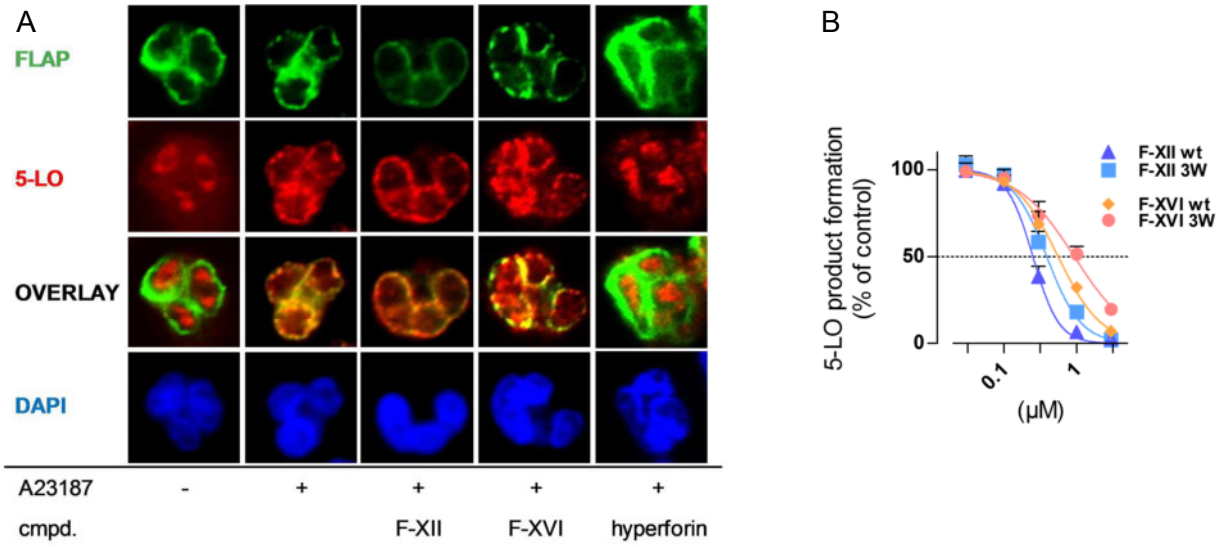

Figure 4.28: Interference of F-XII and F-XVI with subcellular translocation of 5-LO, effects on 5-LO_3W. (A) PMNL were seeded on poly-D-lysine coated glass cover slips, preincubated with 1 µM F-XII, 1 µM F-XVI or 10 µM hyperforin for 15 min, followed by stimulation with 2.5 µM A23187 for 5 min. Cells were fixed with 4% paraformaldehyde solution, permeabilized with 100% acetone and incubated with antibodies against 5-LO (Alexa Fluor 555, red) and FLAP (Alexa Fluor 488, green). Nuclei were stained with DAPI (blue). Images were taken by immunofluorescence microscopy. Images are representative out of 3 independent experiments; scale bar: 5 µM. (B) Impact of F-XII and F-XVI on HEK293 cells stably expressing FLAP and 5-LO_wt or 5-LO_3W mutant lacking the Ca^{2+} binding site, respectively. Cells were preincubated with F-XII or F-XVI at the indicated concentrations or vehicle (0.1% DMSO) for 15 min, followed by stimulation with 2.5 µM A23187 and 3 µM AA for 10 min. 5-LO product formation was detected by RP-HPLC. Data are given as percentage of control (100%); means ± SEM, n = 4.

Ca^{2+} mediates the binding of 5-LO to membrane phospholipids (PC) via distinct tryptophan residues. HEK293 cells stably expressing FLAP and 5-LO_3W, respectively, were used to study if the hydroquinones may act via the PC-binding site of 5-LO (Figure 4.29 B). In the 5-LO_3W mutant the three tryptophans W13, W75 and W102 were replaced by alanine (kindly provided by Dr. Steinhilber, University of Frankfurt), resulting in a disability to bind PCs.

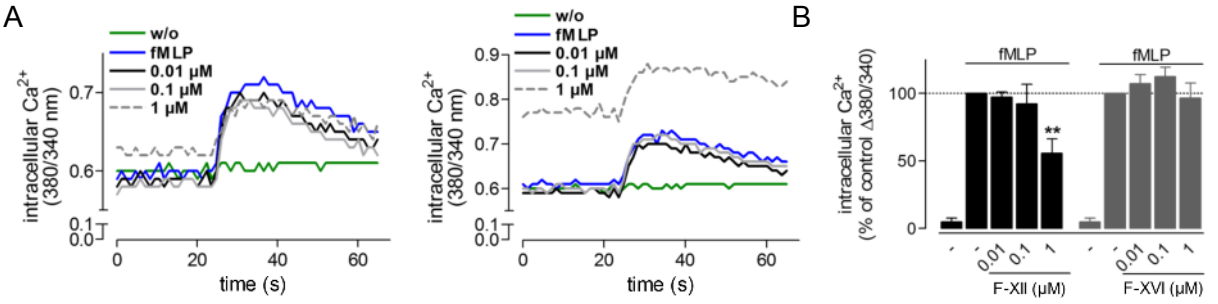

Figure 4.29: Influence of F-XII and F-XVI on intracellular Ca^{2+} levels in PMNL. PMNL were pre-stained with 1 mM Fura-2/AM for 45 min and incubated with compounds at the indicated concentrations or vehicle (1% DMSO) for 10 min. Upon addition of 1 mM Ca^{2+} intracellular Ca^{2+} increase was induced by 1 µM fMLP. (A) Data are given as means of ratio 380/340 nm; n = 3. (B) Data are given as percentage of fMLP stimulated control (ratio 380/340 nM at t_{max} minus t_{min}), means ± SEM, n = 3, **p < 0.01 vs. fMLP stimulated sample. Repeated measures ANOVA followed by Bonferroni post hoc test applied to absolute values.

Interestingly, F-XII and F-XVI showed nearly the same activity (F-XII: 5-LO_wt IC_{50} = 0.3 ± 0.03 µM, 5-LO_3W IC_{50} = 0.4 ± 0.06 µM; F-XVI: 5-LO_wt: IC_{50} = 0.4 ± 0.04 µM, 5-LO_3W IC_{50} = 1.0 ± 0.2 µM), suggesting that W13, W75 and W102 residues as PC-binding sites play no major role in 5-LO inhibition by the hydroquinones. Since the intracellular increase of Ca^{2+} leads to 5-LO activation, the possible interference of F-XII and F-XVI with Ca^{2+} mobilization was assessed (Figure 4.29). PMNL were pre-stained with a Ca^{2+} sensitive dye Fura-2 followed by pre-incubation with F-XII and F-XVI. Subsequent fMLP stimulation led to an intracellular Ca^{2+} increase (Figure 4.29 A). Interestingly, F-XII displayed a decrease of the Ca^{2+} level to about 50% at a concentration of 1 µM (Figure 4.29 B), whereas F-XVI showed no effect.

Activation of 5-LO can not only be achieved by cellular Ca^{2+} increase but also by different kinases via phosphorylation [110, 111]. Therefore, effects of F-XII and F-XVI on the activation of ERK1/2 and p38 MAPK were analyzed. PMNL were preincubated with both hydroquinones and stimulated with fMLP. The selective ERK pathway inhibitor U0126 was used as control. Western blots showed no effect of F-XII and F-XVI on the phosphorylation and thus activation of these protein kinases (Figure 4.30).

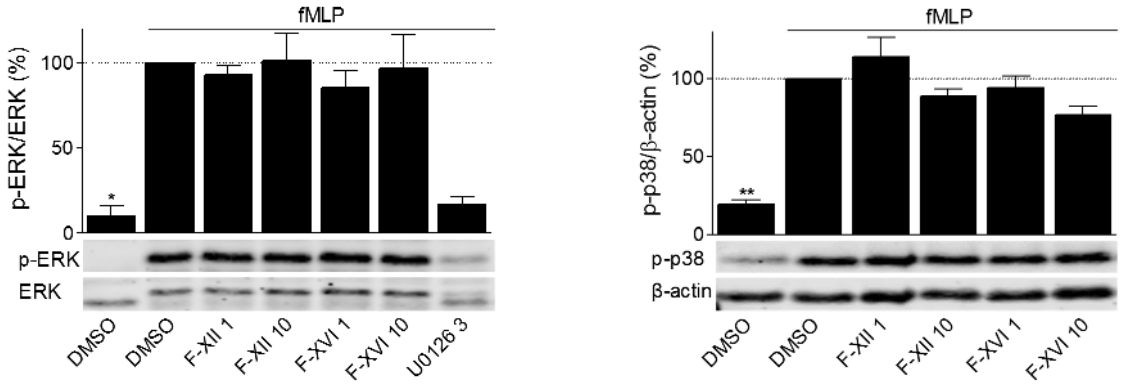

Figure 4.30: F-XII and F-XVI fail to affect activation of MAPKs relevant for 5-LO. PMNL were preincubated with F-XII or F-XVI at the indicated concentrations, 3 µM U0126 or vehicle (0.1% DMSO) for 15 min, followed by stimulation with 1 µM fMLP for 90 s. Cell lysates were obtained by sonication. Phosphorylation of ERK1/2 and p38 was detected via Western blot analysis. Protein amounts are given as percentage of control (fMLP stimulated samples are set to 100%), means ± SEM. Representative Western blots out of 3-5 independent experiments. *p < 0.05, **p < 0.01 vs. fMLP stimulated sample. Repeated measures ANOVA followed by Bonferroni post hoc test applied to absolute values.

4.3.5 Effects of F-XII and F-XVI on other enzymes involved in the biosynthesis of lipid mediators

Besides 5-LO, other enzymes are involved in the formation of inflammatory lipid mediators. F-XII did not impair the activity of mPGES-1, COX-2, LTC_4S or sEH but had a moderate effect on COX-1 activity, with an IC_{50} of 3.8 ± 0.3 µM (Table 4.10). Effects of F-XVI were comparable, but also marginally affected mPGES-1 with an IC_{50} of 8.1 ± 1 µM and also sEH to some degree.

Table 4.10: Effects of F-XII and F-XVI on various enzymes involved in lipid mediator biosynthesis in cell-free assays. F-XII, F-XVI or inhibitors were added to respective enzymes 15 min (mPGES-1, COX-1/2, sEH) or 10 min (LTC_4-S) prior induction of the enzyme reaction. Data are given as IC_{50}-values (µM) or as percentage of control (100%) means ± SEM, n = 3-4. Indo, indomethacin. Assay performed by [a]Katrin Fischer, [b]Stefanie Liening, [c]Erik Romp.

	F-XII (10 µM)	**F-XVI (10 µM)**	**control inhibitor**	
enzyme (cell-free)	remaining activity (%) or IC_{50} (µM)		remaining activity (%)	
mPGES-1[a]	59.6 ± 6.7%	8.1 ± 1 µM	23.04 ± 1.4%	MK886 10 µM
COX-1	3.8 ± 0.3 µM	4.0 ± 0.2 µM	24.4 ± 2.8%	indo 10 µM
COX-2	153.2 ± 19.9%	103.5 ± 19.1%	48.2 ± 17.1%	indo 10 µM
LTC_4S[b]	110.2 ± 7.3%	105.2 ± 9.7%	3.48 ± 0.7%	MK886 10 µM
sEH[c]	94.5 ± 11.7%	46.3 ± 15.3%	11.1 ± 0.5%	AUDA 1 µM

Table 4.11 shows the interactions of the two hydroquinones on further pro-inflammatory enzymes, analyzed in cell-based settings. Here, inhibition of COX-1 activity was similar to the cell-free assay, however, F-XII and F-XVI were more potent on COX-2 (F-XII IC_{50} = 1.1 ± 0.3 µM; F-XVI IC_{50} = 0.4 ± 0.2 µM). Regarding IL-1β, -6 and -8 and TNFα formation, F-XII and F-XVI showed no suppressive effects.

Table 4.11: Effects of F-XII and F-XVI on COX enzymes and cytokine formation in cell-based assays. F-XII, F-XVI or inhibitors were added 15 min (COX-1/2, 12-/15-LO) or 30 min (ILs, TNF_α) prior stimulation of cell system. Data are given as IC_{50}-values or as percentage of control (100%) means ± SEM, n = 3-4. Indo, indomethacin; cele, celecoxib; dexa, dexamethasone. [a]Assays performed by Stefanie König.

		F-XII (10 µM)	**F-XVI (10 µM)**	**control inhibitor**	
enzyme/ mediator	cell type	remaining activity (%) or IC_{50} (µM)		remaining activity (%)	
COX-1	platelets + AA	3.8 ± 0.1 µM	3.2 ± 0.2 µM	6.8 ± 3%	indo 10 µM
COX-2	monocytes + LPS/AA	1.1 ± 0.3 µM	0.4 ± 0.2 µM	31.9 ± 7.7%	cele 1 µM
IL-1β[a]	monocytes + LPS	121.2 ± 6.6%	85.1 ± 12.2%	35.6 ± 7%	dexa 1 µM
IL-6[a]	monocytes + LPS	100.7 ± 11.1%	73 ± 11.6%	51.6 ± 3.4%	dexa 1 µM
IL-8[a]	monocytes + LPS	94.4 ± 3.4%	73.5 ± 3.4%	57.3 ± 3.5%	dexa 1 µM
TNFα[a]	monocytes + LPS	105.9 ± 8.9%	63.1 ± 10.4%	24 ± 1%	dexa 1 µM

To strengthen the data, a complete screening of lipid mediators formed by monocytes following 90 min stimulation with A23187 was performed. Interestingly, a preferential inhibition of all lipid mediators was detectable, where 5-LO was involved in the biosynthesis (Figure 4.31), for example LTB_4 and its isomers or 5-HETE/5-HEPE (IC_{50} around 0.03 µM, white squares). Similar to evaluations in PMNL, 12- and 15-LO, as well as COX enzymes were only affected at much higher concentrations of F-XII and F-XVI (IC_{50} between 1 to 3 µM, white squares).

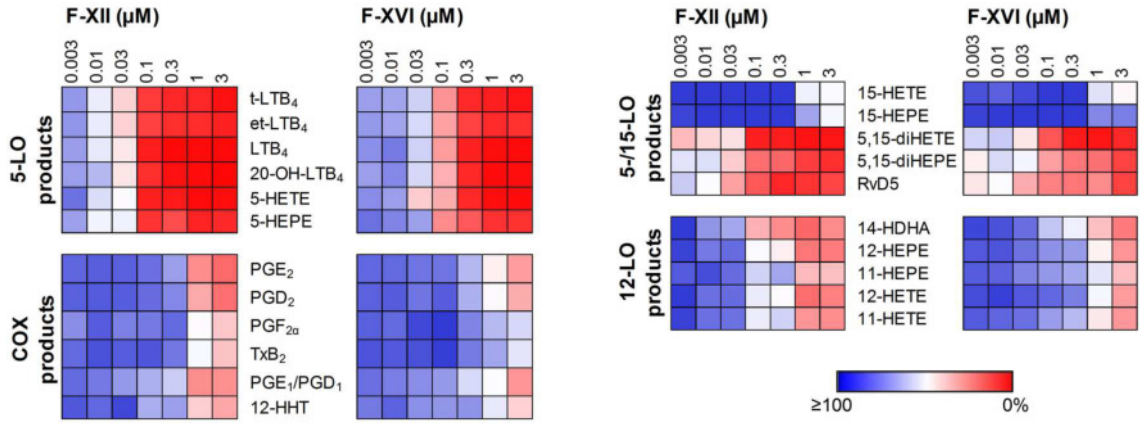

Figure 4.31: Influence of F-XII and F-XVI on the lipid mediator profile of monocytes. Monocytes were preincubated with F-XII or F-XVI at the indicated concentrations or vehicle (0.1% DMSO) for 15 min followed by stimulation with 0.5 µM A23187 for 90 min. Data are given as percentage of control in a heat map (from 100% blue to 0% red), means ± SEM, n = 3-4.

4.3.6 Radical scavenger and antioxidant properties of F-XII and F-XVI

Since antioxidant activity is an underlying mechanism of 5-LO inhibition, the ability of F-XII and F-XVI to scavenge the stable free radical DPPH was determined (Figure 4.32 A). Ascorbic acid as typical antioxidant agent was used as control. Up to 1 µM F-XII and F-XVI were inactive, but scavenged DPPH nearly completely at a concentration of 10 µM. This indicated effective antioxidant activities at concentrations that are about 150-fold higher than needed for 5-LO inhibition.

Additionally, both F-XII and F-XVI showed antioxidant properties in a cellular setting, based on inhibition of ROS formation in PMNL. In fMLP stimulated PMNL they decreased ROS formation to the basal level at a concentration of 1 µM, upon PMA stimulation at a concentration of 10 µM Figure 4.32 B).

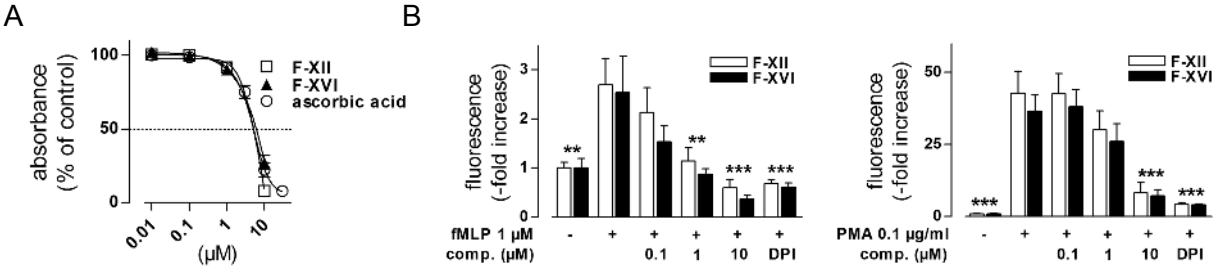

Figure 4.32: Radical scavenger and antioxidant properties of F-XII and F-XVI. (A) Effect on the stable free radical DPPH. F-XII, F-XVI or ascorbic acid were diluted in ethanol to indicated concentrations and 50 µM DPPH was added for 30 min. Radical scavenging was photometrically detected at 520 nm. Data are shown as percentage of DPPH sample (100%), means ± SEM, n = 3-5. (B) Influence on cellular ROS formation. PMNL were preincubated with F-XII and F-XVI at the indicated concentrations, 10 µM DPI or vehicle (1% DMSO) for 15 min. 1 µg/ml DCFH-DA and 1 mM $CaCl_2$ were added 2 min prior stimulation with either 1 µM fMLP for 8 min or 0.1 µg/ml PMA for 6.5 min. Fluorescence of oxidized DCFH-DA was monitored (excitation wavelength: 485 nm, emission wavelength: 535 nm). Data are shown as fold increase of vehicle control, means ± SEM, n = 5. **p < 0.01, ***p < 0.001 vs. fMLP or PMA stimulated sample, repeated measures ANOVA followed by Tukey post hoc test applied to absolute values.

4.3.7 Effects of F-XII and F-XVI in human blood and efficacy *in vivo*

Finally, the pharmacological relevance was investigated in human blood and in an *in vivo* model of acute inflammation in mice. Heparinized blood was preincubated with the compounds and either stimulated with A23187 alone, A23187 with AA or by priming the blood with LPS and subsequent stimulation with fMLP. Compared to F-XVI, compound F-XII was about 4-fold more active in HWB challenged with A23187 alone (IC_{50} = 0.7 ± 0.3 µM vs. 2.3 ± 0.5 µM) , 3-fold in HWB challenged with A23187 plus AA (IC_{50} = 0.6 ± 0.2 µM vs. 1.9 ± 0.5 µM), and 2-fold in HWB challenged with LPS/fMLP (IC_{50} = 1.1 ±0.5 µM vs. 2.4 ± 0.6 µM) (Figure 4.33 A). The zymosan induced peritonitis in mice was performed in the lab of Prof. Lidia Sautebin (University of Naples, Italy) (Figure 4.33 B). The compounds were given intraperitoneally 30 min prior zymosan induced inflammation and were able to suppress the migration of inflammatory cells into the peritoneal cavity (vehicle: 3.1 ± 0.7 ×10^6/ml cells; F-XII: 1.22 ± 0.2 ×10^6/ml cells; F-XVI: 0.8 ± 0.1 ×10^6/ml cells; zileuton: 0.4 ± 0.1 ×10^6/ml cells). F-XII prevented migration about 60%, whereas F-XVI subdued the migration about 75%. Zileuton was used as control (reduction of migrating cells about 87%). These results prove their potential *in vivo* and their possible use in pharmacotherapy in the future.

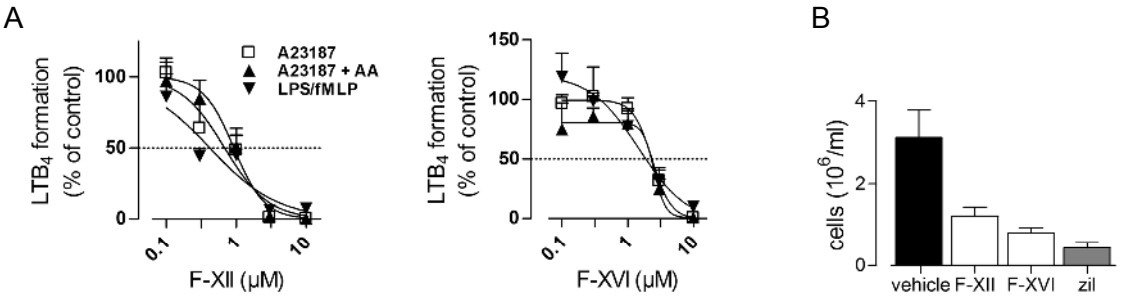

Figure 4.33: Suppression of 5-LO product formation by F-XII and F-XVI in human whole blood and efficacy *in vivo*. (A) 1 ml of HWB was preincubated with compounds at the indicated concentrations or vehicle (0.1% DMSO) for 15 min followed by stimulation with 30 µM A23187 with or without 100 µM AA for 10 min. Alternatively, HWB was primed with 1 µg/ml LPS for 30 min and 0.3 U/ml ADA for 20 min, followed by stimulation with 1 µM fMLP for 15 min. Compounds were added 15 min prior fMLP stimulation. 5-LO product formation was detected by LC-MS/MS. Data are given as percentage of control (100%), means ± SEM, n = 3-5. (B) Effect of catechols on cell migration in zymosan-induced peritonitis in mice. 10 mg/kg F-XII or F-XVI, 10 mg/kg zileuton or vehicle (0.9% saline solution containing 2% DMSO) were given intraperitoneally 30 min before zymosan injection (2 mg/ml in 0.9% w/v saline). Mice were sacrificed after 4 h and peritoneal exudates were collected. Cells were counted using a light microscope in a Burker's chamber after vital trypan blue staining. Data are expressed as percentage of control (100%), means ± SEM, n = 6 animals for each group.

5 DISCUSSION

COX products and 5-LO products are involved in inflammation and reactions of the innate immune response. Dysregulation of the 5-LO/COX pathways can lead to the inability to initiate resolution of inflammation and can escalate into chronic inflammatory diseases like rheumatoid arthritis, multiple sclerosis, atherosclerosis, inflammatory bowel diseases as well as cancer [1, 22]. Moreover, 5-LO-derived leukotrienes play a pivotal role in the development of chronic allergic diseases like asthma and rhinitis [6]. Some of these diseases like systemic lupus erythematosus, rheumatoid arthritis or asthma have been shown to be sex-biased with higher prevalence and severity in females [77]. One possible reason might be sex differences in the production of arachidonic acid-derived lipid mediators like leukotrienes, for which a different regulation of the formation could be detected in mice [194] as well as in human innate immune cells showing higher LT levels in female individuals compared to males. This regulatory effect could be shown to be influenced by the male sex hormone testosterone [4, 88]. Furthermore, the levels of pro-inflammatory interleukins in human whole blood and monocytes was shown to be sex-biased [216, 232]. However, the underlying intracellular mechanisms of the sex-related modulation of immune reactions in inflammation are largely unknown and the question arose, whether the regulation of prostanoid formation in human whole blood is sex-biased as well. First, the prostanoid formation in male and female whole blood and in isolated immune cells will be discussed. Second, the focus will be on the identification of potent 5-LO inhibitors and their mode of action to modulate the leukotriene formation.

5.1 The impact of sex on the prostanoid formation and degradation

The initial investigations addressing the sex-specific prostanoid formation were conducted in human whole blood, where the cells are in a physiological environment, simulating the *in vivo* situation best. Cell counts of the whole blood samples revealed differences in prostanoid-producing cells, with monocyte numbers found to be significantly higher in males, whereas neutrophil numbers were higher in females, consistent with other studies [209, 210]. Since monocytes are the main source of prostanoids in human blood, the enhanced monocyte numbers in males already suggested a sex-regulated prostanoid formation, due to the enhanced capacity to generate prostanoids. On this rationale, the obtained results were normalized on the cell number of monocytes together with neutrophils. The most pronounced effect was detected with significantly enhanced prostanoid levels in HWB, especially of PGE_2, in male samples compared to females after LPS stimulation for 24 h but also with Ca^{2+} ionophore and fMLP, even after normalization. Stimulation with Pam3CSK4, AA and PMA and short-term incubations of whole blood with AA or the Ca^{2+} ionophore displayed no sex difference. Very few studies have been conducted addressing sex-related prostanoid formation in human whole blood of healthy volunteers. However, similar effects were observed in cell based settings, e.g. a study using human platelets, revealing a higher formation of TxB_2 in males [233], as well as higher formation of PGE_2 and TxB_2 in kidney medulla cells of rats [234]. Another study detected higher PGE_2 levels in plasma of male mice suffering haemorrhage and sepsis [235]. On the other hand, several studies reported the opposite findings. Macrophages of rats and mice susceptible to arthritis or after trauma showed higher prostanoid formation in female cells [236-238]. Trying to clarify these inconsistent results obtained in cellular settings,

PBMC were isolated from HWB and challenged with LPS. Incubation in cell culture medium, containing 0.5% of sex hormones-depleted human serum did not result in different prostanoid levels in males compared to females. The lack of a sex difference in isolated cells could be explained by intracellular changes occurring during the isolation and purification process. Kelley et al. reported activation of monocytes due to attachment to plastic surfaces [239] and several other studies revealed changes in the monocyte response upon stimulation [240-242]. This could lead to the loss of contributing mechanisms to the differential prostanoid formation. In contrast, whole blood preparations partially prevent monocyte attachment [243]. Incubation of the isolated PBMC in autologous plasma could not restore the sex difference but increased the PGE_2 level about 8-fold and TxB_2 levels about 2-fold. Pre-incubation of human whole blood with sex hormones had no effect on prostanoid formation in female blood, whereas in blood from males, pre-incubation resulted in a modest increase of prostanoids with all four applied sex hormones. In contrast, in isolated PBMC pre-incubation rather decreased TxB_2 and $PGF_{2\alpha}$ levels in both sexes, whereas PGE_2 remained unaffected. To address transcriptional regulation of the prostanoid production by the steroids, preincubation with sex hormones for 5 h was evaluated as well, but the prolonged pre-incubation time had no effects (data not shown). In contrast, several studies showed regulatory mechanisms of sex hormones regarding the inflammatory response. For example, Miyagi et al. showed suppressing effects of testosterone and estradiol in low concentrations on the PGE_2 production, whereas progesterone appeared to enhance the PGE_2 formation in LPS stimulated human monocytes [244]. Unfortunately, they did not indicate the length of the pre-incubation periods with sex hormones or the LPS stimulation time. Sullivan and colleagues detected higher urinary excretion of PGE_2 metabolites from female spontaneous hypertensive rats concluding higher plasma levels and could furthermore show that gonadectomy of male rats increased PGE_2 levels [214]. This suggests that PGE_2 formation is sensitive to testosterone. On the other hand, Vegeto et al. showed suppressive effects of estradiol on the LPS-activated expression of pro-inflammatory genes like the proteolytic matrix metallo-protease-9 gene in murine RAW267.4 cells [245].

Besides the prostanoid biosynthesis, the catabolism of prostanoids in human whole blood was evaluated as variable affecting overall prostanoid levels. The prostanoid-degrading enzyme is the 15-PGDH, producing 15-keto-prostaglandins with impaired biologic activity [218]. 15-PGDH is known to be counter-regulated to COX-2 [246, 247], and the expression is increased by classical COX-2 inhibitors [220, 248]. At early time points up to six hours after LPS stimulation, the activity of 15-PGDH appeared to be enhanced in female samples compared to males. Treatment with the specific 15-PGDH inhibitor SW033291 [221] elevated PGE_2 levels in female whole blood compared to male blood. Interestingly, after stimulation with LPS for 24 h the inhibitor lost its efficiency, and no differences in the activity could be seen. Further studies are needed to monitor the PGE_2 metabolites during LPS stimulation in order to verify the sex differences in the prostanoid catabolism. Consistent with this result are findings by others showing that progesterone is able to increase 15-PGDH activity in human erythroleukemia cells [220]. However, contrary results in the literature reported an elevated inactivation of prostaglandins in male rat medulla cells [234] and the ability of male sex hormones to induce 15-PGDH expression in hormones-responsive prostate cancer cells [219].

5.2 The effect of sex on intracellular signaling

Since the most pronounced sex difference in prostanoid formation in whole blood was evident following LPS stimulation, the TLR signaling cascade was evaluated in more detail. The expression of TLR4 on the cell surface of isolated monocytes was found to be enhanced in female cells compared to male monocytes, although not significantly. This finding could provide evidence for a negative prerequisite involved in the development of autoimmune diseases, which occur with higher prevalence in females. Several studies could demonstrate that upregulation of TLR4 on immune cells is involved in the pathogenesis of systemic lupus erythematosus [249] and rheumatoid arthritis [250]. However, other findings described in the literature suggested no sex difference regarding the expression of TLR4 on PBMC of gastric cancer patients [85] and the CD14/TLR4 expression on murine macrophages after trauma-haemorrhage [251]. In contrast to the results obtained in this thesis, Mariott et al. reported opposite findings: Higher expression levels of CD14 and TLR4 on male macrophages, and elevated PGE_2 formation in females [87]. Stimulation with LPS requires the formation of a receptor complex consisting of LPS, LBP, CD14, MD-2 and TLR4, which initiates intracellular signaling resulting in the activation of NF-κB and expression of COX-2, taking several hours [44]. However, Mariott at el. examined PGE_2 formation 4 h after LPS stimulation. Investigations in this thesis could barely determine COX-2 expression in human monocytes until 5 h after LPS stimulation and hence nearly no PGE_2 production (data not shown). To evaluate the role of COX-2, mRNA and protein expression was explored. In isolated PBMC, no differences in COX-2 mRNA levels as well as in COX-2 protein expression was observed between males and females. Interestingly, in monocytes sorted by FACS, the COX-2 expression appeared to be higher in female cells, compared to males. This finding was unexpected, thus elevated TLR4 and COX-2 expression in females would suggest enhanced prostanoid levels in female but not in male blood. Literature about sex-dependent COX-2 expression is as controversial as every other aspect of the sexual dimorphism in prostanoid formation. Higher COX-2 protein expression was observed in female rat medulla cells [214] and Martorell and colleagues could demonstrate an increase of COX-2 protein expression in aortic segments from orchidectomized rats [213]. In contrast, Diodato et al. report decreased COX-2 protein levels in liver of female mice exposed to haemorrhage and sepsis, compared to males [235].

Regarding the possibility that mechanisms contributing to the sex difference in prostanoid formation are relevant immediately upon cell stimulation, the constitutively expressed COX-1 protein was evaluated. In PBMC, isolated from HWB, a moderate, but not significant, sex difference in the expression levels could be detected, with higher COX-1 levels in females. Along these lines, stimulating effects of estradiol on COX-1 expression in human umbilical vein endothelial cells were reported in literature [252]. In contrast, higher COX-1 expression was evident in male PMNL, compared to female [5], whereas prostanoid formation was found to be equal in both sexes in PMNL isolated from whole blood. The sex difference was independent of A23187-induced AA release in PMNL within the first two hours, although, AA release should be further elucidated in isolated PBMC or monocytes using LPS as stimulus, regarding the pronounced effect after LPS application in whole blood. Furthermore, this thesis did not address effects of sex on the intracellular Ca^{2+} mobilization required for AA release. Nevertheless, studies of different groups suggest a sex-dependent regulation in different cell types. In ventricular myocytes from mice [253], in vascular smooth muscle cells from rats [254]

and in rat platelets [255] investigations report an increased Ca^{2+} mobilization by male cells suggesting the involvement of sex hormones.

5.3 Sex differences in the cell-cell cross talk

Regarding the fact that immune cells react in an orchestrated manner [256-258], sex-dependent differences in the cell-cell cross talk in human whole blood after stimulation needed to be considered. Therefore, PBMC and PMNL were isolated from human whole blood and stimulated alone or in co-incubations in autologous plasma, concurrent with HWB incubations. Following LPS stimulation only PGE_2 formation appeared to increase in male blood preparations by cell interactions between PBMC and PMNL, whereas all three prostanoids showed the observed sex difference in the whole blood incubations. Stimulation with AA increased prostanoid formation in male samples due to cell interactions between PBMC and PMNL of all three prostanoids. So far, no findings about a sex-specific difference in intercellular cross talk in inflammatory processes could be found in literature. Nevertheless, few studies identified sex-related disparity in the formation of TxA_4 and aspirin-triggered lipoxins [259, 260], indicating differences in cell-cell interactions.

To summarize, regarding the controversial results on sex differences in prostanoid formation obtained in this thesis and the plethora of inconsistent reports in literature, no distinct mechanism could be identified leading to the data obtained for human whole blood. One major drawback is the missing knowledge about the blood donor's personal information. Due to data privacy no specifications about age, hormonal contraception, and the phase of the menstrual cycle of the female donors could be obtained. Furthermore, it became obvious that results strongly depend on cell type, stimulating agent, regarded lipid mediator of interest and the species used for investigations. Nonetheless, elucidation of the sexual dimorphism in prostanoid formation should be pursued to provide optimal pharmacological therapy for both men and women.

5.4 Inhibition of 5-LO by 1,4- and 1,2-benzoquinones

In this study, 16 different 1,4- and 1,2-benzoquinones were investigated regarding their inhibitory potential on 5-LO. These 16 compounds were part of a series, containing 48 structures in total, systematically modified trying to increase the inhibitory efficiency of the lead compound embelin [225]. Literature suggests that quinones are redox-type inhibitors, Michael acceptors reacting with cysteines on 5-LO, or act by defined binding to 5-LO in the active site [150, 167, 169]. Furthermore, the intracellular reducing milieu can transform the quinones to hydroquinones, which are reducing agents and may interfere with the catalytic cycle of 5-LO through their radical scavenging abilities [228, 261]. Nevertheless, recent studies showed that the binding mode is rather a non-redox-type. The inhibitory potential of several 1,4-benzo-quinones did not correlate with the antioxidant properties [262] and exhibited high activity in cell-free systems as well, where reducing agents are missing [168]. In addition, the potential of the 1,4-benzoquinone embelin was independent of the redox form of the quinone moiety and indicated no interaction with the related enzymes 12- and 15-LO. Both LOs possess a

non-heme catalytic iron and exert the same catalytic redox cycle as 5-LO [8]. Variation of another 1,4-benzoquinone series revealed that the inhibitory potential is rather determined by the adjacent residues than the antioxidant capacity [169].

The 16 compounds evaluated in this thesis were varied in the hydroxylation and methylation pattern of the benzoquinone core and in the length of the *n*-alkyl chain in 3-position, since previous studies showed the importance of the linked substituent for the inhibitory efficiency [225]. In cell-free assays, the compounds of all four series showed potent inhibition of 5-LO, with series C (4,5-methoxy-1,2-benzo-quinones) as most potent structures. They exhibited IC_{50} values in a range of 0.04 to 0.6 µM, followed by series D (2,5-hydroxy-1,4-benzoquinones),

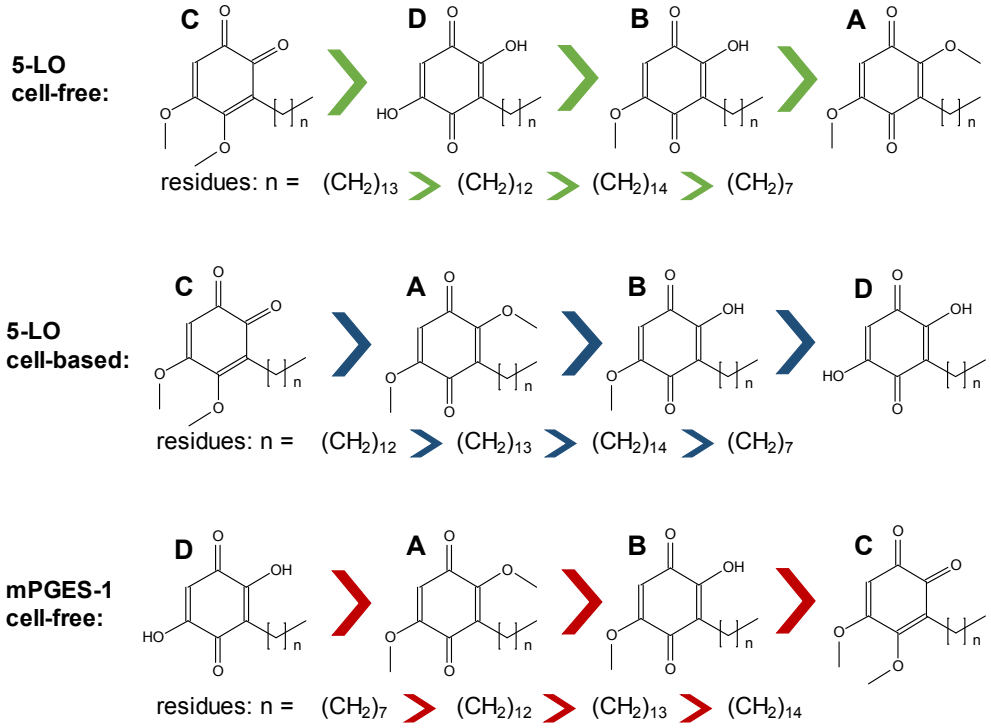

Figure 5.1: Structure-activity relationships of the benzoquinones with 5-LO or with mPGES-1 respectively, in cell-free and cell-based assays. From left highly active to right less active.

series B (2-hydroxy-5-methoxy-1,4-benzoquinone) and series A (2,5-methoxy1,4-benzo-quinones), as shown in Figure 5.1. The lowest efficacy in every group was determined for the structures substituted with a short C8-*n*-alkyl chain (EA-109 A-D) displaying IC_{50} values between 0.3 and 3 µM, whereas an C14-*n*-alkyl residue was examined as most suitable (Figure 5.1). In cell-based assays it became apparent that methylation of the hydroxyl groups increased the inhibitory potential. An explanation could be that the polarity of the bi-hydroxylated compounds and the two incorporated vinyloge acids reduced the permeation into the cells. Compounds of series B containing one hydroxyl group were less efficient with IC_{50} values in a range of 0.3 to 2.3 µM or above 10 µM and compounds of series D with two hydroxy groups nearly lost their activity with IC_{50} values between 2.5 and 5.1 µM or above 10 µM. Series C again showed most potent effects on 5-LO (Figure 5.1) with IC_{50} values in a range of 0.05 to 0.8 µM. However, the compound EA-112C substituted with a C15-*n*-alkyl residue was an exception in this series and showed no activity on 5-LO. In general, efficacy of the

benzoquinones on 5-LO in cellular settings was enhanced along with the number of methylated hydroxyl groups on the benzoquinone moiety, the change from the 1,4-benzoquinone to the 1,2-benzoquinone core, and a *n*-alkyl residue containing 13 to 14 carbon atoms in 3-position (Figure 5.1), revealing compound EA-110C as most potent compound. The activity in intact cells challenged with A23187 together with AA was slightly lower compared to stimulation with A23187 alone, indicating a possible competition with AA for the binding site, which seemed reasonable considering the fatty acid-like structure of the inhibitors. Besides 5-LO, several of the 1,4-benzoquinones showed inhibition of mPGES-1 (Figure 5.1). The most pronounced effects were exerted by the di-hydroxylated compounds of series D, with IC_{50} values between 0.8 and 2.1 µM. EA-109D was the most potent compound of the complete series substituted with a C8-*n*-alkyl chain, whereas in series A, the highest efficacy was obtained by a structure bearing a C13-*n*-alkyl residue. In contrast, series C containing the 1,2-benzoquinone backbone completely lost inhibitory potency on mPGES-1. These results denoted that inhibition of mPGES-1 depends on both, the hydroxyl groups and the length of the substituted residue. In addition, none of the 16 compounds interfered with the related 12- and 15-LO, indicating a rather non-redox-type inhibition, since both enzymes feature activity via a redox cycle based on a non-heme iron. In summary, evaluation of the 16 benzoquinone compounds revealed highly active compounds with EA-110C as most potent and additionally, as selective inhibitor for 5-LO comparable to the activity of the 1,2-benzoquinone RF-22c [170] and superior over the plant-derived 1,2-benzoquinone aethiopinone [263].

5.5 Inhibition of 5-LO by 1,2-benzohydroquinones with linear residues

Encouraged by the identification of EA-110C as highly potent and selective 5-LO inhibitor, further structural modifications were made to yield even more effective compounds. In the literature, natural 1,2-hydroquinones (= catechols) are described as 5-LO inhibitors [149, 227] such as flavonoids and polyphenols. It could be shown that the position of the hydroxyl groups determined the activity. O*rtho*-benzohydroquinones were found to be effective 5-LO inhibitors and substitution in 3-position potentiated the inhibitory effect. In contrast, methylation of one of the hydroxyl groups decreased the activity and *meta*-hydroquinones were poor inhibitors or even inactive [261]. The mechanism by which they inhibit leukotriene formation is supposed to depend on interference with the redox cycle of the catalytically active iron of 5-LO, interference with required lipid peroxides or by complexing the active site iron. Dupon et al. showed that polyhydroxylated naphthalenic derivatives could inhibit 5-LO in cellular settings and additionally exerted radical scavenging properties. Furthermore, these compounds were able to rapidly reduce Fe^{3+} to Fe^{2+} in a cell-free assay at low pH of 1-2 but very slowly at a pH around 8 [264]. Hence, they concluded the radical scavenging and the reduction of the active site iron as responsible mechanism for the inhibitory action. Similarly, Prasad et al. determined the potential inhibition on 5-LO product formation of phenolic compounds and flavonoids in spices. They determined rather high IC_{50} values regarding the interference with 5-LO, for example of quercetin and eugenol (both around 25 µM) [265]. Quercetin was shown to reduce the active site iron to Fe^{2+} and to chelate Fe^{2+} preventing participation in the catalytic redox cycle [266]. Based on these findings, the 1,2-benzoquinone backbone of EA-110C was reduced to a 1,2-hydroquinone backbone (EA-110C RED). Moreover, two more 1,2-hydroquinones of EA-110C with different *O*-methylation patterns were synthesized (EA-110C T

RED, EA-110C P RED), as well as the hydroquinone forms of two other compounds (EA-107C RED and EA-100C RED) [198]. This new series was first analyzed in cell-free and cellular assays to determine the benefit of the quinone core reduction. In comparison with the related 1,2-benzoquinone the hydroquinone EA-107C was superior over its parental compound confirming that the hydroquinone form is the active form in the cellular environment where reducing conditions are present [228, 229]. All five hydroquinones were highly active with IC_{50} values in cell-free assay between 0.06 and 0.29 µM as well as in cellular settings with IC_{50} values in a range of 0.03 to 0.31 µM, whereas trihydroxylation or *para*-dihydroxylation decreased the activity compared with the 1,2-hydroxylation pattern, similar to results of Alanko et al. [261]. The 1,2-hydroquinones displayed a more effective inhibition in cell-based assays indicating either additional targets, intracellular enrichment or activation within the cell. However, the evaluation of these mechanisms were not addressed in this thesis but the binding mode of the hydroquinones to 5-LO and physiological relevance were analyzed more in detail. Incubations of EA-110C and EA-110C RED with various concentrations of AA revealed a non-competitive inhibition. The activity of the hydroquinone was the same, regardless of the different AA concentrations, whereas the benzoquinone EA-110C was less effective with lower AA concentrations (2 and 5 µM). Greiner et al. suggested a second putative binding site of AA positively modulating 5-LO activity, which is blocked by several inhibitors in a AA-uncompetitive manner (e.g. HZ52). Alternatively, higher AA concentrations are needed to form micelles incorporating the inhibitor molecules leading to a more efficient access towards 5-LO [267]. Docking simulations revealed binding of both, the quinone and the hydroquinone moiety in the binding pocket forming hydrogen bonds with Tyr-81, Tyr-383 and Glu-622. In contrast to the quinone core, EA-110C RED was able to form bidirectional hydrogen bonds via the two hydroxyl groups. Furthermore, docking simulations did not suggest direct interaction of the quinone and the hydroquinone with the active site iron.

The anti-inflammatory potential of both the quinone and the hydroquinone could be verified *in vivo*. In carrageenan-induced paw oedema both compounds reduced hind paw swelling in early and late time points along with effective repression of cys-LT formation and migration of inflammatory cells [231]. These results confirm the high efficacy of quinones and hydroquinones to reduce inflammation by potent suppression of 5-LO. This study revealed a 1,2-benzoquinone/-benzohydroquinone backbone with a C13-*n*-alkyl chain in 3 position as optimal structure to interfere selectively with 5-LO. No detailed analysis of the radical scavenging and iron chelating properties were conducted to clarify the mechanism of inhibition, however docking simulation suggested binding to the binding site without direct interaction with the active site iron. This indicated that the inhibitory mechanism is not mainly based on interference with the catalytic redox cycle.

5.6 Inhibition of 5-LO by 1,2-benzohydroquinones with bulky residues

To explore the interference of 1,2-benzohydroquinones with 5-LO and respective SARs, a second set of compounds, substituted with bulky aromatic residues in 4-position was synthesized. A screening on 5-LO activity revealed highly active compounds, with IC_{50} values in cell-free assays in a range of 7 to 210 nM and of 0.07 to 2.1 µM in cell-based settings. Nelson et al showed that the ability of chelating compounds to reduce the ferric state of 5-LO is partly dependent on the electron-withdrawing or electron–donating properties of the

substituent [268]. Nevertheless, it seemed that rather linear structures with lipophilic residues were favored over inflexible hydroxylated substituents in 4-position to yield effective inhibition of 5-LO product formation. Out of this series the two compounds F-XII and F-XVI were outstanding in their ability to suppress LT formation. Thus, they were chosen for detailed investigations of the 5-LO inhibitory mechanisms. In isolated PMNL, they effectively inhibited 5-LO product formation with IC_{50} values in a low nanomolar range (between 60 and 120 nM), irrespective of the used stimulus (A23187, A23187 plus AA, LPS/fMLP). Of note, both compounds were able to outperform zileuton, the only available 5-LO inhibitor on the market (PMNL stimulated with A23187: IC_{50} = 2.5 ± 1.2 µM). Given that the inhibitory potential did not change using A23187 or LPS/fMLP compared to additional exogenous AA indicated that F-XII and F-XVI did not interfere with the $cPLA_2$ enzyme and thus with the AA supply. In contrast, inhibition of AA release could be shown for other 1,2-hydroquinones, like caffeic acid phenyl ester [269]. Strengthening the potent inhibition of LT synthesis in cellular settings, both compounds were equally active on the suppression of LTB_4 and cys-LT formation in isolated human monocytes, indicating that the LTC_4S or LTA_4H are no additional targets. To verify that the inhibitory potential is mediated by the 1,2-hydroquinone moiety the *O*-methylated analogues of F-XII (AF-06) and F-XVI (AF-13) were used as control compounds. Both AF-06 and AF-13 had poor effects on 5-LO product formation in PMNL stimulated with A23187 with or without exogenous AA (AF-06: $IC_{50} \approx 3$ µM; AF-13: remaining activity at 10 µM = 64 - 85%). Furthermore, monitoring the viability of monocytes treated with the hydroquinones confirmed that the potent inhibition is not mediated due to cell toxic effects. In cell-free assays with the isolated 5-LO enzyme, the inhibitory potential of F-XII and F-XVI was even enhanced (IC_{50} = 20 nM) suggesting that the hydrophilic 1,2-benzohydroquinone structure could hamper the permeability into the cells and furthermore, ruling out FLAP as cellular target enzyme. Moreover, the inhibition of the isolated enzyme was independent of the presence of detergents like Triton X-100, excluding acting as nuisance inhibitors. Involvement of the 1,2-hydroquinone core in cell-free assays was again confirmed using the *O*-methylated analogues as control compounds. In PMNL homogenates, efficiency of F-XII was similar but was decreased for F-XVI with a shift of the IC_{50} value to 1.3 µM. This loss of potency could be due to augmented binding to cellular debris or possible interaction with the C2-like domain, which is counteracted by phospholipids as shown for hyperforin and the pyridinylimidazol EP-6 [231, 270]. Detailed study of the binding mode revealed completely reversible inhibition of 5-LO, analyzed by wash out experiments. Interestingly, both compounds displayed a non-competitive mode of inhibition, suggesting that they do not compete with AA for the substrate binding site. The inhibitory potential of F-XII and F-XVI was furthermore independent of interaction with for distinct cysteinyl residues (Cys-159, Cys-300, Cys-416, Cys-418) on the surface of the catalytic C-terminal domain close to the substrate entrance, as shown for several other benzoquinones containing a Michael acceptor function [167]. Using HEK293 cells stably expressing a 5-LO mutant in which the cysteinyl residues were replaced by serines revealed no reduced activity compared to the 5-LO wild type. In accordance with this findings, docking simulation suggested binding to Asp-166, which interacts with Arg-101 connecting the catalytic C-terminal domain with the N-terminal C2-like domain. Additionally, Asp166 is part of a short α2 helix together with Phe-177 and Tyr-181, also called “FY cork” [102]. Interestingly, replacement of the Arg-101 by Asp increased enzyme activity in purified preparations [101], whereas replacement of Asp-166 by Asn decreased 5-LO activity [203]. Further investigations

are needed, to clarify the implication of the hydroquinone - Asp-166 interaction on the inhibitory potential. Probably, binding of the compounds to the α2 helix hampered the ability of the "FY cork" to warrant access of AA to the active site. Since, mutations in the "FY cork" were shown to impair association with the nuclear membrane and FLAP [271], the intracellular distribution of 5-LO in presence of the two hydroquinones was evaluated. The subcellular translocation was not affected by F-XII, whereas F-XVI seemed to interfere partly. Alterations in the intracellular translocation could be mediated by interaction of the hydroquinones with amino acids in the binding site for the membrane phospholipids [106]. In HEK293 cells, stably expressing FLAP and a 5-LO mutant where the respective tryptophans (Trp-13, Trp-75, Trp-102) were replaced by Ala, F-XVI was slightly less active, compared to the 5-LO wild type (5-LO_wt IC_{50} = 0.4 µM; 5-LO_3W IC_{50} = 1 µM). This outcome and the suggested interaction with Asp-166 could contribute to the inhibitory potential on 5-LO. In contrast, only F-XII appeared to influence the intracellular Ca^{2+} mobilization required for 5-LO activation at concentrations from 1 µM upwards. Besides the cellular Ca^{2+} increase, the MAPKs ERK1/2 and p38 activate 5-LO by phosphorylation [110, 111], which however was not influenced by both hydroquinones.

During the inflammatory process several enzymes form a plethora of inflammatory mediators. At concentrations up to 10 µM, F-XII and F-XVI had a nominal effect on mPGES-1 (F-XII: remaining activity at 10 µM = 60%; F-XVI: IC_{50} = 8 µM) and on COX-1 (IC_{50} ≈ 4 µM) in cell-free assays and on COX-2 in monocytes stimulated with LPS plus AA (IC_{50} between 0.4 – 1 µM). Enzymes like LTA_4H, sEH and COX-2 and the formation of interleukins and TNF_α remained unaffected. Furthermore, both benzoquinones did not affect the related enzymes 12- and 15-LO at concentrations up to 1 µM in PMNL and in monocytes. These results suggested that both benzohydroquinones were highly selective for 5-LO at low concentrations. Finally, radical scavenging and antioxidant properties were evaluated. F-XII and F-XVI were able to scavenge the stable free radical DPPH in a cell-free assay, though at concentrations at least 150-fold higher than required for 5-LO inhibition. Similar results were obtained investigating the antioxidant properties. Thus, ROS formation in PMNL was decreased to basal levels with concentrations 10 to 100-fold higher than needed for the suppression of LT formation. These results are consistent with studies from the groups of Dupont [264] and Boudreau [269], where the antioxidant and free radical scavenging potency of hydroquinones was not necessarily related to their ability to inhibit 5-LO. In addition to the striking efficacy of both benzohydroquinones in cellular and cell-free test systems, they both showed promising potential in human whole blood (F-XII: IC_{50} = 0.6 – 1.1 µM; F-XVI: IC_{50} = 1.9 - 2.4 µM) and possessed anti-inflammatory potential *in vivo.* In a zymosan induced peritonitis model in mice, both compounds effectively suppress the migration of inflammatory cells.

To summarize, 1,2-benzhydroquinones represent a group of potent 5-LO inhibitors dependent on their substituted residue in 4-position. The evaluated compounds F-XII and F-XVI were shown to be highly effective in cell-free and in different cell-based settings (PMNL, monocytes, HEK293 cell lines) with negligible impact on other enzymes involved in the inflammatory process. Their inhibitory mode seemed to be rather a non-redox-type or novel type, since concentrations required for antioxidant and radical scavenging properties are noticeably higher than for inhibition of 5-LO product formation and they both did not interfere with the related redox-cycle of 12- and 15-LO. Moreover, F-XVI may interact with the C2-like domain.

Conducting a chrome azurol S (CAS) assay (data not shown) suggested the ability of the compounds to form a Fe(III) complex. However, these complexes were not stable enough to be detectable with mass spectrometry analysis, indicating that chelating the active site iron is not the inhibitory mechanism, what was supported by docking simulations as well. Binding to amino acids, which are part of the salt bridge connecting the two 5-LO domains and/ or the membrane binding site seemed more likely. Additionally, the high efficacy in human whole blood and in inflammatory *in vivo* models identified these 1,2-benzohydroquinones as promising candidates demanding further pharmacological investigations for drug development.

6 LITERATURE

1. Ricciotti, E. and G.A. FitzGerald, *Prostaglandins and inflammation.* Arterioscler Thromb Vasc Biol, 2011. **31**(5): p. 986-1000.
2. Ruggieri, A., et al., *The influence of sex and gender on immunity, infection and vaccination.* Ann Ist Super Sanita, 2016. **52**(2): p. 198-204.
3. Dennis, E.A. and P.C. Norris, *Eicosanoid storm in infection and inflammation.* Nat Rev Immunol, 2015. **15**(8): p. 511-23.
4. Pergola, C., et al., *Testosterone suppresses phospholipase D, causing sex differences in leukotriene biosynthesis in human monocytes.* FASEB J, 2011. **25**(10): p. 3377-87.
5. Pace, S., et al., *Sex differences in prostaglandin biosynthesis in neutrophils during acute inflammation.* Sci Rep, 2017. **7**(1): p. 3759.
6. Haeggstrom, J.Z. and C.D. Funk, *Lipoxygenase and leukotriene pathways: biochemistry, biology, and roles in disease.* Chem Rev, 2011. **111**(10): p. 5866-98.
7. Newcomer, M.E. and N.C. Gilbert, *Location, location, location: compartmentalization of early events in leukotriene biosynthesis.* J Biol Chem, 2010. **285**(33): p. 25109-14.
8. Schaible, A.M., et al., *Potent inhibition of human 5-lipoxygenase and microsomal prostaglandin E(2) synthase-1 by the anti-carcinogenic and anti-inflammatory agent embelin.* Biochem Pharmacol, 2013. **86**(4): p. 476-86.
9. Medzhitov, R., *Inflammation 2010: new adventures of an old flame.* Cell, 2010. **140**(6): p. 771-6.
10. Nathan, C. and A. Ding, *Nonresolving inflammation.* Cell, 2010. **140**(6): p. 871-82.
11. Davies, L.C., et al., *Tissue-resident macrophages.* Nat Immunol, 2013. **14**(10): p. 986-95.
12. Luster, A.D., R. Alon, and U.H. von Andrian, *Immune cell migration in inflammation: present and future therapeutic targets.* Nat Immunol, 2005. **6**(12): p. 1182-90.
13. Sherwood, E.R. and T. Toliver-Kinsky, *Mechanisms of the inflammatory response.* Best Practice & Research Clinical Anaesthesiology, 2004. **18**(3): p. 385-405.
14. Soehnlein, O. and L. Lindbom, *Phagocyte partnership during the onset and resolution of inflammation.* Nat Rev Immunol, 2010. **10**(6): p. 427-39.
15. Ingersoll, M.A., et al., *Monocyte trafficking in acute and chronic inflammation.* Trends Immunol, 2011. **32**(10): p. 470-7.
16. Serbina, N.V., et al., *Monocyte-mediated defense against microbial pathogens.* Annu Rev Immunol, 2008. **26**: p. 421-52.
17. Duffin, R., et al., *Targeting granulocyte apoptosis: mechanisms, models, and therapies.* Immunol Rev, 2010. **236**: p. 28-40.
18. Lawrence, T., D.A. Willoughby, and D.W. Gilroy, *Anti-inflammatory lipid mediators and insights into the resolution of inflammation.* Nat Rev Immunol, 2002. **2**(10): p. 787-95.
19. Medzhitov, R., *Origin and physiological roles of inflammation.* Nature, 2008. **454**(7203): p. 428-35.
20. Nathan, C., *Points of control in inflammation.* Nature, 2002. **420**(6917): p. 846-52.
21. Serhan, C.N. and N.A. Petasis, *Resolvins and protectins in inflammation resolution.* Chem Rev, 2011. **111**(10): p. 5922-43.
22. Serhan, C.N. and J. Savill, *Resolution of inflammation: the beginning programs the end.* Nat Immunol, 2005. **6**(12): p. 1191-7.
23. Serhan, C.N., *Novel lipid mediators and resolution mechanisms in acute inflammation: to resolve or not?* Am J Pathol, 2010. **177**(4): p. 1576-91.
24. Serhan, C.N., *Lipoxins and aspirin-triggered 15-epi-lipoxins are the first lipid mediators of endogenous anti-inflammation and resolution.* Prostaglandins Leukot Essent Fatty Acids, 2005. **73**(3-4): p. 141-62.
25. Schwab, J.M. and C.N. Serhan, *Lipoxins and new lipid mediators in the resolution of inflammation.* Curr Opin Pharmacol, 2006. **6**(4): p. 414-20.
26. Ryan, A. and C. Godson, *Lipoxins: regulators of resolution.* Curr Opin Pharmacol, 2010. **10**(2): p. 166-72.
27. Karin, M., T. Lawrence, and V. Nizet, *Innate immunity gone awry: linking microbial infections to chronic inflammation and cancer.* Cell, 2006. **124**(4): p. 823-35.

28. Lawrence, T. and D.W. Gilroy, *Chronic inflammation: a failure of resolution?* Int J Exp Pathol, 2007. **88**(2): p. 85-94.
29. Lawrence, T., *The nuclear factor NF-kappaB pathway in inflammation.* Cold Spring Harb Perspect Biol, 2009. **1**(6): p. a001651.
30. Brockmann, L., et al., *Regulation of TH17 Cells and Associated Cytokines in Wound Healing, Tissue Regeneration, and Carcinogenesis.* Int J Mol Sci, 2017. **18**(5).
31. Aoki, T. and S. Narumiya, *Prostaglandins and chronic inflammation.* Trends Pharmacol Sci, 2012. **33**(6): p. 304-11.
32. Nasef, N.A., S. Mehta, and L.R. Ferguson, *Susceptibility to chronic inflammation: an update.* Arch Toxicol, 2017. **91**(3): p. 1131-1141.
33. Hussain, S.P. and C.C. Harris, *Inflammation and cancer: an ancient link with novel potentials.* Int J Cancer, 2007. **121**(11): p. 2373-80.
34. Grivennikov, S.I., F.R. Greten, and M. Karin, *Immunity, inflammation, and cancer.* Cell, 2010. **140**(6): p. 883-99.
35. Coussens, L.M. and Z. Werb, *Inflammation and cancer.* Nature, 2002. **420**(6917): p. 860-7.
36. Mantovani, A., et al., *Cancer-related inflammation.* Nature, 2008. **454**(7203): p. 436-44.
37. Karin, M. and F.R. Greten, *NF-kappaB: linking inflammation and immunity to cancer development and progression.* Nat Rev Immunol, 2005. **5**(10): p. 749-59.
38. Korniluk, A., et al., *From inflammation to cancer.* Ir J Med Sci, 2017. **186**(1): p. 57-62.
39. Ben-Neriah, Y. and M. Karin, *Inflammation meets cancer, with NF-kappaB as the matchmaker.* Nat Immunol, 2011. **12**(8): p. 715-23.
40. Mantovani, A., et al., *Macrophage polarization: tumor-associated macrophages as a paradigm for polarized M2 mononuclear phagocytes.* TRENDS in Immunology, **2002**. **23**(11): p. 549-555.
41. West, A.P., A.A. Koblansky, and S. Ghosh, *Recognition and signaling by toll-like receptors.* Annu Rev Cell Dev Biol, 2006. **22**: p. 409-37.
42. Akira, S., S. Uematsu, and O. Takeuchi, *Pathogen recognition and innate immunity.* Cell, 2006. **124**(4): p. 783-801.
43. Akashi-Takamura, S. and K. Miyake, *TLR accessory molecules.* Curr Opin Immunol, 2008. **20**(4): p. 420-5.
44. Kawai, T. and S. Akira, *The role of pattern-recognition receptors in innate immunity: update on Toll-like receptors.* Nat Immunol, 2010. **11**(5): p. 373-84.
45. Kagan, J.C., et al., *TRAM couples endocytosis of Toll-like receptor 4 to the induction of interferon-beta.* Nat Immunol, 2008. **9**(4): p. 361-8.
46. Tanimura, N., et al., *Roles for LPS-dependent interaction and relocation of TLR4 and TRAM in TRIF-signaling.* Biochem Biophys Res Commun, 2008. **368**(1): p. 94-9.
47. Smith, W.L., D.L. DeWitt, and R.M. Garavito, *Cyclooxygenases: structural, cellular, and molecular biology.* Annu Rev Biochem, 2000. **69**: p. 145-82.
48. Tanabe, T. and N. Tohnai, *Cyclooxygenase isozymes and their gene structures and expression.* Prostaglandins Other Lipid Mediat, 2002. **68-69**: p. 95-114.
49. Herschman, H.R., *Regulation of prostaglandin synthase-1 and prostaglandin synthase-2.* Cancer Metastasis Rev, 1994. **13**(3-4): p. 241-56.
50. Morita, I., *Distinct functions of COX-1 and COX-2.* Prostaglandins Other Lipid Mediat, 2002. **68-69**: p. 165-75.
51. Zidar, N., et al., *Cyclooxygenase in normal human tissues--is COX-1 really a constitutive isoform, and COX-2 an inducible isoform?* J Cell Mol Med, 2009. **13**(9B): p. 3753-63.
52. Wallace, J.L., et al., *NSAID-induced gastric damage in rats: requirement for inhibition of both cyclooxygenase 1 and 2.* Gastroenterology, 2000. **119**(3): p. 706-14.
53. Picot, D., P.J. Loll, and R.M. Garavito, *The X-ray crystal structure of the membrane protein prostaglandin H2 synthase-1.* Nature, 1994. **367**(6460): p. 243-9.
54. Smith, W.L., Y. Urade, and P.J. Jakobsson, *Enzymes of the cyclooxygenase pathways of prostanoid biosynthesis.* Chem Rev, 2011. **111**(10): p. 5821-65.

55. Morita, I., et al., *Different intracellular locations for prostaglandin endoperoxide H synthase-1 and -2.* J Biol Chem, 1995. **270**(18): p. 10902-8.
56. Spencer, A.G., et al., *Subcellular localization of prostaglandin endoperoxide H synthases-1 and -2 by immunoelectron microscopy.* J Biol Chem, 1998. **273**(16): p. 9886-93.
57. Kang, Y.J., et al., *Regulation of intracellular cyclooxygenase levels by gene transcription and protein degradation.* Prog Lipid Res, 2007. **46**(2): p. 108-25.
58. Kim, S.F., *The role of nitric oxide in prostaglandin biology; update.* Nitric Oxide, 2011. **25**(3): p. 255-64.
59. Schneider, C., et al., *Control of oxygenation in lipoxygenase and cyclooxygenase catalysis.* Chem Biol, 2007. **14**(5): p. 473-88.
60. Seo, M.J. and D.K. Oh, *Prostaglandin synthases: Molecular characterization and involvement in prostaglandin biosynthesis.* Prog Lipid Res, 2017. **66**: p. 50-68.
61. Hirata, T. and S. Narumiya, *Prostanoid receptors.* Chem Rev, 2011. **111**(10): p. 6209-30.
62. Surh, Y.J., et al., *15-Deoxy-Delta(1)(2),(1)(4)-prostaglandin J(2), an electrophilic lipid mediator of anti-inflammatory and pro-resolving signaling.* Biochem Pharmacol, 2011. **82**(10): p. 1335-51.
63. Jakobsson, P.J., et al., *Identification of human prostaglandin E synthase: a microsomal, glutathione-dependent, inducible enzyme, constituting a potential novel drug target.* Proc Natl Acad Sci U S A, 1999. **96**(13): p. 7220-5.
64. Thoren, S. and P.J. Jakobsson, *Coordinate up- and down-regulation of glutathione-dependent prostaglandin E synthase and cyclooxygenase-2 in A549 cells. Inhibition by NS-398 and leukotriene C4.* Eur J Biochem, 2000. **267**(21): p. 6428-34.
65. Park, J.Y., M.H. Pillinger, and S.B. Abramson, *Prostaglandin E2 synthesis and secretion: the role of PGE2 synthases.* Clin Immunol, 2006. **119**(3): p. 229-40.
66. Jegerschold, C., et al., *Structural basis for induced formation of the inflammatory mediator prostaglandin E2.* Proc Natl Acad Sci U S A, 2008. **105**(32): p. 11110-5.
67. Sjogren, T., et al., *Crystal structure of microsomal prostaglandin E2 synthase provides insight into diversity in the MAPEG superfamily.* Proc Natl Acad Sci U S A, 2013. **110**(10): p. 3806-11.
68. Sreeramkumar, V., M. Fresno, and N. Cuesta, *Prostaglandin E2 and T cells: friends or foes?* Immunol Cell Biol, 2012. **90**(6): p. 579-86.
69. Ueno, N., et al., *Coupling between cyclooxygenase, terminal prostanoid synthase, and phospholipase A2.* J Biol Chem, 2001. **276**(37): p. 34918-27.
70. Sasaki, Y., et al., *Role of prostacyclin synthase in carcinogenesis.* Prostaglandins Other Lipid Mediat, 2017.
71. Liu, M., et al., *12-Hydroxyheptadecatrienoic acid promotes epidermal wound healing by accelerating keratinocyte migration via the BLT2 receptor.* J Exp Med, 2014. **211**(6): p. 1063-78.
72. Smyth, E.M., *Thromboxane and the thromboxane receptor in cardiovascular disease.* Clin Lipidol, 2010. **5**(2): p. 209-219.
73. Williams, C.S., M. Mann, and R.N. DuBois, *The role of cyclooxygenases in inflammation, cancer, and development.* Oncogene, 1999. **18**(55): p. 7908-16.
74. Goldman, A.P., et al., *Meloxicam inhibits the growth of colorectal cancer cells.* Carcinogenesis, 1998. **19**(12): p. 2195-9.
75. Washburn, T.C., D.N. Medearis, Jr., and B. Childs, *Sex Differences in Susceptibility to Infections.* Pediatrics, 1965. **35**: p. 57-64.
76. Bouman, A., M.J. Heineman, and M.M. Faas, *Sex hormones and the immune response in humans.* Hum Reprod Update, 2005. **11**(4): p. 411-23.
77. Whitacre, C.C., *Sex differences in autoimmune disease.* Nat Immunol, 2001. **2**(9): p. 777-80.
78. Abdullah, M., et al., *Gender effect on in vitro lymphocyte subset levels of healthy individuals.* Cell Immunol, 2012. **272**(2): p. 214-9.
79. Gubbels Bupp, M.R., *Sex, the aging immune system, and chronic disease.* Cell Immunol, 2015. **294**(2): p. 102-10.

80. Pan, Z. and C. Chang, *Gender and the regulation of longevity: implications for autoimmunity.* Autoimmun Rev, 2012. **11**(6-7): p. A393-403.
81. Mathur, P., et al., *Gender-Related Differences in Atherosclerosis.* Cardiovasc Drugs Ther, 2015. **29**(4): p. 319-27.
82. Ng, M.K., *New perspectives on Mars and Venus: unravelling the role of androgens in gender differences in cardiovascular biology and disease.* Heart Lung Circ, 2007. **16**(3): p. 185-92.
83. Liu, P.Y., A.K. Death, and D.J. Handelsman, *Androgens and cardiovascular disease.* Endocr Rev, 2003. **24**(3): p. 313-40.
84. Jones, R.D., T. Hugh Jones, and K.S. Channer, *The influence of testosterone upon vascular reactivity.* Eur J Endocrinol, 2004. **151**(1): p. 29-37.
85. Ono, S., et al., *Sex differences in cytokine production and surface antigen expression of peripheral blood mononuclear cells after surgery.* Am J Surg, 2005. **190**(3): p. 439-44.
86. Temple, S.E., et al., *Endotoxin induced TNF and IL-10 mRNA production is higher in male than female donors: correlation with elevated expression of TLR4.* Cell Immunol, 2008. **251**(2): p. 69-71.
87. Marriott, I., K.L. Bost, and Y.M. Huet-Hudson, *Sexual dimorphism in expression of receptors for bacterial lipopolysaccharides in murine macrophages: a possible mechanism for gender-based differences in endotoxic shock susceptibility.* J Reprod Immunol, 2006. **71**(1): p. 12-27.
88. Pergola, C., et al., *ERK-mediated regulation of leukotriene biosynthesis by androgens: a molecular basis for gender differences in inflammation and asthma.* Proc Natl Acad Sci U S A, 2008. **105**(50): p. 19881-6.
89. Radmark, O., et al., *5-Lipoxygenase, a key enzyme for leukotriene biosynthesis in health and disease.* Biochim Biophys Acta, 2015. **1851**(4): p. 331-9.
90. Borgeat, P., M. Hamberg, and B. Samuelsson, *Transformation of arachidonic acid and homo-gamma-linolenic acid by rabbit polymorphonuclear leukocytes. Monohydroxy acids from novel lipoxygenases.* J Biol Chem, 1976. **251**(24): p. 7816-20.
91. Borgeat, P. and B. Samuelsson, *Arachidonic acid metabolism in polymorphonuclear leukocytes: effects of ionophore A23187.* Proc Natl Acad Sci U S A, 1979. **76**(5): p. 2148-52.
92. Kuhn, H., S. Banthiya, and K. van Leyen, *Mammalian lipoxygenases and their biological relevance.* Biochim Biophys Acta, 2015. **1851**(4): p. 308-30.
93. Samuelsson, B., et al., *Leukotrienes and lipoxins: structures, biosynthesis, and biological effects.* Science, 1987. **237**(4819): p. 1171-6.
94. Mandhane, S.N., J.H. Shah, and R. Thennati, *Allergic rhinitis: an update on disease, present treatments and future prospects.* Int Immunopharmacol, 2011. **11**(11): p. 1646-62.
95. Sanak, M., *Eicosanoid Mediators in the Airway Inflammation of Asthmatic Patients: What is New?* Allergy Asthma Immunol Res, 2016. **8**(6): p. 481-90.
96. Mashima, R. and T. Okuyama, *The role of lipoxygenases in pathophysiology; new insights and future perspectives.* Redox Biol, 2015. **6**: p. 297-310.
97. Moore, G.Y. and G.P. Pidgeon, *Cross-Talk between Cancer Cells and the Tumour Microenvironment: The Role of the 5-Lipoxygenase Pathway.* Int J Mol Sci, 2017. **18**(2).
98. Seuter, S., et al., *Functional characterization of vitamin D responding regions in the human 5-Lipoxygenase gene.* Biochim Biophys Acta, 2007. **1771**(7): p. 864-72.
99. Uhl, J., et al., *The 5-lipoxygenase promoter is regulated by DNA methylation.* J Biol Chem, 2002. **277**(6): p. 4374-9.
100. Radmark, O., et al., *5-Lipoxygenase: regulation of expression and enzyme activity.* Trends Biochem Sci, 2007. **32**(7): p. 332-41.
101. Rakonjac Ryge, M., et al., *A mutation interfering with 5-lipoxygenase domain interaction leads to increased enzyme activity.* Arch Biochem Biophys, 2014. **545**: p. 179-85.
102. Gilbert, N.C., et al., *The structure of human 5-lipoxygenase.* Science, 2011. **331**(6014): p. 217-9.

103. Chasteen, N.D., et al., *Characterization of the non-heme iron center of human 5-lipoxygenase by electron paramagnetic resonance, fluorescence, and ultraviolet-visible spectroscopy: redox cycling between ferrous and ferric states.* Biochemistry, 1993. **32**(37): p. 9763-71.
104. Radmark, O., *Arachidonate 5-lipoxygenase.* Prostaglandins Other Lipid Mediat, 2002. **68-69**: p. 211-34.
105. Hammarberg, T. and O. Radmark, *5-lipoxygenase binds calcium.* Biochemistry, 1999. **38**(14): p. 4441-7.
106. Kulkarni, S., et al., *Molecular basis of the specific subcellular localization of the C2-like domain of 5-lipoxygenase.* J Biol Chem, 2002. **277**(15): p. 13167-74.
107. Radmark, O. and B. Samuelsson, *5-Lipoxygenase: mechanisms of regulation.* J Lipid Res, 2009. **50 Suppl**: p. S40-5.
108. Provost, P., et al., *5-Lipoxygenase interacts with coactosin-like protein.* J Biol Chem, 2001. **276**(19): p. 16520-7.
109. Rakonjac, M., et al., *Coactosin-like protein supports 5-lipoxygenase enzyme activity and up-regulates leukotriene A4 production.* Proc Natl Acad Sci U S A, 2006. **103**(35): p. 13150-5.
110. Werz, O., et al., *5-lipoxygenase is phosphorylated by p38 kinase-dependent MAPKAP kinases.* Proc Natl Acad Sci U S A, 2000. **97**(10): p. 5261-6.
111. Werz, O., et al., *Extracellular signal-regulated kinases phosphorylate 5-lipoxygenase and stimulate 5-lipoxygenase product formation in leukocytes.* FASEB J, 2002. **16**(11): p. 1441-3.
112. Werz, O., et al., *Arachidonic acid promotes phosphorylation of 5-lipoxygenase at Ser-271 by MAPK-activated protein kinase 2 (MK2).* J Biol Chem, 2002. **277**(17): p. 14793-800.
113. Luo, M., et al., *Protein kinase A inhibits leukotriene synthesis by phosphorylation of 5-lipoxygenase on serine 523.* J Biol Chem, 2004. **279**(40): p. 41512-20.
114. Werz, O., *5-lipoxygenase: cellular biology and molecular pharmacology.* Curr Drug Targets Inflamm Allergy, 2002. **1**(1): p. 23-44.
115. Surette, M.E., et al., *Mechanisms of the priming effect of lipopolysaccharides on the biosynthesis of leukotriene B4 in chemotactic peptide-stimulated human neutrophils.* FASEB J, 1998. **12**(14): p. 1521-31.
116. Sala, A., et al., *Differential metabolism of exogenous and endogenous arachidonic acid in human neutrophils.* J Biol Chem, 1999. **274**(40): p. 28264-9.
117. Peters-Golden, M. and T.G. Brock, *5-lipoxygenase and FLAP.* Prostaglandins Leukot Essent Fatty Acids, 2003. **69**(2-3): p. 99-109.
118. Miller, D.K., et al., *Identification and isolation of a membrane protein necessary for leukotriene production.* Nature, 1990. **343**(6255): p. 278-81.
119. Abramovitz, M., et al., *5-lipoxygenase-activating protein stimulates the utilization of arachidonic acid by 5-lipoxygenase.* Eur J Biochem, 1993. **215**(1): p. 105-11.
120. Mancini, J.A., et al., *5-lipoxygenase-activating protein is an arachidonate binding protein.* FEBS Lett, 1993. **318**(3): p. 277-81.
121. Werz, O., J. Gerstmeier, and U. Garscha, *Novel leukotriene biosynthesis inhibitors (2012-2016) as anti-inflammatory agents.* Expert Opin Ther Pat, 2017. **27**(5): p. 607-620.
122. Maas, R.L., et al., *Stereospecific removal of the DR hydrogen atom at the 10-carbon of arachidonic acid in the biosynthesis of leukotriene A4 by human leukocytes.* J Biol Chem, 1982. **257**(22): p. 13515-9.
123. Powell, W.S. and J. Rokach, *The eosinophil chemoattractant 5-oxo-ETE and the OXE receptor.* Prog Lipid Res, 2013. **52**(4): p. 651-65.
124. Romano, M., et al., *Lipoxins and aspirin-triggered lipoxins in resolution of inflammation.* Eur J Pharmacol, 2015. **760**: p. 49-63.
125. Borgeat, P. and B. Samuelsson, *Arachidonic acid metabolism in polymorphonuclear leukocytes: unstable intermediate in formation of dihydroxy acids.* Proc Natl Acad Sci U S A, 1979. **76**(7): p. 3213-7.

126. Peters-Golden, M., M.M. Gleason, and A. Togias, *Cysteinyl leukotrienes: multi-functional mediators in allergic rhinitis.* Clin Exp Allergy, 2006. **36**(6): p. 689-703.
127. Maclouf, J., R.C. Murphy, and P.M. Henson, *Transcellular sulfidopeptide leukotriene biosynthetic capacity of vascular cells.* Blood, 1989. **74**(2): p. 703-7.
128. Murakami, M., et al., *Recent progress in phospholipase A(2) research: from cells to animals to humans.* Prog Lipid Res, 2011. **50**(2): p. 152-92.
129. Dennis, E.A., et al., *Phospholipase A2 enzymes: physical structure, biological function, disease implication, chemical inhibition, and therapeutic intervention.* Chem Rev, 2011. **111**(10): p. 6130-85.
130. Burke, J.E. and E.A. Dennis, *Phospholipase A2 structure/function, mechanism, and signaling.* J Lipid Res, 2009. **50 Suppl**: p. S237-42.
131. Haeggstrom, J.Z., *Leukotriene A4 hydrolase/aminopeptidase, the gatekeeper of chemotactic leukotriene B4 biosynthesis.* J Biol Chem, 2004. **279**(49): p. 50639-42.
132. Rudberg, P.C., et al., *Leukotriene A4 hydrolase: selective abrogation of leukotriene B4 formation by mutation of aspartic acid 375.* Proc Natl Acad Sci U S A, 2002. **99**(7): p. 4215-20.
133. Ago, H., et al., *Crystal structure of a human membrane protein involved in cysteinyl leukotriene biosynthesis.* Nature, 2007. **448**(7153): p. 609-12.
134. Martinez Molina, D., et al., *Structural basis for synthesis of inflammatory mediators by human leukotriene C4 synthase.* Nature, 2007. **448**(7153): p. 613-6.
135. Saino, H., et al., *The catalytic architecture of leukotriene C4 synthase with two arginine residues.* J Biol Chem, 2011. **286**(18): p. 16392-401.
136. Le Bel, M., A. Brunet, and J. Gosselin, *Leukotriene B4, an endogenous stimulator of the innate immune response against pathogens.* J Innate Immun, 2014. **6**(2): p. 159-68.
137. Funk, C.D., *Leukotriene modifiers as potential therapeutics for cardiovascular disease.* Nat Rev Drug Discov, 2005. **4**(8): p. 664-72.
138. Griffiths, R.J., et al., *Leukotriene B4 plays a critical role in the progression of collagen-induced arthritis.* Proc Natl Acad Sci U S A, 1995. **92**(2): p. 517-21.
139. Jame, A.J., et al., *Human bronchial epithelial cells express an active and inducible biosynthetic pathway for leukotrienes B4 and C4.* Clin Exp Allergy, 2007. **37**(6): p. 880-92.
140. Piper, P.J., *Formation and actions of leukotrienes.* Physiol Rev, 1984. **64**(2): p. 744-61.
141. Nakamura, M. and T. Shimizu, *Leukotriene receptors.* Chem Rev, 2011. **111**(10): p. 6231-98.
142. Nicosia, S., V. Capra, and G.E. Rovati, *Leukotrienes as mediators of asthma.* Pulm Pharmacol Ther, 2001. **14**(1): p. 3-19.
143. Singh, R.K., et al., *Cysteinyl leukotrienes and their receptors: molecular and functional characteristics.* Pharmacology, 2010. **85**(6): p. 336-49.
144. Zhu, J., et al., *Localization and upregulation of cysteinyl leukotriene-1 receptor in asthmatic bronchial mucosa.* Am J Respir Cell Mol Biol, 2005. **33**(6): p. 531-40.
145. Paruchuri, S., et al., *Leukotriene E4-induced pulmonary inflammation is mediated by the P2Y12 receptor.* J Exp Med, 2009. **206**(11): p. 2543-55.
146. Riendeau, D., et al., *Sensitivity of immunoaffinity-purified porcine 5-lipoxygenase to inhibitors and activating lipid hydroperoxides.* Biochem Pharmacol, 1989. **38**(14): p. 2313-21.
147. Nelson, M.J., et al., *Reduction of the active-site iron by potent inhibitors of lipoxygenases.* J Biol Chem, 1991. **266**(13): p. 8225-9.
148. Rouzer, C.A., et al., *Inhibition of human leukocyte 5-lipoxygenase by a 4-hydroxybenzofuran, L-656,224. Evidence for enzyme reduction and inhibitor degradation.* Biochem Pharmacol, 1991. **41**(9): p. 1365-73.
149. Werz, O., *Inhibition of 5-lipoxygenase product synthesis by natural compounds of plant origin.* Planta Med, 2007. **73**(13): p. 1331-57.
150. Young, R.N., *Inhibitors of 5-lipoxygenase: a therapeutic potential yet to be fully realized?* Eur. J. Med. Chem., 1999. **34**: p. 671-685.

151. McMillan, R.M. and E.R. Walker, *Designing therapeutically effective 5-lipoxygenase inhibitors.* Trends Pharmacol Sci, 1992. **13**(8): p. 323-30.
152. Corey, E.J., et al., *Rationally designed, potent competitive inhibitors of leukotriene biosynthesis.* J Am Chem Soc 1984. **106**: p. 1503-1504.
153. Falgueyret, J.P., J.H. Hutchinson, and D. Riendeau, *Criteria for the identification of non-redox inhibitors of 5-lipoxygenase.* Biochem Pharmacol, 1993. **45**(4): p. 978-81.
154. Tateson, J.E., et al., *Selective inhibition of arachidonate 5-lipoxygenase by novel acetohydroxamic acids: biochemical assessment in vitro and ex vivo.* Br J Pharmacol, 1988. **94**(2): p. 528-39.
155. Chamulitrat, W., R.P. Mason, and D. Riendeau, *Nitroxide metabolites from alkylhydroxylamines and N-hydroxyurea derivatives resulting from reductive inhibition of soybean lipoxygenase.* J Biol Chem, 1992. **267**(14): p. 9574-9.
156. Carter, G.W., et al., *5-lipoxygenase inhibitory activity of zileuton.* J Pharmacol Exp Ther, 1991. **256**(3): p. 929-37.
157. Lehnigk, B., et al., *Effects of a 5-lipoxygenase inhibitor, ABT-761, on exercise-induced bronchoconstriction and urinary LTE4 in asthmatic patients.* Eur Respir J, 1998. **11**(3): p. 617-23.
158. Tardif, J.C., et al., *Treatment with 5-lipoxygenase inhibitor VIA-2291 (Atreleuton) in patients with recent acute coronary syndrome.* Circ Cardiovasc Imaging, 2010. **3**(3): p. 298-307.
159. Crawley, G.C., et al., *Methoxytetrahydropyrans. A new series of selective and orally potent 5-lipoxygenase inhibitors.* J Med Chem, 1992. **35**(14): p. 2600-9.
160. McMillan, R.M., J.M. Girodeau, and S.J. Foster, *Selective chiral inhibitors of 5-lipoxygenase with anti-inflammatory activity.* Br J Pharmacol, 1990. **101**(3): p. 501-3.
161. Kusner, E.J., et al., *The 5-lipoxygenase inhibitors ZD2138 and ZM230487 are potent and selective inhibitors of several antigen-induced guinea-pig pulmonary responses.* Eur J Pharmacol, 1994. **257**(3): p. 285-92.
162. Werz, O., et al., *Nonredox 5-lipoxygenase inhibitors require glutathione peroxidase for efficient inhibition of 5-lipoxygenase activity.* Mol Pharmacol, 1998. **54**(2): p. 445-51.
163. Fischer, L., et al., *Phosphorylation- and stimulus-dependent inhibition of cellular 5-lipoxygenase activity by nonredox-type inhibitors.* FASEB J, 2003. **17**(8): p. 949-51.
164. Shirumalla, R.K., et al., *RBx 7,796: A novel inhibitor of 5-lipoxygenase.* Inflamm Res, 2006. **55**(12): p. 517-27.
165. Grimm, E.L., et al., *Substituted coumarins as potent 5-lipoxygenase inhibitors.* Bioorg Med Chem Lett, 2006. **16**(9): p. 2528-31.
166. Mano, T., et al., *Optimization of imidazole 5-lipoxygenase inhibitors and selection and synthesis of a development candidate.* Chem Pharm Bull (Tokyo), 2005. **53**(8): p. 965-73.
167. Maucher, I.V., et al., *Michael acceptor containing drugs are a novel class of 5-lipoxygenase inhibitor targeting the surface cysteines C416 and C418.* Biochem Pharmacol, 2017. **125**: p. 55-74.
168. Filosa, R., et al., *Discovery and biological evaluation of novel 1,4-benzoquinone and related resorcinol derivatives that inhibit 5-lipoxygenase.* Eur J Med Chem, 2013. **67**: p. 269-79.
169. Schaible, A.M., et al., *Elucidation of the molecular mechanism and the efficacy in vivo of a novel 1,4-benzoquinone that inhibits 5-lipoxygenase.* Br J Pharmacol, 2014. **171**(9): p. 2399-412.
170. Schaible, A.M., et al., *The 5-lipoxygenase inhibitor RF-22c potently suppresses leukotriene biosynthesis in cellulo and blocks bronchoconstriction and inflammation in vivo.* Biochem Pharmacol, 2016. **112**: p. 60-71.
171. Siemoneit, U., et al., *On the interference of boswellic acids with 5-lipoxygenase: mechanistic studies in vitro and pharmacological relevance.* Eur J Pharmacol, 2009. **606**(1-3): p. 246-54.
172. Sengupta, K., et al., *A double blind, randomized, placebo controlled study of the efficacy and safety of 5-Loxin for treatment of osteoarthritis of the knee.* Arthritis Res Ther, 2008. **10**(4): p. R85.

173. Koeberle, A., et al., *Licofelone suppresses prostaglandin E2 formation by interference with the inducible microsomal prostaglandin E2 synthase-1.* J Pharmacol Exp Ther, 2008. **326**(3): p. 975-82.
174. Maier, T.J., et al., *Celecoxib inhibits 5-lipoxygenase.* Biochem Pharmacol, 2008. **76**(7): p. 862-72.
175. Araico, A., et al., *Phenylsulphonyl urenyl chalcone derivatives as dual inhibitors of cyclo-oxygenase-2 and 5-lipoxygenase.* Life Sci, 2006. **78**(25): p. 2911-8.
176. Scholz, M., et al., *Diaryl-dithiolanes and -isothiazoles: COX-1/COX-2 and 5-LOX-inhibitory, *OH scavenging and anti-adhesive activities.* Bioorg Med Chem, 2009. **17**(2): p. 558-68.
177. Koeberle, A., et al., *Pirinixic acid derivatives as novel dual inhibitors of microsomal prostaglandin E2 synthase-1 and 5-lipoxygenase.* J Med Chem, 2008. **51**(24): p. 8068-76.
178. Koeberle, A., et al., *The molecular pharmacology and in vivo activity of 2-(4-chloro-6-(2,3-dimethylphenylamino)pyrimidin-2-ylthio)octanoic acid (YS121), a dual inhibitor of microsomal prostaglandin E2 synthase-1 and 5-lipoxygenase.* J Pharmacol Exp Ther, 2010. **332**(3): p. 840-8.
179. Karg, E.M., et al., *Structural optimization and biological evaluation of 2-substituted 5-hydroxyindole-3-carboxylates as potent inhibitors of human 5-lipoxygenase.* J Med Chem, 2009. **52**(11): p. 3474-83.
180. Koeberle, A., et al., *Discovery of benzo[g]indol-3-carboxylates as potent inhibitors of microsomal prostaglandin E(2) synthase-1.* Bioorg Med Chem, 2009. **17**(23): p. 7924-32.
181. Pettersen, D., O. Davidsson, and C. Whatling, *Recent advances for FLAP inhibitors.* Bioorg Med Chem Lett, 2015. **25**(13): p. 2607-12.
182. Gillard, J., et al., *L-663,536 (MK-886) (3-[1-(4-chlorobenzyl)-3-t-butyl-thio-5-isopropylindol-2-yl]-2,2 - dimethylpropanoic acid), a novel, orally active leukotriene biosynthesis inhibitor.* Can J Physiol Pharmacol, 1989. **67**(5): p. 456-64.
183. Bain, G., et al., *Pharmacodynamics, pharmacokinetics and safety of GSK2190915, a novel oral anti-inflammatory 5-lipoxygenase-activating protein inhibitor.* Br J Clin Pharmacol, 2013. **75**(3): p. 779-90.
184. Follows, R.M., et al., *Efficacy, safety and tolerability of GSK2190915, a 5-lipoxygenase activating protein inhibitor, in adults and adolescents with persistent asthma: a randomised dose-ranging study.* Respir Res, 2013. **14**: p. 54.
185. Pergola, C., et al., *The novel benzimidazole derivative BRP-7 inhibits leukotriene biosynthesis in vitro and in vivo by targeting 5-lipoxygenase-activating protein (FLAP).* Br J Pharmacol, 2014. **171**(12): p. 3051-64.
186. Banoglu, E., et al., *4,5-Diarylisoxazol-3-carboxylic acids: A new class of leukotriene biosynthesis inhibitors potentially targeting 5-lipoxygenase-activating protein (FLAP).* Eur J Med Chem, 2016. **113**: p. 1-10.
187. Lorrain, D.S., et al., *Pharmacological characterization of 3-[3-tert-butylsulfanyl-1-[4-(6-methoxy-pyridin-3-yl)-benzyl]-5-(pyridin-2-ylmeth oxy)-1H-indol-2-yl]-2,2-dimethyl-propionic acid (AM103), a novel selective 5-lipoxygenase-activating protein inhibitor that reduces acute and chronic inflammation.* J Pharmacol Exp Ther, 2009. **331**(3): p. 1042-50.
188. Stock, N.S., et al., *5-Lipoxygenase-activating protein (FLAP) inhibitors. Part 4: development of 3-[3-tert-butylsulfanyl-1-[4-(6-ethoxypyridin-3-yl)benzyl]-5-(5-methylpyridin-2-y lmethoxy)-1H-indol-2-yl]-2,2-dimethylpropionic acid (AM803), a potent, oral, once daily FLAP inhibitor.* J Med Chem, 2011. **54**(23): p. 8013-29.
189. Tanis, V.M., et al., *Azabenzthiazole inhibitors of leukotriene A(4) hydrolase.* Bioorg Med Chem Lett, 2012. **22**(24): p. 7504-11.
190. Eccles, W., et al., *Identification of benzofuran central cores for the inhibition of leukotriene A(4) hydrolase.* Bioorg Med Chem Lett, 2013. **23**(3): p. 811-5.
191. Stsiapanava, A., et al., *Binding of Pro-Gly-Pro at the active site of leukotriene A4 hydrolase/aminopeptidase and development of an epoxide hydrolase selective inhibitor.* Proc Natl Acad Sci U S A, 2014. **111**(11): p. 4227-32.

192. Kleinschmidt, T.K., et al., *Tandem Benzophenone Amino Pyridines, Potent and Selective Inhibitors of Human Leukotriene C4 Synthase.* J Pharmacol Exp Ther, 2015. **355**(1): p. 108-16.
193. Liening, S., et al., *Development of smart cell-free and cell-based assay systems for investigation of leukotriene C4 synthase activity and evaluation of inhibitors.* Biochim Biophys Acta, 2016. **1861**(11): p. 1605-1613.
194. Rossi, A., et al., *In vivo sex differences in leukotriene biosynthesis in zymosan-induced peritonitis.* Pharmacol Res, 2014. **87**: p. 1-7.
195. Peters-Golden, M. and W.R. Henderson, Jr., *Leukotrienes.* N Engl J Med, 2007. **357**(18): p. 1841-54.
196. Wenzel, S.E. and A.K. Kamada, *Zileuton: the first 5-lipoxygenase inhibitor for the treatment of asthma.* Ann Pharmacother, 1996. **30**(7-8): p. 858-64.
197. Matsuse, H. and S. Kohno, *Leukotriene receptor antagonists pranlukast and montelukast for treating asthma.* Expert Opin Pharmacother, 2014. **15**(3): p. 353-63.
198. Peduto, A., et al., *Optimization of benzoquinone and hydroquinone derivatives as potent inhibitors of human 5-lipoxygenase.* Eur J Med Chem, 2017. **127**: p. 715-726.
199. Albert, D., et al., *Hyperforin is a dual inhibitor of cyclooxygenase-1 and 5-lipoxygenase.* Biochem Pharmacol, 2002. **64**(12): p. 1767-75.
200. Livak, K.J. and T.D. Schmittgen, *Analysis of relative gene expression data using real-time quantitative PCR and the 2(-Delta Delta C(T)) Method.* Methods, 2001. **25**(4): p. 402-8.
201. Mosmann, T., *Rapid colorimetric assay for cellular growth and survival: application to proliferation and cytotoxicity assays.* J Immunol Methods, 1983. **65**(1-2): p. 55-63.
202. Grynkiewicz, G., M. Poenie, and R.Y. Tsien, *A new generation of Ca2+ indicators with greatly improved fluorescence properties.* J Biol Chem, 1985. **260**(6): p. 3440-50.
203. Hammarberg, T., et al., *Mutations at the C-terminal isoleucine and other potential iron ligands of 5-lipoxygenase.* Eur J Biochem, 1995. **230**(2): p. 401-7.
204. Brungs, M., et al., *Sequential induction of 5-lipoxygenase gene expression and activity in Mono Mac 6 cells by transforming growth factor beta and 1,25-dihydroxyvitamin D3.* Proc Natl Acad Sci U S A, 1995. **92**(1): p. 107-11.
205. Waltenberger, B., et al., *Discovery of Potent Soluble Epoxide Hydrolase (sEH) Inhibitors by Pharmacophore-Based Virtual Screening.* J Chem Inf Model, 2016. **56**(4): p. 747-62.
206. Wixtrom, R.N., M.H. Silva, and B.D. Hammock, *Affinity purification of cytosolic epoxide hydrolase using derivatized epoxy-activated Sepharose gels.* Anal Biochem, 1988. **169**(1): p. 71-80.
207. **Blois, M.S.**, *Antioxidant determinations by the use of a stable free radical.* Nature, 1958. **181**(4671): p. 1199-1200.
208. Steinhilber, D., T. Herrmann, and H.J. Roth, *Separation of lipoxins and leukotrienes from human granulocytes by high-performance liquid chromatography with a Radial-Pak cartridge after extraction with an octadecyl reversed-phase column.* J Chromatogr, 1989. **493**(2): p. 361-6.
209. Bain, B.J., *Ethnic and sex differences in the total and differential white cell count and platelet count.* J Clin Pathol, 1996. **49**(8): p. 664-6.
210. Rathod, K.S., et al., *Accelerated resolution of inflammation underlies sex differences in inflammatory responses in humans.* J Clin Invest, 2017. **127**(1): p. 169-182.
211. O'Flaherty, J.T., et al., *Neutrophil aggregation and degranulation. Effect of arachidonic acid.* Am J Pathol, 1979. **95**(2): p. 433-44.
212. Heumann, D., et al., *Role of plasma, lipopolysaccharide-binding protein, and CD14 in response of mouse peritoneal exudate macrophages to endotoxin.* Infect Immun, 2001. **69**(1): p. 378-85.
213. Martorell, A., et al., *Orchidectomy increases the formation of prostanoids and modulates their role in the acetylcholine-induced relaxation in the rat aorta.* Cardiovasc Res, 2008. **77**(3): p. 590-9.
214. Sullivan, J.C., et al., *Sexual dimorphism in renal production of prostanoids in spontaneously hypertensive rats.* Hypertension, 2005. **45**(3): p. 406-11.

215. Lasa, M., et al., *Dexamethasone destabilizes cyclooxygenase 2 mRNA by inhibiting mitogen-activated protein kinase p38.* Mol Cell Biol, 2001. **21**(3): p. 771-80.
216. Imahara, S.D., et al., *The influence of gender on human innate immunity.* Surgery, 2005. **138**(2): p. 275-82.
217. Dale, D.C., L. Boxer, and W.C. Liles, *The phagocytes: neutrophils and monocytes.* Blood, 2008. **112**(4): p. 935-45.
218. Ensor, C.M. and H.H. Tai, *15-Hydroxyprostaglandin dehydrogenase.* J Lipid Mediat Cell Signal, 1995. **12**(2-3): p. 313-9.
219. Tong, M. and H.H. Tai, *Induction of NAD(+)-linked 15-hydroxyprostaglandin dehydrogenase expression by androgens in human prostate cancer cells.* Biochem Biophys Res Commun, 2000. **276**(1): p. 77-81.
220. Xun, C.Q., C.M. Ensor, and H.H. Tai, *Regulation of synthesis and activity of NAD(+)-dependent 15-hydroxy-prostaglandin dehydrogenase (15-PGDH) by dexamethasone and phorbol ester in human erythroleukemia (HEL) cells.* Biochem Biophys Res Commun, 1991. **177**(3): p. 1258-65.
221. Zhang, Y., et al., *TISSUE REGENERATION. Inhibition of the prostaglandin-degrading enzyme 15-PGDH potentiates tissue regeneration.* Science, 2015. **348**(6240): p. aaa2340.
222. Li, J., et al., *Platelet-neutrophil interactions under thromboinflammatory conditions.* Cell Mol Life Sci, 2015. **72**(14): p. 2627-43.
223. Vanichakarn, P., et al., *Neutrophil CD40 enhances platelet-mediated inflammation.* Thromb Res, 2008. **122**(3): p. 346-58.
224. von Hundelshausen, P. and C. Weber, *Platelets as immune cells: bridging inflammation and cardiovascular disease.* Circ Res, 2007. **100**(1): p. 27-40.
225. Filosa, R., et al., *Novel series of benzoquinones with high potency against 5-lipoxygenase in human polymorphonuclear leukocytes.* Eur J Med Chem, 2015. **94**: p. 132-9.
226. De Lucia, D., et al., *Design, synthesis and evaluation of semi-synthetic triazole-containing caffeic acid analogues as 5-lipoxygenase inhibitors.* Eur J Med Chem, 2015. **101**: p. 573-83.
227. Levy, R.M., L. Pillai, and B.P. Burnett, *Nutritional benefits of flavocoxid in patients with osteoarthritis: efficacy and safety.* Nutr Diet Suppl., 2010. **2010(2)**: p. 27-38.
228. Ohkawa, S., et al., *Reduction of 2,3,5-trimethyl-6-(3-pyridylmethyl)-1,4-benzoquinone by PB-3c cells and biological activity of its hydroquinone.* Chem Pharm Bull (Tokyo), 1991. **39**(4): p. 917-21.
229. Rouzer, C.A. and B. Samuelsson, *The importance of hydroperoxide activation for the detection and assay of mammalian 5-lipoxygenase.* FEBS Lett, 1986. **204**(2): p. 293-6.
230. Wiegard, A., et al., *Pyrrole alkanoic acid derivatives as nuisance inhibitors of microsomal prostaglandin E2 synthase-1.* Eur J Med Chem, 2012. **48**: p. 153-63.
231. Feisst, C., et al., *Hyperforin is a novel type of 5-lipoxygenase inhibitor with high efficacy in vivo.* Cell Mol Life Sci, 2009. **66**(16): p. 2759-71.
232. Bouman, A., et al., *Gender difference in the non-specific and specific immune response in humans.* Am J Reprod Immunol, 2004. **52**(1): p. 19-26.
233. Pinto, S., et al., *Sex related differences in platelet TxA2 generation.* Prostaglandins Leukot Essent Fatty Acids, 1990. **40**(3): p. 217-21.
234. Gecse, A., et al., *Sex differences in prostaglandin metabolism.* Biochem Biophys Res Commun, 1979. **86**(3): p. 643-7.
235. Diodato, M.D., et al., *Gender differences in the inflammatory response and survival following haemorrhage and subsequent sepsis.* Cytokine, 2001. **14**(3): p. 162-9.
236. Du, J.T., et al., *Sex differences in arachidonate cyclo-oxygenase products in elicited rat peritoneal macrophages.* Biochim Biophys Acta, 1984. **794**(2): p. 256-60.
237. Leslie, C.A., W.A. Gonnerman, and E.S. Cathcart, *Gender differences in eicosanoid production from macrophages of arthritis-susceptible mice.* J Immunol, 1987. **138**(2): p. 413-6.

238. Stapleton, P.P., et al., *Gender affects macrophage cytokine and prostaglandin E2 production and PGE2 receptor expression after trauma.* J Surg Res, 2004. **122**(1): p. 1-7.
239. Kelley, J.L., et al., *Activation of human blood monocytes by adherence to tissue culture plastic surfaces.* Exp Mol Pathol, 1987. **46**(3): p. 266-78.
240. Bauer, G.J., et al., *Adherence regulates macrophage signal transduction and primes tumor necrosis factor production.* Shock, 2000. **14**(4): p. 435-40.
241. Bernardo, J., et al., *Adherence-dependent calcium signaling in monocytes: induction of a CD14-high phenotype, stimulus-responsive subpopulation.* J Immunol Methods, 1997. **209**(2): p. 165-75.
242. Petit-Bertron, A.F., et al., *Adherence influences monocyte responsiveness to interleukin-10.* J Leukoc Biol, 2003. **73**(1): p. 145-54.
243. Krause, S.W., M. Kreutz, and R. Andreesen, *Differential effects of cell adherence on LPS-stimulated cytokine production by human monocytes and macrophages.* Immunobiology, 1996. **196**(5): p. 522-34.
244. Miyagi, M., M. Morishita, and Y. Iwamoto, *Effects of sex hormones on production of prostaglandin E2 by human peripheral monocytes.* J Periodontol, 1993. **64**(11): p. 1075-8.
245. Vegeto, E., et al., *Regulation of the lipopolysaccharide signal transduction pathway by 17beta-estradiol in macrophage cells.* J Steroid Biochem Mol Biol, 2004. **91**(1-2): p. 59-66.
246. Liu, Z., et al., *Expression of 15-PGDH is downregulated by COX-2 in gastric cancer.* Carcinogenesis, 2008. **29**(6): p. 1219-27.
247. Wolf, I., et al., *15-hydroxyprostaglandin dehydrogenase is a tumor suppressor of human breast cancer.* Cancer Res, 2006. **66**(15): p. 7818-23.
248. Tai, H.H., X. Chi, and M. Tong, *Regulation of 15-hydroxyprostaglandin dehydrogenase (15-PGDH) by non-steroidal anti-inflammatory drugs (NSAIDs).* Prostaglandins Other Lipid Mediat, 2011. **96**(1-4): p. 37-40.
249. Wong, C.K., et al., *Activation profile of Toll-like receptors of peripheral blood lymphocytes in patients with systemic lupus erythematosus.* Clin Exp Immunol, 2010. **159**(1): p. 11-22.
250. Abdollahi-Roodsaz, S., et al., *Inhibition of Toll-like receptor 4 breaks the inflammatory loop in autoimmune destructive arthritis.* Arthritis Rheum, 2007. **56**(9): p. 2957-67.
251. Eisenmenger, S.J., et al., *Differences in the expression of LPS-receptors are not responsible for the sex-specific immune response after trauma and hemorrhagic shock.* Cell Immunol, 2004. **230**(1): p. 17-22.
252. Sobrino, A., et al., *Estradiol selectively stimulates endothelial prostacyclin production through estrogen receptor-{alpha}.* J Mol Endocrinol, 2010. **44**(4): p. 237-46.
253. Parks, R.J., et al., *Sex differences in SR Ca(2+) release in murine ventricular myocytes are regulated by the cAMP/PKA pathway.* J Mol Cell Cardiol, 2014. **75**: p. 162-73.
254. Crews, J.K. and R.A. Khalil, *Gender-specific inhibition of Ca2+ entry mechanisms of arterial vasoconstriction by sex hormones.* Clin Exp Pharmacol Physiol, 1999. **26**(9): p. 707-15.
255. Morikawa, M., et al., *Sex difference in the effect of aspirin on rat platelet aggregation and arachidonic acid metabolism.* Jpn J Pharmacol, 1985. **37**(4): p. 317-23.
256. Halvorsen, H., J.O. Olsen, and B. Osterud, *Granulocytes enhance LPS-induced tissue factor activity in monocytes via an interaction with platelets.* J Leukoc Biol, 1993. **54**(4): p. 275-82.
257. Magnarin, M., et al., *Human neutrophils specifically interact with human monocyte-derived macrophage monolayers.* Inflammation, 2000. **24**(1): p. 89-98.
258. Zarbock, A., R.K. Polanowska-Grabowska, and K. Ley, *Platelet-neutrophil-interactions: linking hemostasis and inflammation.* Blood Rev, 2007. **21**(2): p. 99-111.
259. Wang, S.B., et al., *Estrogen negatively regulates epithelial wound healing and protective lipid mediator circuits in the cornea.* FASEB J, 2012. **26**(4): p. 1506-16.

260. Chiang, N., et al., *Aspirin has a gender-dependent impact on antiinflammatory 15-epi-lipoxin A4 formation: a randomized human trial.* Arterioscler Thromb Vasc Biol, 2006. **26**(2): p. e14-7.
261. Alanko, J., et al., *Modulation of arachidonic acid metabolism by phenols: relation to their structure and antioxidant/prooxidant properties.* Free Radic Biol Med, 1999. **26**(1-2): p. 193-201.
262. Wurm, G. and S. Schwandt, *Methylierte 2-Aryl-1,4-naphthochinonderivate, 5-Lipoxygenase-Inhibitoren mit reduzierter antioxidativer Aktivität.* Pharmazie, 2003. **58**(8): p. 531-538.
263. Benrezzouk, R., et al., *Inhibition of 5-lipoxygenase activity by the natural anti-inflammatory compound aethiopinone.* Inflamm Res, 2001. **50**(2): p. 96-101.
264. Dupont, R., et al., *New bis-catechols 5-lipoxygenase inhibitors.* Bioorg Med Chem, 2001. **9**(2): p. 229-35.
265. Prasad, N.S., et al., *Spice phenolics inhibit human PMNL 5-lipoxygenase.* Prostaglandins Leukot Essent Fatty Acids, 2004. **70**(6): p. 521-8.
266. Fernandez, M.T., et al., *Iron and copper chelation by flavonoids: an electrospray mass spectrometry study.* J Inorg Biochem, 2002. **92**(2): p. 105-11.
267. Greiner, C., et al., *2-(4-(Biphenyl-4-ylamino)-6-chloropyrimidin-2-ylthio)octanoic acid (HZ52)--a novel type of 5-lipoxygenase inhibitor with favourable molecular pharmacology and efficacy in vivo.* Br J Pharmacol, 2011. **164**(2b): p. 781-93.
268. Nelson, M.J., *Catecholate Complexes of Ferric Soybean Lipoxygenase-1.* Biochemistry, 1988. **27**(12): p. 4273-4278.
269. Boudreau, L.H., et al., *Caffeic acid phenethyl ester and its amide analogue are potent inhibitors of leukotriene biosynthesis in human polymorphonuclear leukocytes.* PLoS One, 2012. **7**(2): p. e31833.
270. Wisniewska, J.M., et al., *Molecular characterization of EP6--a novel imidazo[1,2-a]pyridine based direct 5-lipoxygenase inhibitor.* Biochem Pharmacol, 2012. **83**(2): p. 228-40.
271. Gerstmeier, J., et al., *5-Lipoxygenase-activating protein rescues activity of 5-lipoxygenase mutations that delay nuclear membrane association and disrupt product formation.* FASEB J, 2016. **30**(5): p. 1892-900.

APPENDIX 1: Acknowledgements

Ein außerordentlicher Dank gebührt Herrn Prof. Dr. Oliver Werz, der es mir ermöglicht hat in seinem Arbeitskreis zu promovieren. Ich möchte mich für das spannende und herausfordernde Thema bedanken, welches uns so manches Kopfzerbrechen bereitet hat, für seine Unterstützung, hervorragende Betreuung und die vielen konstruktiven Diskussionen.

Ich bedanke mich herzlich bei Herrn Prof. Dr. Gerhard Scriba für die Übernahme des Zweitgutachtens.

Bei Herrn Prof. Dr. Nils Helge Schebb möchte ich mich herzlich für die Übernahme des externen Gutachtens für meine Arbeit bedanken.

Ein großer Dank gilt den Mitarbeitern der Transfusionsmedizin des Uniklinikums in Jena, besonders Frau Dr. Silke Rummler und Frau Dr. Christina Weinigel für die Bereitstellung der Buffycoats. Außerdem bedanke ich mich bei dem gesamten Schwesternteam der Blutspende in der Bachstraße, besonders bei Frau Silvana Tiersch und Frau Simone Krieger, für die harmonische Zusammenarbeit. Und nicht zuletzt den eifrigen Blutspendern aus Jena.

Ich bedanke mich bei Frau Prof. Dr. Rosanna Filosa und ihrer Arbeitsgruppe für die Synthese und Bereitstellung der potentiellen 5-LO Inhibitoren und der guten Zusammenarbeit hinsichtlich gemeinsamer Publikationen.

Bedanken möchte ich mich außerdem bei Frau Dr. Daniela Schuster für die Erstellung der Docking-Modelle sowie bei Herrn Prof. Bruno D'Agostino und seiner Arbeitsgruppe für die Durchführung einiger Tierexperimente.

Von Herzen bedanke ich mich bei allen Mitarbeitern des Philosophenweg 14, ohne sie wäre diese Arbeit nicht möglich gewesen und Jena nicht zu meiner zweiten Heimat geworden. Vielen Dank für die schöne gemeinsame Zeit und eine wunderbare Arbeitsatmosphäre! Vielen Dank an:

Herrn PD Dr. Andreas Koeberle für die Einführung in die LC-MS/MS-Analytik, der geduldigen Beantwortung aller Fragen dazu und die Hilfe bei so manchem Statistikproblem.

Frau Dr. Ulrike Garscha für ihre Hilfe im Bereich Molekularbiologie, für ihr jederzeit offenes Ohr und die Bereitschaft sich bei Fragen und Problemen Zeit zu nehmen um diese kritisch zu diskutieren. Danke für die vielen aufbauenden und motivierenden Worte!

Frau Dr. Simona Pace, mein Partner „in crime" in Sachen geschlechtsspezifischer Untersuchungen. Das Thema hat uns so manches Mal an uns zweifeln lassen, trotzdem haben wir nicht aufgegeben! Danke außerdem für die Durchführung einiger Tierexperimente und das ein oder andere leckere original italienische Abendessen.

Herrn PD Andreas Seeling für die Einführung in die Praktika „Arzneistoffanalytik unter besonderer Berücksichtigung der Arzneibücher (Qualitätskontrolle und –sicherung bei Arzneistoffen)" und „Biochemische Untersuchungsmethoden einschließlich Klinischer Chemie (Biotransformation)". Außerdem bedanke ich mich bei allen Mitbetreuern des Praktikums, bei

Helmut Pein, Felix Nikels, Susanna Völker, Konstantin Löser und Stephanie Zergiebel für die unterhaltsame Zeit.

Danke an Monika Listing und Bärbel Schmalwasser für ihre Unterstützung bei den unzähligen Substanzen die getestet werden mussten! Danke an Heidi Traber für ihre Geduld mich mit dem Novostar und so manchem Experiment vertraut zu machen. Ich danke Petra Wiecha für ihre Unterstützung im alltäglichen Laborgeschehen und Uwe Beck für seinen unermüdlichen handwerklichen Einsatz.

Ich bedanke mich herzlich bei Katrin Fischer, HPLC-Expertin, MS-Expertin und zusammen mit Nadja Gerlitz außerdem DIE Expertinnen in Sachen Verbrauchsmaterialien und Bestellungen. Sie behalten den Überblick und vermeiden, dass das Labor im Chaos versinkt, vielen Dank für alles!

Ich bedanke mich von ganzem Herzen bei Stefanie Liening, die nun schon seit Diplomzeiten an meiner Seite ist und alle Höhen und Tiefen dieser Promotion zusammen mit mir gemeistert hat. Zusammen mit Stefanie König hat sie mich aufgebaut, wenn mal wieder so rein gar nichts klappen wollte und mich motiviert weiterzumachen. Beide waren mir eine unverzichtbare Stütze und Hilfe sowohl im Labor, als auch im wahren Leben. Zusammen mit Erik Romp, Helmut Pein, Konstantin Löser, Maria Thürmer, Lea Thomas, Katrin Schubert und Felix Nikels haben sie Jena zu meiner zweiten Heimat gemacht und ohne sie wäre diese Zeit nur halb so schön gewesen! An Felix Nikels, Helmut Pein und Markus Werner außerdem vielen Dank für die Hilfe bei jeglichen IT- und Computerproblemen. Vielen Dank auch an meine beiden Sportskanonen Maria Thürmer und Lea Thomas die mich nicht nur im Labor tatkräftig unterstützt haben, sondern auch bei meinen sportlichen Aktivitäten. Herzlichen Dank an Friederike Dehm, von der ich das Thema übernehmen durfte und die mich in das Arbeiten mit Vollblut eingeführt hat. Danke für viele schöne und lustige gemeinsame Stunden. Ich bedanke mich bei Shanice Liebeskind und Theresa Hildebrandt für die Hilfe bei allen administrativen Fragen. Außerdem bedanke ich mich bei allen andern Mitarbeitern, Doktoranden, Diplomanden, Masteranden und Studenten für die schöne und gute Zusammenarbeit, sie alle haben meine Zeit in Jena zu etwas Besonderem gemacht.

Ein besonderer Dank gebührt meinen Eltern und meinem Bruder, die mir diesen Weg ermöglicht haben. Ohne euren Glauben an mich und euer Vertrauen wäre ich heute nicht da, wo ich jetzt bin. Ihr habt mich während dieser nicht immer einfachen Zeit zu 100% unterstützt und mir Kraft gegeben.

APPENDIX 2: Publications and conference contributions

Publications

König S, Romp E, **Krauth V**, Rühl M, Dörfer M, Hofmann B, Häfner A-K, Steinhilber D, Karas M, Garscha U, Hoffmeister D, Werz O (2018)

„Melleolides from honey mushroom inhibit 5-lipoxygenase via Cys159.“ Cell Chem Biol (submitted)

Pace S, Rossi A, **Krauth V**, Dehm F, Troisi F, Bilanca R, Weinigel C, Rummler S, Werz O, Sautebin L (2017)

„Sex differences in prostaglandin biosynthesis in neutrophils during acute inflammation.” Sci Rep. 19;7(1):3759

Svouraki A, Garscha U, Kouloura E, Pace S, Pergola C, **Krauth V**, Rossi A, Sautebin L, Halabalaki M, Werz O, Gaboriaud-Kolar N, Skaltsounis AL (2017)

„Evaluation of dual 5-lipoxygenase/microsomal prostaglandin E_2 Synthase-1 inhibitory effect of natural and synthetic acronychia-type isoprenylated acetophenons.” J Nat Prod. 24;80(3):699-706

Scuotto M*, Peduto A*, **Krauth V***, Roviezzo F, Rossi A, Temml V, Esposito V, Stuppner H, Schuster D, D'Agostino B, Schiraldi C, de Rosa M, Werz O, Filosa R (2017)

„Optimization of benzoquinone and hydroquinone derivatives as potent inhibitors of human 5-lipoxygenase.“ Eur J Med Chem. 15;127:715-726

*authors contributed equally

Aligiannis N, Halabalaki M, Chaita E, Kouloura E, Argyropoulou A, Benaki D, Kalpoutzakis E, Angelis A, Stathopoulou K, Antoniou S, Sani M, **Krauth V**, Werz O, Schütz B, Schäfer H, Spraul M, Mikros E, Skaltsounis LA (2016)

„Heterocovariance based metabolomics as a powerful tool accelerating bioactive natural product identification.“ Chemistry Select Jul 1;1(10):2531-2535

Schaible AM, Filosa R, **Krauth V**, Temml V, Pace S, Garscha U, Liening S, Weinigel C, Rummler S, Schieferdecker S, Nett M, Peduto A, Collarile S, Scuotto M, Roviezzo F, Spaziano G, de Rosa M, Stuppner H, Schuster D, D'Agostino B, Werz O. (2016)

„The 5-lipoxygenase inhibitor RF-22c potently suppresses leukotriene biosynthesis in cellulo and blocks bronchoconstriction and inflammation in vivo.” Biochem Pharmacol. 15;112:60-71

Peduto A, **Krauth V**, Collarile S, Dehm F, Ambruosi M, Belardo C, Guida F, Massa A, Esposito V, Maione S, de Rosa M, Werz O, Filosa R. (2016)

„Exploring the role of chloro and methyl substitutions in 2-phenylthiomethyl-benzoindole derivatives for 5-LOX enzyme inhibition.“ Eur J Med Chem. 27;108:466-75

Ciffolilli S, Wallert M, Bartolini D, **Krauth V**, Werz O, Piroddi M, Sebastiani B, Torquato P, Lorkowski S, Birringer M, Galli F. (2015)

„Human serum determination and in vitro anti-inflammatory activity of the vitamin E metabolite α-(13'-hydroxy)-6-hydroxychroman." Free Radic Biol Med. 89:952-62

Wallert M, Schmölz L, Koeberle A, **Krauth V**, Glei M, Galli F, Werz O, Birringer M, Lorkowski S. (2015)

„α-Tocopherol long-chain metabolite α-13'-COOH affects the inflammatory response of lipopolysaccharide-activated murine RAW264.7 macrophages." Mol Nutr Food Res. 59(8):1524-34

Filosa R, Peduto A, Schaible AM, **Krauth V**, Weinigel C, Barz D, Petronzi C, Bruno F, Roviezzo F, Spaziano G, D'Agostino B, De Rosa M, Werz O. (2015)

„Novel series of benzoquinones with high potency against 5-lipoxygenase in human polymorphonuclear leukocytes." Eur J Med Chem. 13;94:132-9

Peduto A, Bruno F, Dehm F, **Krauth V**, de Caprariis P, Weinigel C, Barz D, Massa A, De Rosa M, Werz O, Filosa R. (2014)

"Further studies on ethyl 5-hydroxy-indole-3-carboxylate scaffold: design, synthesis and evaluation of 2-phenylthiomethyl-indole derivatives as efficient inhibitors of human 5-lipoxygenase." Eur J Med Chem. 23;81:492-8

Schaible AM, Filosa R, Temml V, **Krauth V**, Matteis M, Peduto A, Bruno F, Luderer S, Roviezzo F, Di Mola A, de Rosa M, D'Agostino B, Weinigel C, Barz D, Koeberle A, Pergola C, Schuster D, Werz O. (2014)

„Elucidation of the molecular mechanism and the efficacy in vivo of a novel 1,4-benzoquinone that inhibits 5-lipoxygenase." Br J Pharmacol. 171(9):2399-412

Filosa R, Peduto A, Aparoy P, Schaible AM, Luderer S, **Krauth V**, Petronzi C, Massa A, de Rosa M, Reddanna P, Werz O. (2013)

„Discovery and biological evaluation of novel 1,4-benzoquinone and related resorcinol derivatives that inhibit 5-lipoxygenase." Eur J Med Chem. 67:269-79

Poster presentations

Krauth V, Filosa R, Peduto A, Schaible AM, Werz O (2015). "Potent inhibition of 5-lipoxygenase in human polymorphonuclear leukocytes by new benzoquinone derivatives." 14th International Conference on Bioactive Lipids in Cancer, Inflammation and related Diseases, Budapest, Hungary.

Krauth V, Pace S, Schaibl AM, Garscha U, Filosa R, Temml V, Schuster D, Stuppner H, D'Agostino B, Werz O (2016). "Potent suppression of 5-lipoxygenase activity *in vitro* and *in vivo* by the novel inhibitor RF22c." 6th European Workshop on Lipid Mediators, Frankfurt (Main), Germany.

APPENDIX 3: Eigenständigkeitserklärung

Hiermit erkläre ich, dass mir die Promotionsordnung der Biologisch-Pharmazeutischen Fakultät der Friedrich-Schiller-Universität Jena bekannt ist. Die vorliegende Dissertation habe ich selbst angefertigt, keine Textabschnitte eines Dritten oder eigener Prüfungsarbeiten ohne Kennzeichnung übernommen und alle von mir benutzten Hilfsmittel, persönliche Mitteilungen und Quellen wurden als solche kenntlich gemacht. Bei der Auswahl und der Auswertung des Materials sowie bei der Herstellung der Manuskripte hat mich Prof. Dr. Oliver Werz unterstützt.

Ich versichere, dass ich die Hilfe eines Promotionsberaters nicht in Anspruch genommen habe und dass Dritte weder unmittelbar noch mittelbar geldwerte Leistungen von mir für Arbeiten erhalten haben, die im Zusammenhang mit dem Inhalt der vorgelegten Dissertation stehen.

Diese Dissertation wurde für keine staatliche oder andere wissenschaftliche Prüfung als Prüfungsarbeit von mir eingereicht. Weiterhin versichere ich, dass ich die gleiche, eine in wesentlichen Teilen ähnliche oder eine andere Abhandlung nicht bei einer anderen Universität als Dissertation eingereicht habe.

_____ _____

Ort, Datum Verena Krauth